Novel in vitro models for pathogen detection based on organic transistors integrated with living cells.

Scherrine Tria

Ecole Nationale Supérieure des Mines
SAINT-ETIENNE

NNT : 2013 EMSE 0712

THÈSE

présentée par

Scherrine Tria

pour obtenir le grade de
Docteur de l'École Nationale Supérieure des Mines de Saint-Étienne

Spécialité: Bioelectronics

Novel *in vitro* models for pathogen detection based on organic transistors integrated with living cells.

soutenue à Gardanne, le 18 Octobre 2013

Membres du jury

Président :	Lena ALEXOPOULOU	DR1, Centre d'Immunologie de Marseille-Luminy
Rapporteurs :	Fréderic LUTON	CR1 Institut de Pharmacologie Moléculaire et Cellulaire, Valbonne
Co encadrants :	Roisin OWENS	Professeur Assistant, ENSMSE, Gardanne
	Romaric DEYDIER	PDG, CDL Pharma, Marseille
Directeur de thèse :	Georges MALLIARAS	Professeur, ENSMSE, Gardanne

Spécialités doctorales : SCIENCES ET GENIE DES MATERIAUX MECANIQUE ET INGENIERIE GENIE DES PROCEDES SCIENCES DE LA TERRE SCIENCES ET GENIE DE L'ENVIRONNEMENT MATHEMATIQUES APPLIQUEES INFORMATIQUE IMAGE, VISION, SIGNAL GENIE INDUSTRIEL MICROELECTRONIQUE	**Responsables :** K. Wolski Directeur de recherche S. Drapier, professeur F. Gruy, Maître de recherche B. Guy, Directeur de recherche D. Graillot, Directeur de recherche O. Roustant, Maître-assistant O. Boissier, Professeur JC. Pinoli, Professeur A. Dolgui, Professeur

EMSE : Enseignants-chercheurs et chercheurs autorisés à diriger des thèses de doctorat (titulaires d'un doctorat d'État ou d'une HDR)

AVRIL	Stéphane	PR2	Mécanique et ingénierie	CIS
BATTON-HUBERT	Mireille	PR2	Sciences et génie de l'environnement	FAYOL
BENABEN	Patrick	PR1	Sciences et génie des matériaux	CMP
BERNACHE-ASSOLLANT	Didier	PR0	Génie des Procédés	CIS
BIGOT	Jean Pierre	MR(DR2)	Génie des Procédés	SPIN
BILAL	Essaid	DR	Sciences de la Terre	SPIN
BOISSIER	Olivier	PR1	Informatique	FAYOL
BORBELY	Andras	MR(DR2)		SMS
BOUCHER	Xavier	PR2	Génie Industriel	FAYOL
BRODHAG	Christian	DR	Sciences et génie de l'environnement	FAYOL
BURLAT	Patrick	PR2	Génie Industriel	FAYOL
COLLOT	Philippe	PR0	Microélectronique	CMP
COURNIL	Michel	PR0	Génie des Procédés	DIR
DARRIEULAT	Michel	IGM	Sciences et génie des matériaux	SMS
DAUZERE-PERES	Stéphane	PR1	Génie Industriel	CMP
DEBAYLE	Johan	CR	Image Vision Signal	CIS
DELAFOSSE	David	PR1	Sciences et génie des matériaux	SMS
DESRAYAUD	Christophe	PR2	Mécanique et ingénierie	SMS
DOLGUI	Alexandre	PR0	Génie Industriel	FAYOL
DRAPIER	Sylvain	PR1	Mécanique et ingénierie	SMS
FEILLET	Dominique	PR2	Génie Industriel	CMP
FOREST	Bernard	PR1	Sciences et génie des matériaux	CIS
FORMISYN	Pascal	PR0	Sciences et génie de l'environnement	DIR
FRACZKIEWICZ	Anna	DR	Sciences et génie des matériaux	SMS
GARCIA	Daniel	MR(DR2)	Génie des Procédés	SPIN
GIRARDOT	Jean-jacques	MR(DR2)	Informatique	FAYOL
GOEURIOT	Dominique	DR	Sciences et génie des matériaux	SMS
GRAILLOT	Didier	DR	Sciences et génie de l'environnement	SPIN
GROSSEAU	Philippe	DR	Génie des Procédés	SPIN
GRUY	Frédéric	PR1	Génie des Procédés	SPIN
GUY	Bernard	DR	Sciences de la Terre	SPIN
GUYONNET	René	DR	Génie des Procédés	SPIN
HAN	Woo-Suck	CR		SMS
HERRI	Jean Michel	PR1	Génie des Procédés	SPIN
INAL	Karim	PR2	Microélectronique	CMP
KLOCKER	Helmut	DR	Sciences et génie des matériaux	SMS
LAFOREST	Valérie	MR(DR2)	Sciences et génie de l'environnement	FAYOL
LERICHE	Rodolphe	CR	Mécanique et ingénierie	FAYOL
LI	Jean Michel		Microélectronique	CMP
MALLIARAS	Georges	PR1	Microélectronique	CMP
MOLIMARD	Jérôme	PR2	Mécanique et ingénierie	CIS
MONTHEILLET	Franck	DR	Sciences et génie des matériaux	SMS
PERIER-CAMBY	Laurent	PR2	Génie des Procédés	DFG
PIJOLAT	Christophe	PR0	Génie des Procédés	SPIN
PIJOLAT	Michèle	PR1	Génie des Procédés	SPIN
PINOLI	Jean Charles	PR0	Image Vision Signal	CIS
ROUSTANT	Olivier	MA(MDC)		FAYOL
STOLARZ	Jacques	CR	Sciences et génie des matériaux	SMS
SZAFNICKI	Konrad	MR(DR2)	Sciences et génie de l'environnement	CMP
TRIA	Assia		Microélectronique	CMP
VALDIVIESO	François	MA(MDC)	Sciences et génie des matériaux	SMS
VIRICELLE	Jean Paul	MR(DR2)	Génie des Procédés	SPIN
WOLSKI	Krzystof	DR	Sciences et génie des matériaux	SMS
XIE	Xiaolan	PR1	Informatique	CIS

ENISE : Enseignants-chercheurs et chercheurs autorisés à diriger des thèses de doctorat (titulaires d'un doctorat d'État ou d'une HDR)

FORTUNIER	Roland	PR	Sciences et Génie des matériaux	ENISE
BERGHEAU	Jean-Michel	PU	Mécanique et Ingénierie	ENISE
DUBUJET	Philippe	PU	Mécanique et Ingénierie	ENISE
LYONNET	Patrick	PU	Mécanique et Ingénierie	ENISE
SMUROV	Igor	PU	Mécanique et Ingénierie	ENISE
ZAHOUANI	Hassan	PU	Mécanique et Ingénierie	ENISE
BERTRAND	Philippe	MCF	Génie des procédés	ENISE
HAMDI	Hédi	MCF	Mécanique et Ingénierie	ENISE
KERMOUCHE	Guillaume	MCF	Mécanique et Ingénierie	ENISE
RECH	Joël	MCF	Mécanique et Ingénierie	ENISE
TOSCANO	Rosario	MCF	Mécanique et Ingénierie	ENISE
GUSSAROV Andrey	Andrey	Enseignant contractuel	Génie des procédés	ENISE

PR 0	Professeur classe exceptionnelle
PR 1	Professeur 1ère classe
PR 2	Professeur 2ème classe
PU	Professeur des Universités
MA (MDC)	Maître assistant
DR	Directeur de recherche

Ing.	Ingénieur
MCF	Maître de conférences
MR (DR2)	Maître de recherche
CR	Chargé de recherche
EC	Enseignant-chercheur
IGM	Ingénieur général des mines

SMS	Sciences des Matériaux et des Structures
SPIN	Sciences des Processus Industriels et Naturels
FAYOL	Institut Henri Fayol
CMP	Centre de Microélectronique de Provence
CIS	Centre Ingénierie et Santé

Mise à jour : 04/09/2012

Content

Acknowledgement

First of all I would like to say that these 3 years of PhD was a great chance for me, I really appreciate this experience. I came away stronger scientifically and technically but also culturally. I spent beautiful years in a lab where I met remarkable and amazing people who have enriched me and that made this unforgettable adventure.

For the honor they have done me to participate in my thesis committee and for their analysis this thesis, I also express my thanks to Lena Alexopoulou who was rapporteur then after a happy event experienced by Guisseppe Scarpa, she was president of my jury as well as Frédéric Luton.

I would like first to thanks the Region PACA and Romaric Deydier from CDL Pharma, without which this project could not be financed. This thesis took place in the Microelectronics Center of Provence, Site Georges Charpak Ecole Nationale Supérieure des Mines de Saint-Etienne. I thank Philippe Collot and Stéphane Dauzères-Pérez, director of the Center, for their hospitality. I also want to express my gratitude to George Malliras and Róisín Owens

I also address my thanks to the informatics and infrastructure service without which the center will not beat. In particular, a big thanks you to Veronique who pampers PhD as no one else, Barbara and Michelle for their assistance in orders and missions and Sabine for the most part literary. Gracien, thank you for always had been there for express repairs, without forgetting Manon, Stephane and Jonathan.

I also thank all the scientific staff of the CMP for all the good times past. I also think of all those who helped me during these three years, Jessica for your help and your explanations for the SEM, Romain Etienne C and for their advice and special procedures PhD. In addition to that, I thank them for their good humor and laughter filled lunch break with the help of Thierry and Brice.

I also want to thank my aunt, Assia, who allowed me to meet Roisin and George during his HDR

My greatest of thanks go firstly to Roisin Owens for choosing me and helped make my goal in his team. Over the years it has transmitted me his expertise and experience. It was an extraordinary bordering, who guided me and make me change to reach the end of this adventure. I also thank George Malliaras who accept in my laboratory, a laboratory in his exceptional scientific and cultural wealth.

Then I also want to thank my fellow adventurers, especially what with all that to start, and this at any point, we started our project together but also

create the beginning this lab. I think of Dion, Pierre, Thomas, Esma, Moshe, Jin, Eleni, Erica, Jacqueline Tong, Sylvain and Sebastian. Dion (Kido), you are the only PhD student in BEL when I arrived, I remember our seeming discussion when I didn't talk English and you didn't speak French, but we found a way to communicate. Esma, you were the only French speaking non-permanent at the beginning, you help me a lot as much for English as science. It was during this first year that I met my teammate on my project, Leslie Jimison. By your perseverance and your organization, you showed me how to conduct good research and should look like and very good scientist. You taught me a lot about areas that I was still very abstract. Then I met Adel with whom I shared a lot and whose advice in these areas of expertise have been an important asset. Pierre, we share the same office and a lot of adventure between our conference and travel, I also appreciate all of our discussion and your explanation about electronics and other subject. We had amazing funny time all together with our Wednesday in Aix and Thursday at Ti'Bar. Others then arrived to enrich this fabulous team: Xenofon, Jonathan, Michele, Marc R and Marc F, Miriam, Manuelle, Cassandra, Liza, Duc and Dimitris.

Finally I would like to thank all of my friends, my family, my father Mehrez, my Mother Catherine and my brother Alexandre. Thank you for putting up with me. Thank you for making me smile, laugh and relax. Special thanks to my boyfriend Romain for his undying support, encouragement and love.

Abbreviations:

A: Area

Ag/AgCl: Silver/Silver chloride

AJ: Adherens Junction

BSA: Bovine Serum Albumin

C_o: initial concentration of Lucifer yellow on the apical side

Caco-2: heterogeneous human epithelial colorectal adenocarcinoma cells line

Ccell: Capacitance of the cell layer,

C_{CP}: Capacitance conducting polymer

C_{filter}: Capacitance of the porous filter

CFU: Colony-Forming Unit

CP: Conducting Polymer

CPE: Constant Phase Elements

DAPI: 4',6-diamidino-2-phenylindole

DBSA : DodecylBenzeneSulfonic Acid

DMEM : Advanced Dulbecco's Modified Eagle Medium

DNA: DeoxyriboNucleic Acid

ECIS system : Electric Cell-substrate Impedance Sensing

EGTA : Ethylene Glycol-bis(2-aminoethyl-ether)-N, N, N', N',-tetraacetic acid

EIS: Electronic Impedance Spectroscopy

ELISA: Enzyme-Linked ImmunoSorbent Assay

EtOH; Ethanol

EVOM: Epithelial VoltOhmMeter

FBS: Fetal Bovine Serum

FRAP: Fluorescence Recovery After Photobleaching

GOPS: 3-glycidoxypropyltrimethoxysilane

GUK: GUanylate Kinase

H_2O_2: Hydrogen peroxide

HCl: Hydrogen Chloride

HRP: HorseRadish Peroxidase

IBD: Inflammatory Bowel Disease

I_D: drain current

I_G: gate current

IgG: Immunoglobulin G

I_o: drain current when V_G is off

JAM: Junctional Adhesion Molecule

LB: Luria Broth

LDH: Lactate DeHydrogenase

LY: Lucifer Yellow

MAGUK: Membrane-Associated GUanylate Kinase

MDCK: Madin-Darby Canine Kidney

MEA: MicroElectrodes Arrays

MOI: Multiplicity Of Infection

NH_4Cl: Ammonium chloride

NI: Non-Invasive

NR: Normalized Response

OD: Optical Density

OECT: Organic ElectroChemical Transistor

P app: apparent permeability

PBS: Phosphate Buffered Saline

PBST: Phosphate Buffered Saline with Tween

PCR: Polymerase Chain Reaction

PDMS: PolyDiMethylSiloxane

PEDOT: PSS: (poly(3,4-ethylenedioxythiophene)-poly(styrenesulfonate)

Pen-strep: penicillin–streptomycin

P-gp: Permeability glycoprotein

Ppy:PSS: polypyrrole doped with polystyrene sulfonate

R_{filter} : resistance of the porous filter

R_{med} : resistance of the media

ROS: Reactive Oxygen Species

Ser: Serine

Ţ: Tau

TER: TransEpithelial Resistance

Thr: Threonine

TJ: Tight Junction

Tyr: Tyrosine

V_G: gate voltage

WT: WildType

ZO: Zonula Occludens

ZONAB : (ZO-1)-associated nucleic acid binding protein

ΔI_D : drain current modulation in response to the application of the gate voltage

Abstract

In vitro cell models for barrier tissue abound, and depending on the tissue type, and the cell type, are more or less successful at mimicking *in vivo* conditions. The validity of the model also depends on the method used to assess it. The main parameters to assess barrier tissue integrity are permeability and transepithelial resistance. These parameters generally correlate as an intact barrier tissue exhibit high electrical resistance and a low permeability. Different methods to measure these parameters were developed. Typically, the permeability is measured by the passage of a radio labeled or fluorescent compound across the epithelial barrier. For the measurement of the transepithelial resistance (TER), different devices have been developed. Some, such as the handheld volt Ohm meter are relatively inexpensive but are not compatible with high throughput screening, other such as impedance spectroscopy, are more automatized and reproducible but remain expensive.

The advent of organic electronics has created a unique opportunity to interface the worlds of electronics and biology, using devices such as the organic electrochemical transistor (OECT). This device provides a very sensitive way to detect minute ionic currents in an electrolyte, as the transistor amplifies the gate current. These devices have unprecedented sensitivity, in a format that can be mass produced at low-cost. So, the OECT represent a new exciting method for assessing barrier tissue cell layers.

The aim of this study is to integrate barrier tissue layers with OECTs to yield devices that can detect minute disruptions in barrier function, as seen by a decrease in transepithelial resistance. A disruption in the barrier (*eg*. caused by a pathogen) will be detected electrically through a measurement of the drain current. The resulting integration will yield devices that can detect minute disruptions in barrier function, with unprecedented sensitivity, by means of a simple electrical measurement, and in a format that can be mass produced using low-cost manufacturing techniques.

Firstly, gastro-intestinal cell monolayers that form a barrier tissue layer were characterized using established techniques such as immunofluorescence, permeability assays with Lucifer Yellow and measurement of the transepithelial resistance using a commercially available EIS system. Second, gastro-intestinal cell were integrated with the OECT. The technique was then validated using toxic compounds (Ethanol and hydrogen peroxide) and a calcium chelator. Finally the system was transitioned to an *in situ* measurement setup for longer term measurements under physiological conditions and used to detect *Salmonella typhimurium* in classic and complex media.

In summary, a novel device which can be fabricated at low cost, which is capable of label-free monitoring of barrier tissue, has been developed. This device shows greater sensitivity and higher temporal resolution than existing methods. The integration of *in vitro* models with devices such as the OECT can be a great alternative to animal testing for drug discovery and toxicology.

Motivation

Electrical monitoring of cell health has been broadly used in basic research but such methods are urgently needed for high throughput screening. The main part of the European REACH regulation is to develop new strategies to limit the use of animals to test the toxicity of new products. This regulation has much more interest than the more than 30,000 chemical substances that are imported into Europe. This regulation can be applied only by the development of a competent validation method with an accurate *in vitro* model to produce data needed to ensure a high level of protection of human health or the environment.

Different methods available but most of them used labels. Labelling adds cost, time, steps and can generate artefacts. Therefore it is important to create a device without labels to measure barrier tissue integrity which is low cost, sensitive, rapid and adaptable to high throughput screening.

Due to the transistor geometry an inherent amplification takes place resulting in much more sensitive OECTs. OECT require very simple electronics to read out), making the devices easily portable. They are fully compatible to roll-to-roll techniques so they can be fabricated at a low cost. Coupling OECT with live epithelial cell layer will create a device that is very sensitive and tailored to detect all manner of pathogens and toxins.

1 Chapter 1

Introduction

1.1 Barrier tissue

In most multicellular organisms, all cells are not identical. There are important differences in their morphology and function and those due to the process of differentiation. Differentiation leads to changes in many aspects of cell physiology: its size, shape, polarity, metabolic activity, sensitivity to signals and gene expression can all be modified during differentiation. Differentiation of stem cells is a mechanism that allows humans to renew its cells. The basal portion of the skin is comprised of stem cells, which are differentiated so as asymmetric: a stem cell gives an epithelial cell and a skin stem cell. Epithelial cells are commonly found throughout the body of multicellular organisms, and constitute the border between the internal and external environments. Epithelia cells can have varied morphology depending on their location (figure 1.1). Due to their localization, some epithelial cells become stratified because they are exposed to chemical and mechanical stress. Elsewhere in the body, the epithelia form monolayers. These barrier layers can be columnar in the intestine, squamous in the lungs, or tubular in the renal tubule.

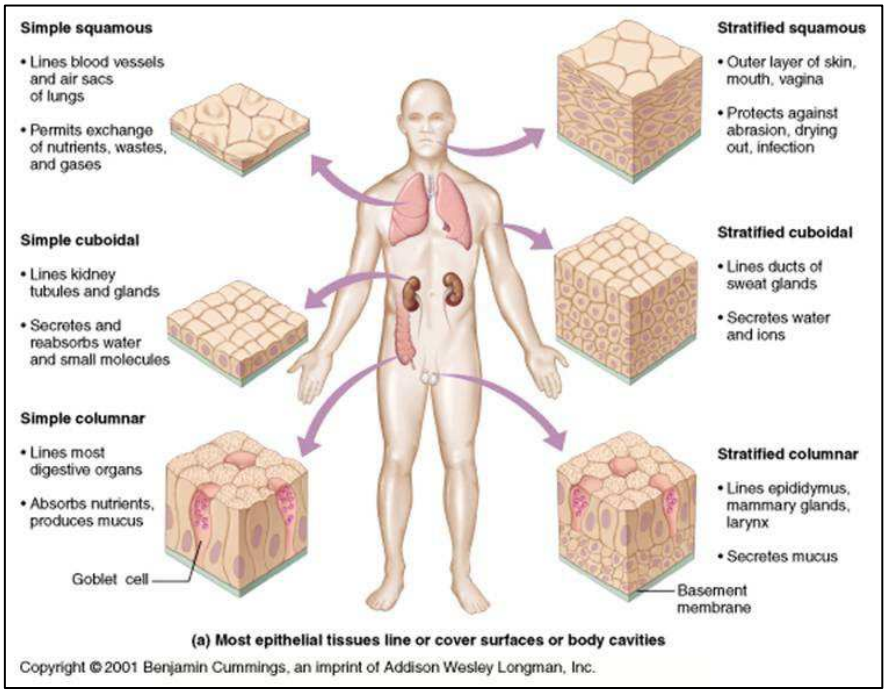

Figure 1.1: different types of epithelia

Epithelial and endothelial cell layers serve as functional barriers in many different parts of the body. These cell layers form selectively permeable interfaces that control not only diffusive permeation of solutes along paracellular routes between adjacent cells, but can also actively transport substances along transcellular pathways. Individual epithelial and endothelial cells are joined to each other by specialized complexes, including the adherens

junction and the Zonula occludens, commonly referred to as tight junction [1] (figure 1.2).

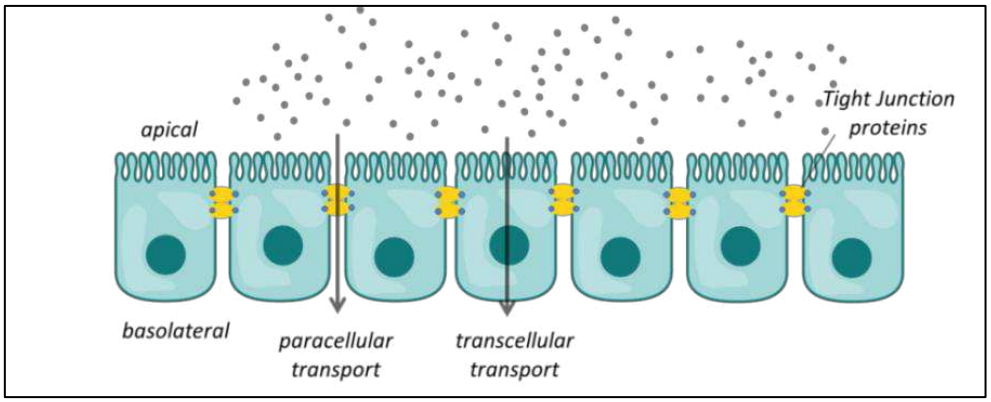

Figure 1.2: Transport across barrier tissues

Tight junctions are composed of several proteins, such as the transmembrane proteins occludin and claudin and the intracellular proteins ZO-1 and ZO-2. The tight junctions seal the intercellular space between adjacent cells to create a barrier, thereby restricting paracellular diffusion [2]. These tight junctions are of particular relevance for the active barrier functionality of the cell layer. They regulate the passage of molecules across the barrier as they selectively open and close in response to various signals from the inside and outside of the cells. There are many different types of barrier tissue in the body.

1.2 Structure and function of the tight junction

Tight junction was first described as Zonula occludens in a study from Schneeberger *et al.* [3] where horseradish peroxidase (HRP) was injected into mice to determine alveolar-capillary membrane permeability. Upon fixation, tissues sections were examined under electron microscopy. They found that HRP pass endothelial junction but cannot reach alveolar space because HRP was stop by junction between epithelial cells. Similar results were observed when HRP were instilled intranasally. These finding demonstrate that these junction form a barrier to the passage of HRP.

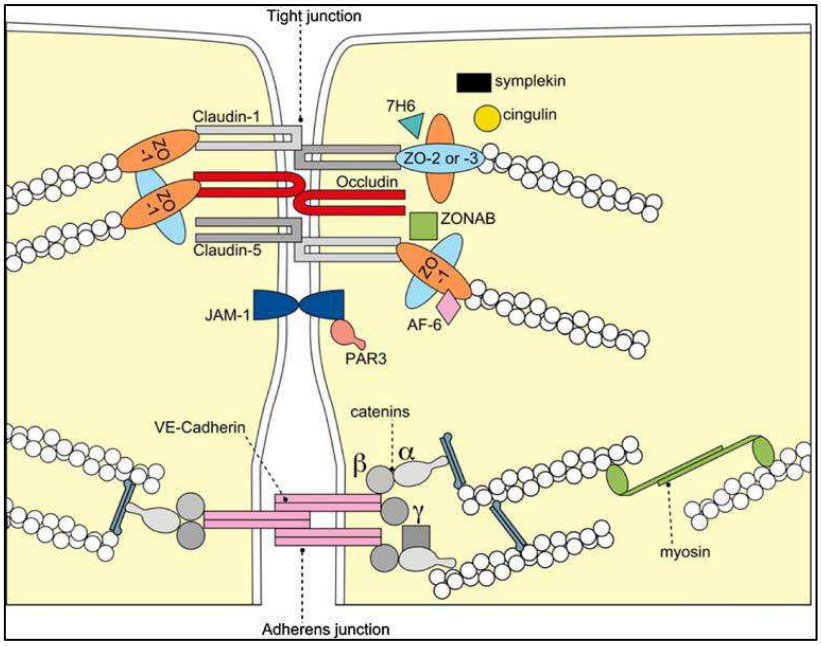

Figure 1.3: Molecular composition of tight junctions. The transmembrane proteins occludin, the claudin(s) and junctional adhesion molecule-1 (JAM-1) constitute the barrier formed by TJs, sealing the paracellular space. From Förster, 2008 [4].

By electron microscopy TJ appear as kissing points at the outer leaflets of the plasma membrane of adjacent cells, which seal the intercellular space [5]. When TJs are observed by immunofluorescence, they are found at the cell border [6]. Following a freeze fracture technique they are observed to be a network of fibrils which circle the apical plasma membrane [7]. From this observation, TJ have been described as a scaffold of both integral and peripheral proteins (figure 1.3). The former play a role in the establishment of cell-cell contact while the latter act as a bridge to link the integral protein to the cytoskeleton.

1.2.1 Structure of the tight junction

1.2.1.1 Integral proteins

The integral proteins responsible for occluding of intercellular space are mainly occludin, claudin, and junctional adhesion molecule (JAM) protein.

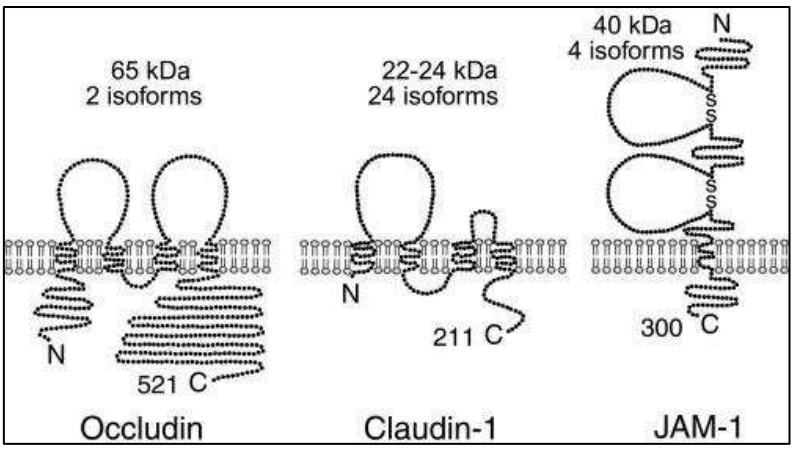

Figure 1.4. Integral membrane TJ proteins from Schneeberger *et al*, [8]

Occludin was the first TJ transmembrane protein identified [9]. The four transmembrane domains of occludin (figure 1.4) are separated by hydrophilic extracellular loops rich in tyrosine and serine. In epithelial cell lines, highly phosphorylated occludins are found at the TJ, so the action of phosphatase/kinase can modulate the assembly of the filament at the TJ [10]. The carboxyl terminal of the protein can directly interact with actin [11] or bind to the peripheral protein ZO-1 [12].Experiments using synthetic peptides homologous to the region of the first extracellular loop suggest that extracellular loops are critical in the formation of the paracellular barrier [13]. Truncated protein experiments also demonstrated that the carboxyl terminal of occludin is necessary for the function of TJs [14]. Although occludin has been shown to be a constituent of TJ filaments, its role remains unclear as occludin knock-out mice are viable with well-defined TJs [15].

Claudin proteins, like occludin, form four transmembrane domains and two extracellular loops (figure 1.4). By using different size of polyethylene glycol, it has been demonstrated that the permeability has two components,: One pathway is formed by claudin pore and is charge selective, where only molecules less than 4Å in diameter can pass through the pore. Molecule larger than 4Å in diameter can also pass across a intact TJ, but require a dynamic and temporary opening of the TJ [16]. The first extracellular loop, rich in charged amino acids, creates the ionic selectivity. Through the presence of disulfide bonds, the stability of the extracellular loop in claudins is enhanced and thus facilitates the pore formation [17]. The transepithelial resistance (TER) reflects

the passage of ion and charge molecules through the TJ. The pore form by claudins is the main pathway for ions, so pores are the key determinants in ion permeability. The second extracellular loop takes part in the interaction with claudin in the neighboring cell plasma membrane and within the same. The expression of claudin proteins in fibroblasts demonstrates that claudin constitutes the backbone of a TJ strand [18]. It has been shown that claudin is the key regulator of the TJ formation [19,20]. By co-cultivating fibroblasts which express different claudin [21], it has been found that claudins form selective interactions and that this interaction determines the barrier properties [22].

JAM proteins are single transmembrane proteins (figure 1.4), and members of the immunoglobulin superfamily [23]. These proteins have been shown to interact with peripheral TJ proteins such as ZO-1 via their carboxy terminus [24], but are not able to from TJ strands in fibroblasts [25]. They are concentrated at the TJ and appear to be associated laterally to claudin proteins [26]. Thus, JAM proteins are involved in the formation and assembly of TJ in epithelial cells but are not involved in the barrier function.

1.2.1.2 Peripheral protein

A number of proteins are located in the submembraneous region of TJ. Most of these proteins function as molecular scaffolds by containing multiple protein-protein binding sites.

Zonula occludens -1 (ZO-1) was the first TJ associated protein identified [27]. Later, two homologues, ZO-2 and ZO-3 were discovered [28,29]. These proteins are members of the membrane-associated guanylate kinase (MAGUK). Due to its protein-protein binding site, ZO-1 plays a central role in TJ scaffolding (Figure 1.5).

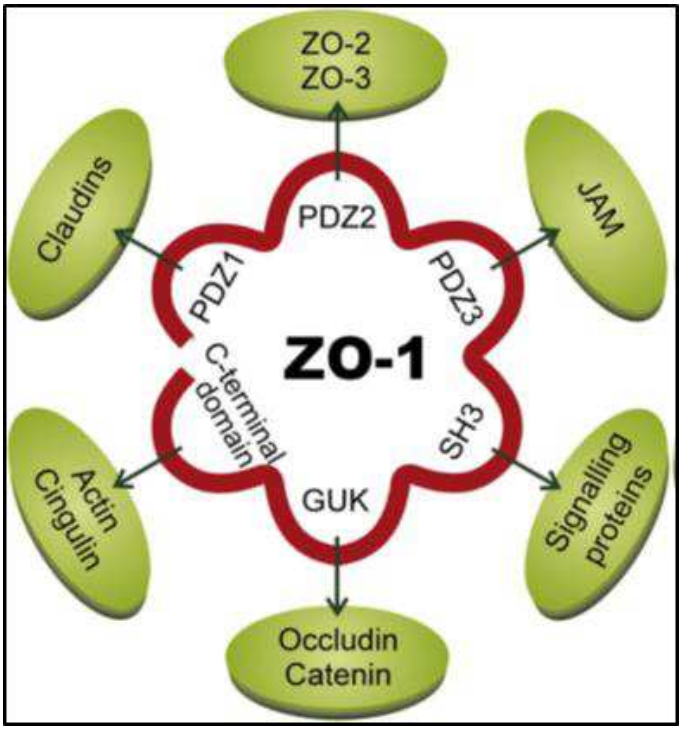

Figure 1.5: Schematic diagram of interactions of ZO-1 with transmembrane, cytosolic and cytoskeletal proteins, from Kosińska, et al [30].

Via its PDZ domain, ZO-1 interacts with claudin [31], other ZO proteins [11] and JAM [32], with occludin via guanylate kinase (GUK) homology domain and with F-actin through its C-terminal domain. Through its interaction with signaling proteins, ZO-1 can also regulate gene expression, cell proliferation and paracellular permeability [33].

1.2.1.3 Tricellular tight junction

It should be noted that for many years, TJ has been described as cell-cell sealing proteins between two adjacent cells. However, at the meeting point of three epithelial cells, junctions are also present and contribute to the sealing of the paracellular pathway. These structures are named tricellular TJ [34] (figure 1.6). Tricellulin is the protein involved in tricellular junction, which has been demonstrated using two different experiments. A delay in barrier formation has been observed in tricellulin knock down [35]. Moreover, a mutation in this protein induces a decrease in transepithelial resistance and an increase in permeability. Interestingly, the loss of tricellulin also destabilized bicellular TJ by disturbing occludin strands [34]. Furthermore, occludin knock-down leads to a mislocation of tricellulin to bicellular TJ [35]. Together these results demonstrate that tricellulin may compensate for the role of occludin proteins. It has been shown that the region homolog to occludin, in the carboxy terminal domain, bind to ZO-1 [36]. Krug et al also demonstrate that tricellulin

selectively restricts the passage of macromolecules without affecting the passage of ions [37]. Through these studies, the action of tricellulin in TJ has been demonstrated, but the mechanisms by which these proteins interact with other proteins remain unclear.

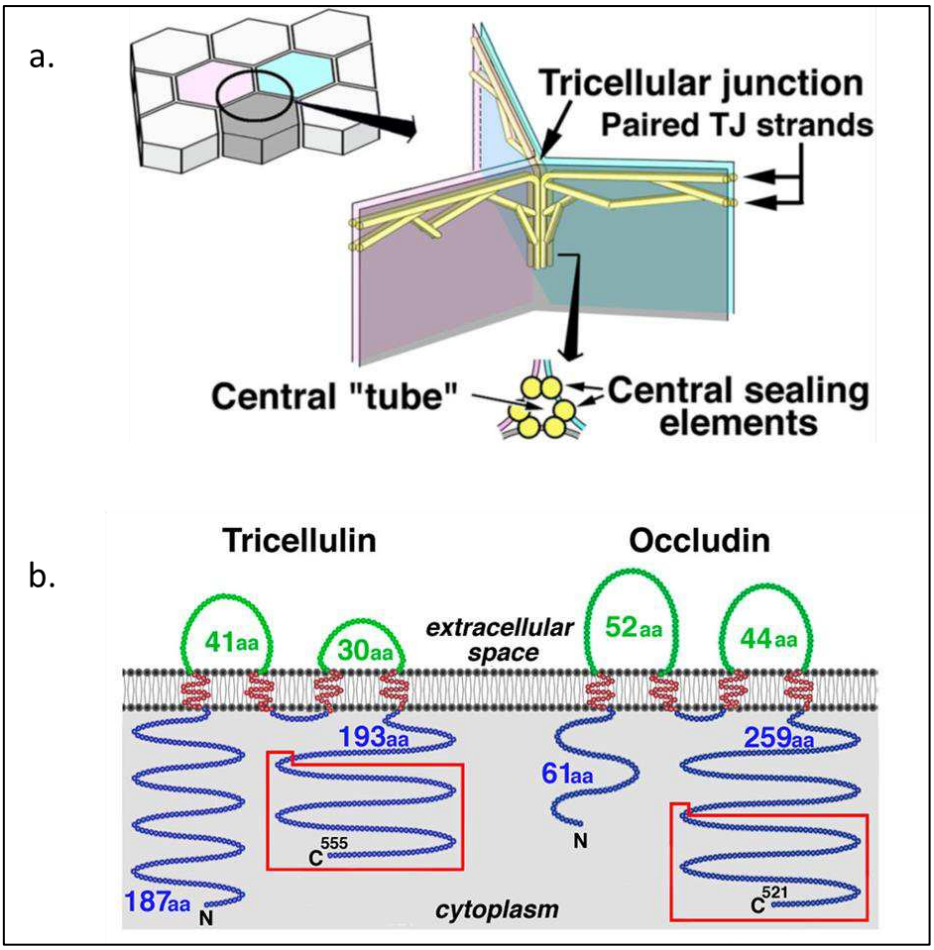

Figure 1.6: (A) Schematic drawing of the organization of tTJs. One tricellular contact (left drawing) is enlarged in the right drawing. (B). Structure and expression of mouse tricellulin. Adapted from Ikenouchi *et al* [34].

1.2.2 Function of the tight junction

Tight junctions are complexes of protein that contain cytoplasmic protein associated with transmembrane protein. These cytoplasmic proteins can have different roles to the tight junction.

When epithelial cells adhere one to the other, tight junction protein JAM and ZO-1 are present in high concentration. TJ proteins will interact with polarity complex [38]. Based on recent data [39], the interaction of polarity complex and TJ protein is crucial for the apical basal polarity and maturation of apical junction. The presences of apical and basal domains confer two roles to the tight junction: a gate and a fence function [40,41].

The regulation of the passage of ions and molecules across barrier tissues is determined by the opening of TJs. This action refers to the gate function of TJ and can be measured by the TER of barrier tissues. The value of TER results from the sum of the transcellular and paracellular resistance [4]. The transcellular resistance, which is defined by the resistance of the apical and basal membrane, remains stable. Therefore, the fluctuation of the TER value is due to a modification of the paracellular flux resulting from the opening of the tight junction.

The fence function corresponds to the ability of lipids to move within the membrane from the apical to the basal domain. The polarity of the membrane is maintained by this function and can be measured by the free diffusion of fluorescent lipids across the barrier [42].

Tight junction proteins are also involved in signaling event from and to the environment of the cell. Through its interaction with different kinase, occludin protein can induce the proliferation of cells [43-45]. Recent data also suggests that transition from epithelial to endothelial transition imply the targeting of TGF-β by occludin [46]. Other studies demonstrated that ZO-1 localizes in the nuclear region to regulate proliferation during maturation of cells by interacting with ZONAB [47]. Through this interaction, ZO-1 protein plays a role in signaling. Protein involved in TJ have also play a role in tumor genesis [48] membrane trafficking [49] and transcriptional regulation [50].

1.3 Importance of measuring barrier function

Measuring barrier tissue integrity is important as the degree of intactness can be an indicator for disease state [2,51] and also of the suitability of a particular *in vitro* model for use in toxicology and drug screening.

Pathogens have devised multiple mechanisms to destroy the integrity of the intestinal epithelial barrier, for example. The effect of individual pathogens/toxins on the intestinal epithelium has been well characterized: these pathogens disrupt barrier tissue in a variety of ways, such as by targeting tight junction proteins. Enteropathogenic and Enterohaemorrhagic E. coli are known to target occludin and ZO-1 respectively [52,53], while rotaviruses appear to disrupt the extracellular domains of tight junctions [54]. Once the barrier tissue is destroyed, the normal absorption of water in the intestine is severely compromised and diarrheal disease usually results [55]. In Europe, 5609 food-borne outbreaks were reported in 2007, affecting 39,727 (you can round to 39,700 or say “nearly 40,000”)people, resulting in 3921 (round) hospitalizations, and causing 19 deaths [56]. The global incidence of food-borne disease is difficult to estimate, but it was reported that in 2005 alone 1.8 million people died from diarrheal diseases. A great proportion of these cases can be attributed to contamination of food and drinking water. Additionally, diarrhea is a major cause of malnutrition in infants and young children [57]. The action

mechanism of toxins or pathogens targeting other barrier tissues are less well known, possibly because *in vitro* models are less well developed.

Thousands of new chemical products are tested every year to determine their organ toxicity following a long-term exposure to chemicals, their carcinogenic potential, toxicity to reproductive functions and to the developing fetus, and to their long-term toxicity to the aquatic environment. The uses of *in vitro* models based on barrier tissues are one of the first steps of toxicity tests. To induce toxicity, a chemical product should be able to cross the human epithelial barrier. Pharmaceutical industries, beside the toxicity aspect, want to know if the use of excipient modifies the barrier properties and if this modification is reversible or induce adverse effects.

1.4 Methods to assess barrier tissues integrity

Several methods exist to assess barrier tissue integrity. Many molecular biology techniques require chromophores or fluorophores. These methods require the realization of different steps, which increase the time and the cost of the experiment. They also require specific kits and sophisticated instruments to measure the read-out. Measurements of transepithelial resistance have been demonstrated to be an indicator of barrier tissue integrity. Since then, different methods have emerged to measure the TER or cell permeability. These include the use of transwell devices as a permeability assay for high throughput screening, which is extensively used in the pharmaceutical industry. Cells are seeded on a porous membrane, compounds are added upon confluency, and samples are subsequently harvested from the chamber below and analyzed by mass spectrometry. Permeability is often measured using radiolabeled compounds or molecules such as Lucifer yellow which are normally impermeable to barrier tissue, although the degree of permeability needs to be defined depending on the tissue type. For measuring TER there are a variety of tools available: traditionally TER has been measured using an epithelial voltohmmeter, which measures resistance across the cell monolayer. This technique, however, requires the use of a bulky probe which must be physically placed into a tissue culture plate and causes large scale disruptions to the cell layers. The CellZscope is an automated device for measuring the impedance of cell layers on permeable membranes (www.nanoanalytics.com), thus combining the ability to measure permeability and TER. New technology has evolved to allow the growth of epithelial cells directly on planar capacitors using the ECIS system (Electric Cell-substrate Impedance Sensing; Applied Biophysics). However, this system is rather costly, and the sensor heads are difficult to fabricate and require a very specific geometry to accommodate the electrodes.

1.4.1 Biological methods to assess barrier tissue integrity

1.4.1.1 Immunofluorescence

Immunofluorescence uses the specificity of antibodies to target a specific molecule by an antibodies/antigen reaction. This technique needs instruments such as a fluorescent microscope or a confocal microscope as the antibodies are coupled with fluorescent probes.

There are two types of immunofluorescence techniques, direct or indirect.

In the case of direct or primary immunofluorescence, a single antibody which is coupled with a fluorophore is used to target the protein of interest and label it. The advantage of using single antibodies is the reduction of the steps and background by decreasing the risk of cross reactivity or non-specificity. But since the number of fluorescent probe linked to the antibodies is limited, the signal is lower than in indirect techniques.

Secondary, or indirect, immunofluorescence uses two antibodies. The first antibody targets the molecule of interest while the second antibody which is coupled with the fluorophore targets the first antibody. As many secondary antibodies can recognize the primary antibody, the sensitivity of the signal is increased. This technique is more time consuming but offers more flexibility in the choice of antibody.

Limitations of immunofluorescence common with all techniques that use fluorescence are photobleaching and the fixation process. The former can be avoided by reducing the intensity and exposure time or by employing robust fluorophores such as AlexaFluor. For the latter, the used of fixative agent can induce a cross linking of cell proteins leading to non-specific bounding.

To avoid the use of antibodies, recombinant proteins can be a good alternative as they can also be used in living cells to follow, for example, trafficking proteins. Even if this technique seems to be elegant, they require transfection or transduction assays.

Beyond these constraints, the protocol should be adjusted for each type of experiment, as the fixative agent, the blocking step and the incubation temperature can have dramatic effects on the staining. Also, the use of monoclonal or polyclonal antibodies can affect the sensitivity of the binding.

1.4.1.2 Permeability assays

The permeability of a barrier reflects the ability of a molecule to pass across the barrier. This technique requires the use of radiolabeled or fluorescent compounds which are normally impermeable to the barrier. A barrier tissue is size and charge selective. As described above, claudins proteins are the major player in selective permeability. As each cell line express different claudin, the compound of interest should be chosen according to the cell line used.

Radioactive mannitol has been widely used in fundamental studies and pharmaceutical industry as it can diffuse across the intestinal epithelium with a specific rate according to the stomach segment [58]. The uses of radioactive labels require the specific equipment, room, and safety equipment to confine the radioactivity to one area. The safety procedures induce high cost and risks for laboratories, which now try to exclude technics based on radioactivity.

An alternative is to use of Dextran or polyethylene glycol, which can be available in different size depending on synthetic control. Thus, the permeability to different sizes can be tested with the same compound. They also offer a wide possibility of branching sites which allow different detection technique (colorimetric, fluorescence…) [59,60].

Another permeability marker commonly used is Lucifer Yellow. It was first used as an intracellular dye for nerve cells [61]. Later, this dye was used to test the permeability of barrier tissues, in particular for the Caco-2 cell line. This dye can be used to follow the differentiation of the monolayer forming barrier tissue as well as the effect of toxic compounds on the barrier tissue and the absorption of drugs.

1.4.2 Electronic methods to monitor cells

As biological techniques uses labels, the generation of artifact is possible. The emergence of electronic methods for live cell sensing permits the data acquisition of a wide variety of measurements. Furthermore, these techniques have the advantage of providing dynamic and real time measurements since they are label free and non-invasive.

Pharmaceutical companies could be the main entities interested in electronic methods as they need to test at the same time the ability of the drug to reach their target and the toxicity of the drug. For the moment they use permeability measurements which are cell line and molecule dependent, so different marker (size and charge) must be used to determine the toxicity and the efficiency of drug. The diagnostic industry also is also interested in the use of such techniques to detect pathogens. Monitoring cell health with electronic

methods has applications in food and water safety as well as medical diagnostic and environmental protection.

Integrity of epithelia has been assessed by the measurement of ion flow across epithelial tissue generally termed the transepithelial resistance (TER). As describe before in this chapter the ion flux across the epithelium is controlled by TJ and the tightness of these junctions depend of the proteins complex composition, particularly the claudins [62,63]. Steady-state ion flux via the paracellular pathway goes either through the pore pathway formed by transmembrane tight junction proteins, or via the non-pore pathway, postulated to be caused by dynamic breaking and resealing of tight junction strands [63]. The distinction between these pathways is often not considered. As permeability measurement use molecule that pass through the non-pore pathway, it cannot be used as an accurate measurement to assess the function of the pore pathway [64]. Electrical measurement will provide a direct assessment of ions flux by taking account of both pathway, and so an accurate method to assess barrier tissue integrity.

The first *in vitro* model for measuring electrical parameters of cells was based on using chambers (figure 1.7), where it was demonstrated that cell forming barrier tissue develop the same transport and permeability characteristics as *in vivo*. Later on, Cereijido and co-workers grew monolayers of cells on filters and placed it between two chambers (filled with the same electrolyte) and measured the electrical potential difference. They demonstrate that cells provide an electrical resistance known as Trans epithelial resistance (TER or TEER). The value is calculated as the inverse of the conductance, expressed in $\Omega.cm^2$ and was found to increase over time and settle, remaining stable for a few weeks [65]. Later on, Cereijido and co-workers grew monolayers of cells on filters and placed it between two chambers (filled with the same electrolyte) and measure the electrical potential difference. As researchers were interested in understanding what is influencing the variation of ions flux among different cell lines, different studies were performed. One of them lead to the development of a microelectrode array to study and measure electrical activity of cell culture *in vitro* [66].

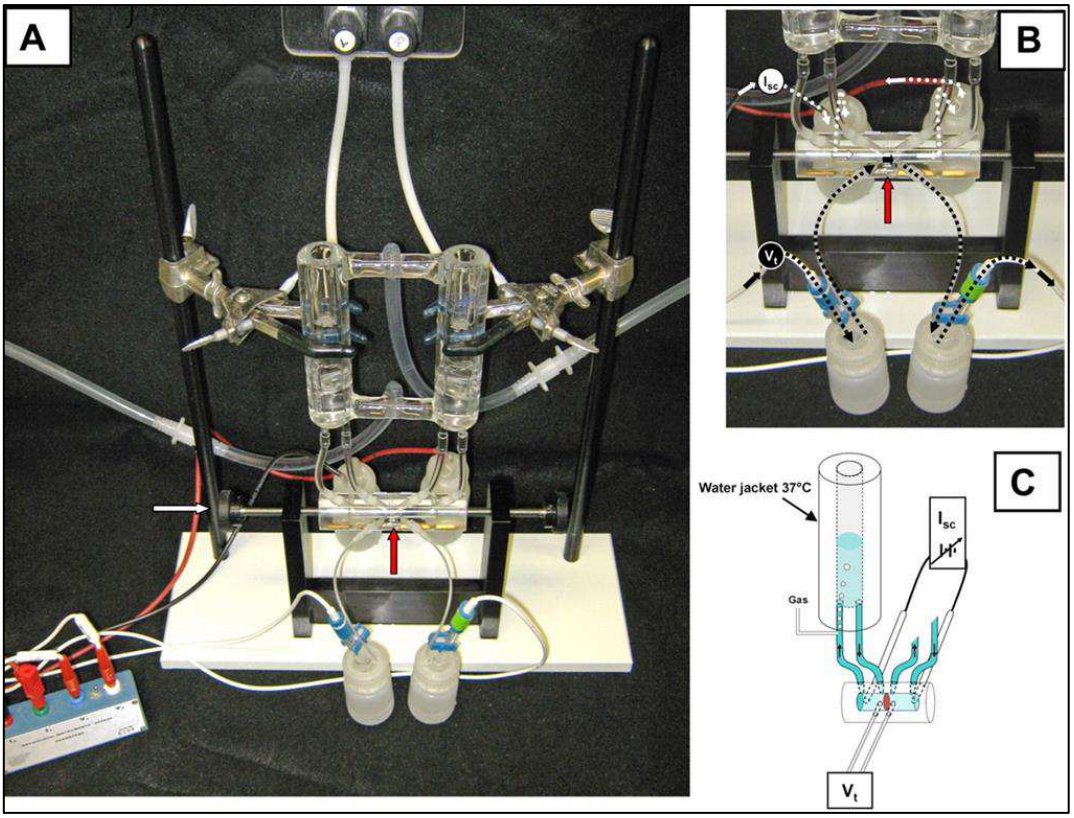

Figure 1.7: A classical Ussing chamber. A: assembled apparatus with water-jacketed reservoirs, Ussing chamber (intestinal preparation is mounted vertically; red arrow) secured by thumb wheel screws (white arrow), and electrodes attached to voltage clamp head stage. B: close-up view of voltage (Vt)-measuring and short-circuit current (Isc)-passing pathways. Calomel half-cell electrodes used for Vt measurements are connected by 3 M KCl salt bridges at each side of intestinal preparation (red arrow). Ag-AgCl electrodes used for Isc passing across the intestinal preparation are connected to the chamber by Krebs bicarbonate Ringer (KBR) salt bridges at each end of the chamber. C: schematic cut-away diagram of Vt and Isc circuits of the Ussing chamber. Short circuiting (Isc) is provided by an automatic voltage clamp (symbol). Note superfusion circulation of KBR is driven by gas lift using 95%O2-5% CO2. Intestinal preparation (red disc) separates the mucosal and serosal baths. From Clarke, L.L [67].

1.4.2.1 Impedance based monitoring of tissue/cells

The opposition that a circuit presents to an alternative current defines the electrical impedance. Electrical impedance is usually measured in a range of frequencies and corresponds to the ratio of voltage and current. This technique uses low voltage [68] and is, therefore, compatible with biological systems. The first device using this technology was monitoring cell attachment and spreading on a gold electrode [69]. This method, named electrical cell substrate impedance sensing (ECIS), serves as a new method to monitor arrays of cells *in vitro* (figure 1.8).

1.4.2.2 Electrical cell substrate impedance sensing

ECIS is now a commercially available product (www.biophysics.com) and has been used for applications such as kinetics of cell spreading [70] analysis of adherent cells after electroporation [71]. This system is composed of an interdigitated electrode, or two gold electrodes immersed in cell culture media. When cells are cultured on top of the working electrode, the flow is restricted and the impedance is modified. This technique has the advantage of monitoring the TER change in real time but is not compatible with cell culture insert.

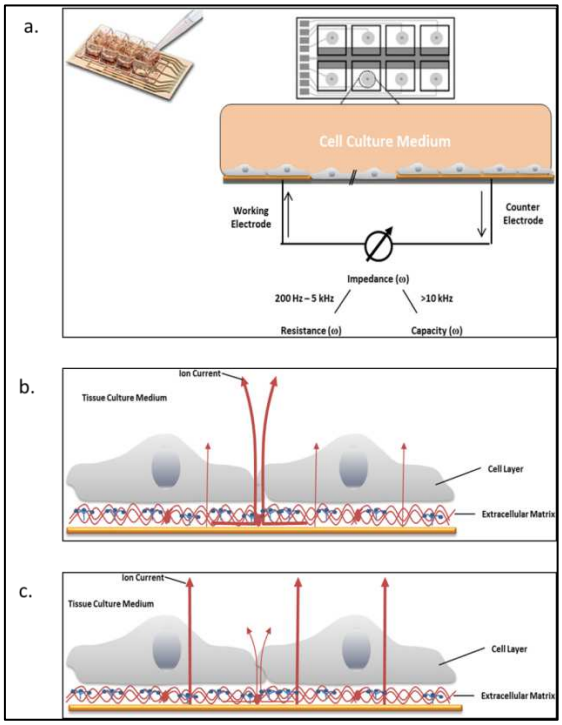

Figure 1.8: The ECIS system. a. Schematic drawing of an ECIS array and principle of the electric cell-substrate impedance sensing (ECIS) method. Cell layers are grown to confluence on integrated gold-film electrodes. An applied AC current flows between small working electrodes and the larger counter electrode using normal culture medium as an electrolyte. By a variation of the frequency ω, a spectrum can be obtained. Applying higher frequencies the current flow is dominated by the capacity of the total system, at mid-range frequencies the ohmic resistance of the total system is mirrored b. The current pathway at low frequencies on a cerebral endothelial cell monolayer (ECIS method, 400 Hz). At low frequencies the current predominantly flows paracellular (through extracellular matrix proteins) and between adjacent cells (through tight junctions) and the electrolyte (medium), see bold arrows. c. By applying high frequencies (ECIS method, > 40 kHz), the capacitive amount of measured impedance is especially sensitive for adhered cells. The current passes through the insulating cell monolayer, especially through cell membranes. Adapted from Benson *et al*, 2013 [72].

1.4.2.3 Non planar electrodes

A number of different cell lines need to be cultured in cell culture insert to become differentiated. Indeed, some cells line need to be fed by the basal and apical side to become polarized and exhibit a fully differentiation. This cells lines are often use for transport assays. The integrity prior and during experiment is measured by the electrical properties of the cell monolayer. The development of chopstick electrodes allows measurement the resistance across the monolayer based on the current recorded between electrodes. However, studies demonstrate that the use of DC current can damage cell layers [73,74].

To avoid this problem, the EVOM setup (Epithelial Voltohmmeter; world precision instruments) was developed (Figure 1.9). It can measure the resistance of a cell layer at low frequency with a square current pulse. However, this setup still presents disadvantages. The main issue is that the measurement is operator dependent, and, depending on where the electrodes are placed, the TER values significantly fluctuate. Also, the measurements are carried out outside the incubator which leads to a perturbation of physiologic parameters and thus to a variation of TER values. Despite this drawback, the EVOM system was used in several studies, from basic research to the effect of pathogenic organisms infecting cell layers [75-79]. Based on the same technology, an automated system was developed to allow the measurement on 24 and 96 well plates. To improve the EVOM system, industry developed the Endohm system in which the electrodes are circular, to improve measurement heterogeneity.

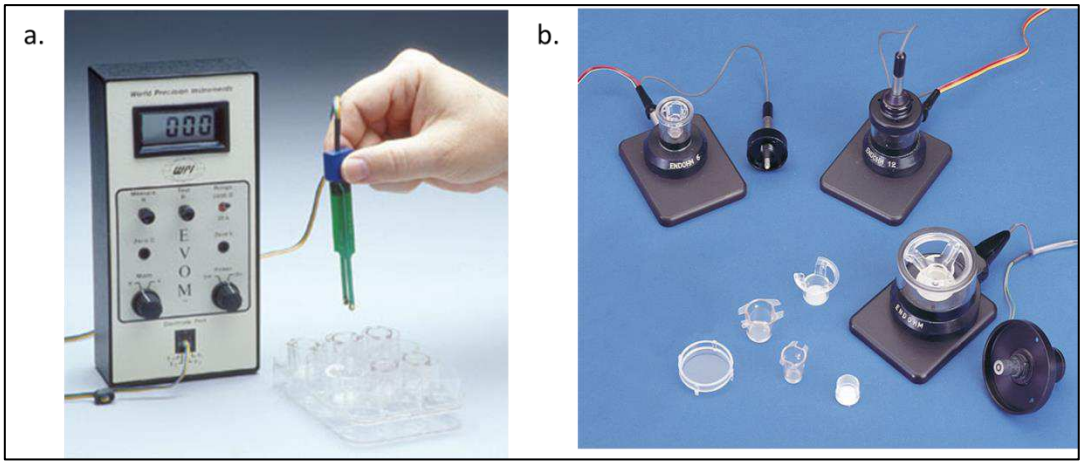

Figure 1.9: Hand voltometers. a. EVOM device; b. Endohm system. Adapted from wpiinc.com.

In 2004, Wegener *et al.* [80] developed a new device which solves two of the main problems of the devices presented above, maintaining physiological conditions by measuring the TER in an incubator, and homogenous results by using round fix electrodes. This device is named the CellZscope and is commercially available (NanoAnalytics GmbH) (figure 1.10). The experiment is controlled with a PC interface and the electrical measurements are performed

with a data acquisition board. 6 to 24 well formats can be used; each filter can be controlled individually. The cell culture insert is placed between two electrodes. The bottom electrode is common for all wells, while the top one is small and dipped in each well. A small AC current is applied between the two electrodes; the impedance frequency on a range from 1 to 105 Hz is recorded. The TER and the capacitance are extracted from an equivalent circuit model. The capacitance is also an important parameter as it can be indicative of membrane folding, an increase in capacitance reflects more folding or ruffling of the membrane [81]. The equivalent circuit and the model used allow the extraction of the resistance due to the filter and/or media, as the addition of compound or the change of media can induce variation of the TER result. To permit the comparison of the result with other techniques and experiments, the device gives the result of TER as $\Omega.cm^2$.

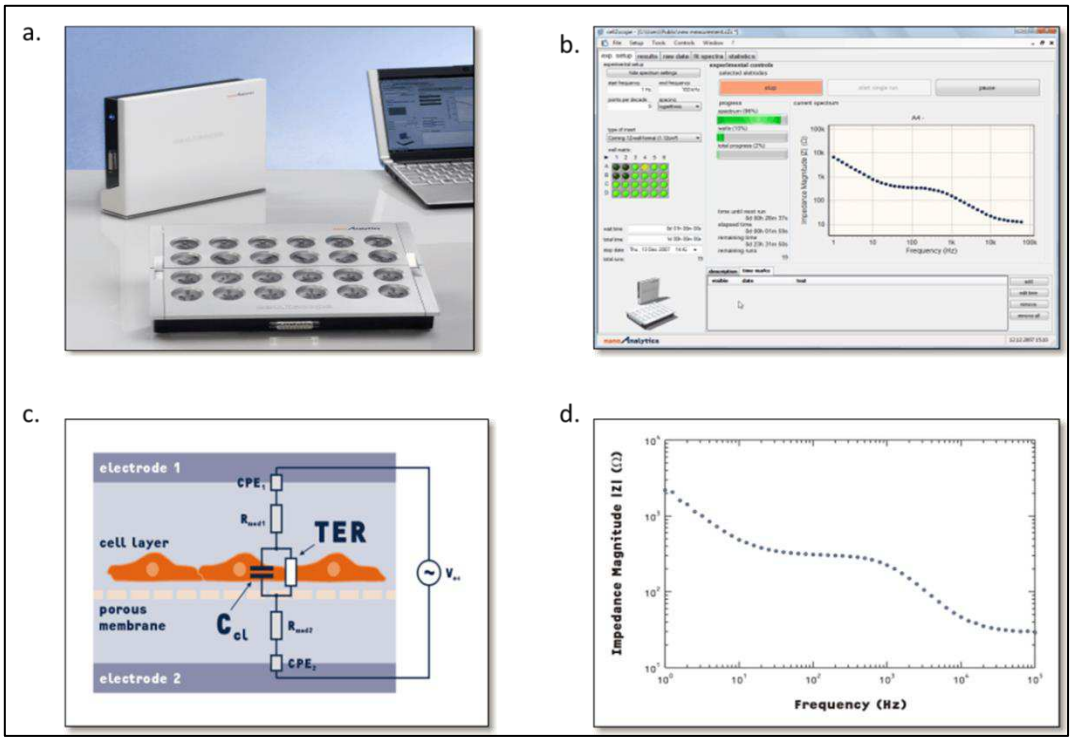

Figure 1.10: The CellZscope a. Overview of CellZscope device, b. Overview of CellZscope data acquisition window, c. Equivalent circuit for epithelial cell layer grown on porous filter, d. Typical Impedance frequency scan. Adapted from technical bulletin, Nanoanalytics.com.

The ECIS system cannot be used with cell culture insert, because cells must be grown directly on top of the electrodes. To overcome this disadvantage, Sun et al [82] developed transwell filters that are enclosed in a polycarbonate holder and separated from the gold plated dot ring electrode by an insulating epoxy layer (figure 1.11). The electrode are fabricated by electrochemical deposition of a conducting polymer (polypyrrole doped with polystyrene sulfonate (Ppy: PSS)) on the gold plated electrodes. This deposition was realized to solve the effect of the electrical double layer, which usually

appear at the interface between the surface and an ionic fluid. This layer corresponds to the formation of a first layer of ion adsorbed onto the surface and a second layer composed of ion attracted to the first charge layer. The deposition of this conducting layer increases the sensitivity of the measurement at low frequency, which is known to be dominated by the paracellular resistance. The model used to extract TER is very similar to the one used for the CellZscope. The differences reside in the epithelial cells impedance; they shown that the electrical field which enters in the cell layer has a longitudinal and orthogonal component. The impedance was therefore divided in two parts. They also demonstrate that the Ppy electrode have an impedance lower than gold electrode by one order in magnitude. To validate this method, they authors used Triton X 100 and the calcium chelator EGTA (ethylene glycol-bis(2-aminoethyl-ether)-N, N, N', N',-tetraacetic acid) to induce a destruction of a barrier tissue.

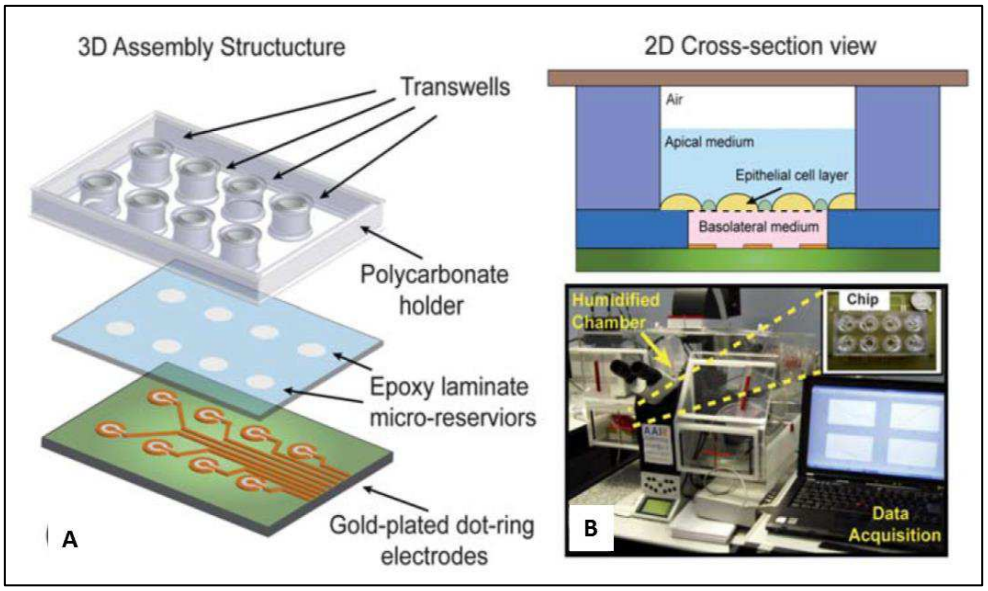

Figure 1.11: Conducting polymer coated electrodes for impedance scanning. A. Diagram shows the 3D assembly structure and 2D cross-section view of the bio-impedance chip. B. Image showing the experimental system instrumentation. From Sun *et al* [82].

1.4.2.4 Organic electronic at the interface with biology

Organic electronics refers to devices using carbon based polymers and small molecules as the electrically active component. Organic electronics offer a number of unique advantages including their ease of processing, ionic and electronic conductivity, and their flexible mechanical properties. The soft nature of these materials and their compatibility with soft substrates makes them ideal for flexible displays and solid state lighting, and also for interfacing with biological systems.

Organic bioelectronics, first named by Berggren and Richter-Dahlfors [83], couple device based on organic semiconductors with biological elements. This coupling is bi-directional: a signal from a biological event can be transduce to the electronic device or the device can stimulate a biological element to induce a reaction or an event into this biological element (figure 1.12).

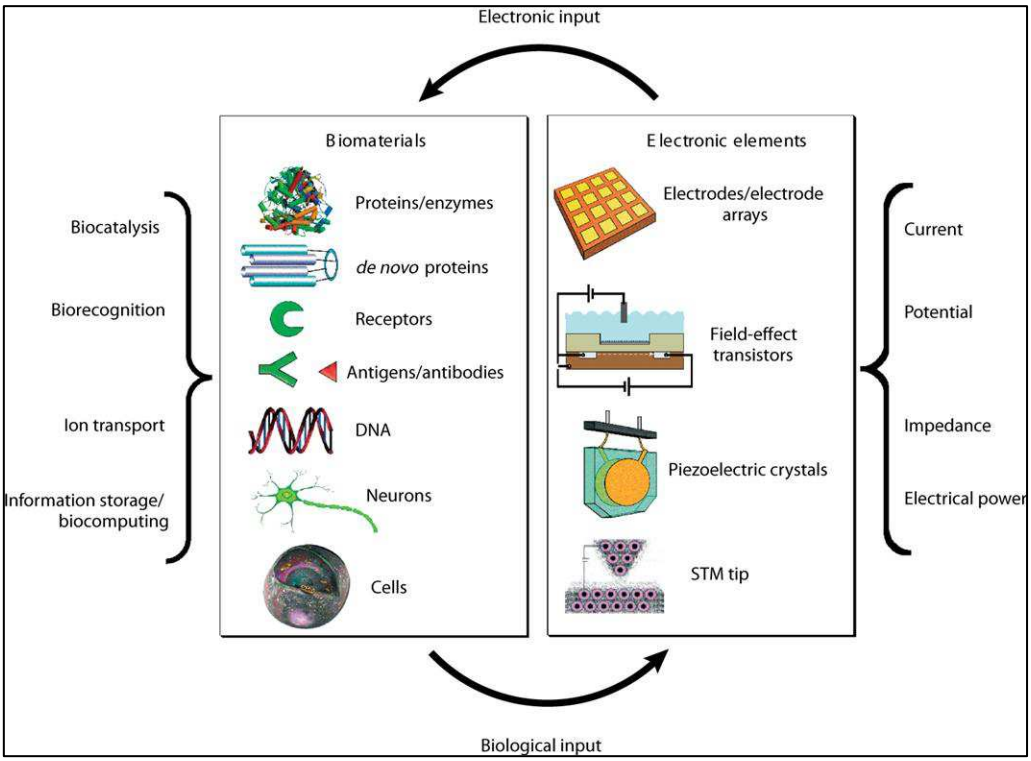

Figure 1.12: Integrated systems of biomaterials and electronic elements for bioelectronics applications. From Itamar Willner and Eugenii Katz, 2005

A numbers of biological elements are capable of recognition, including enzymes, oligonucleotide and DNA. Coupling these elements with electronic device to build biosensors has been of great interest. The major challenge with this type of sensor is the optimization of the information transfer between the two parts of the device. The information sent by the biomaterial should be translated to the recognition element such that the output signal could be differentiated from the background signal. Glucose sensors were developed in 1960 to monitor glucose level in blood diabetic patents. As OECT provide an inherent amplification, detection of glucose in human saliva can be achieve using an all polymer sensor [84]. Using the same approach, OECTs were integrated with microfluidic to detect multi-analytes [85]. Another type of transistor (organic field effect transistor) was developed with microfluidic to sense in aqueous solution without recognition elements [86]. In this device, detection of glucose is attributed to an interaction of the glucose with the conducting polymer.

Organic electronic materials can also be used to control biological elements. Investigation of the influence of the redox state of conducting

polymers on cells proliferation and differentiation was the first application [87]. Applications in the biomedical field come out with the functionalization of conducting polymer with biomolecules [88] [89]. Further, Wan et al, developed a device in which a redox gradient is patterned [90]; this gradient is critical to understanding cellular mechanisms in normal and pathologic tissues; similar work was also done by Berggen *et al.* [91]. To move toward more relevant cell-cell interactions, a 3D scaffold was developed; nanofibers coated with conductive polymer were used to induce calcium signaling on nerve cells [92]. Finally, to control release of biomolecules, organic electronic ion pumps were develop for *in vitro* [93] and *in vivo* [94] used.

In the last area, organic electronic can stimulate biological structure and in return sense or record a response to the stimulus. This field focuses on developing tools for neuroscience. The soft conducting polymer offer great opportunities to replace silicon based probes or electrodes. The first advances in this field demonstrate higher performance of these new electrodes compared to the state of the art devices [95]. These improvement were combined with hydrogels and then biomolecules were incorporated [96-98]. The combination of conducting polymers, biomolecules and hydrogel improve the biocompatibility of the device and also permit the exploration of electrical stimulation. Based on this work, microelectrodes were used as sensors of neurotransmitter release [99]. Evolution of this work and advantages of the conducting polymers device were discussed in a review by Kim *et al.* [88]. Electrodes were then fabricated in a network to create microelectrodes arrays (MEA). The first generation of these MEA were too thick and would limit their conformability [100]. Recently, a new way of fabrication demonstrated the use of dense arrays of electrode for *in vivo* recording [101]. These polymers electrodes were shown to have better performance than gold electrodes.

1.4.2.5 Transistor to measure barrier tissue integrity

Impedance spectroscopy provides significant contributions in the field of measurement of capacitance and resistance of a cell layer. This technique is more automated and reproducible than other technique but still presents limitation in temporal resolution and sensitivity as well as cost. Transistors provide a good alternative to conventional electrodes for *in vitro* and *in vivo* monitoring of cells. Organic electrochemical transistors (OECT) have been recently introduced for biomedical applications. Unlike field effect transistors and inorganic transistors, the electrolyte plays an important role in the device operating mechanism. OECT based on the conducting polymer PEDOT: PSS (poly(3,4-ethylenedioxythiophene)-poly(styrenesulfonate) were shown to be stable in media in physiological condition [102-104].Organic materials are compatible with roll to roll, large scale processing for low cost processing of disposable devices. The key advantage of OECT is that it converts ionic signals

to electronic signal efficiently and can operate at low voltage which is fully compatible with biological environments.

The first study based on this technology was the observation of cells detachment upon treatment with trypsin on a cell layer [104]. Authors determined that the change detected by the OECT was due to an electrostatic effect, whereas it is instead an effect of ion penetrating the conducting polymer [105].

Previously, bilayer lipid membrane were used to control the gating of an OECT [106]. When an intact bilayer lipid membrane was placed on top of an OECT, the gating was suppressed. Whereas, the addition of ion channel into the bilayer lipid membrane restore the gating. This work demonstrates that OECT can be used as biosensors as they convert ion to electron and that movement of ions across a membrane can be detected by an OECT. In this project, we use this property to create a new device to detect pathogens. Gastrointestinal cells will be grown as monolayer in cell culture insert to form an epithelial barrier and integrated with an OECT.

1.5 References

1. Anderson, J.M.; Van Itallie, C.M., Physiology and function of the tight junction. *Cold Spring Harb Perspect Biol* **2009**, *1*, a002584.

2. Balkovetz, D.F.; Katz, J., Bacterial invasion by a paracellular route: Divide and conquer. *Microbes and infection / Institut Pasteur* **2003**, *5*, 613-619.

3. Schneeberger-Keeley, E.E.; Karnovsky, M.J., The ultrastructural basis of alveolar-capillary membrane permeability to peroxidase used as a tracer. *The Journal of cell biology* **1968**, *37*, 781-793.

4. Forster, C., Tight junctions and the modulation of barrier function in disease. *Histochemistry and cell biology* **2008**, *130*, 55-70.

5. Furuse, M., Molecular basis of the core structure of tight junctions. *Cold Spring Harb Perspect Biol* **2010**, *2*.

6. Li, N.; Lewis, P.; Samuelson, D.; Liboni, K.; Neu, J., Glutamine regulates caco-2 cell tight junction proteins. *American journal of physiology. Gastrointestinal and liver physiology* **2004**, *287*, G726-733.

7. Gonzalez-Mariscal, L.; Betanzos, A.; Nava, P.; Jaramillo, B.E., Tight junction proteins. *Progress in biophysics and molecular biology* **2003**, *81*, 1-44.

8. Schneeberger, E.E.; Lynch, R.D., The tight junction: A multifunctional complex. *American journal of physiology. Cell physiology* **2004**, *286*, C1213-1228.

9. Furuse, M.; Hirase, T.; Itoh, M.; Nagafuchi, A.; Yonemura, S.; Tsukita, S., Occludin - a novel integral membrane-protein localizing at tight junctions. *Journal of Cell Biology* **1993**, *123*, 1777-1788.

10. Anderson, J.M.; Van Itallie, C.M., Tight junctions and the molecular basis for regulation of paracellular permeability. *The American journal of physiology* **1995**, *269*, G467-475.

11. Wittchen, E.S.; Haskins, J.; Stevenson, B.R., Protein interactions at the tight junction. Actin has multiple binding partners, and zo-1 forms independent complexes with zo-2 and zo-3. *The Journal of biological chemistry* **1999**, *274*, 35179-35185.

12. Furuse, M.; Itoh, M.; Hirase, T.; Nagafuchi, A.; Yonemura, S.; Tsukita, S., Direct association of occludin with zo-1 and its possible involvement in the localization of occludin at tight junctions. *The Journal of cell biology* **1994**, *127*, 1617-1626.

13. Van Itallie, C.M.; Anderson, J.M., Occludin confers adhesiveness when expressed in fibroblasts. *Journal of cell science* **1997**, *110 (Pt 9)*, 1113-1121.

14. Balda, M.S.; Whitney, J.A.; Flores, C.; Gonzalez, S.; Cereijido, M.; Matter, K., Functional dissociation of paracellular permeability and transepithelial electrical resistance and disruption of the apical-basolateral intramembrane diffusion barrier by expression of a mutant tight junction membrane protein. *The Journal of cell biology* **1996**, *134*, 1031-1049.

15. Saitou, M.; Furuse, M.; Sasaki, H.; Schulzke, J.D.; Fromm, M.; Takano, H.; Noda, T.; Tsukita, S., Complex phenotype of mice lacking occludin, a component of tight junction strands. *Molecular biology of the cell* **2000**, *11*, 4131-4142.

16. Knipp, G.T.; Ho, N.F.H.; Barsuhn, C.L.; Borchardt, R.T., Paracellular diffusion in caco-2 cell monolayers: Effect of perturbation on the transport of hydrophilic compounds that vary in charge and size. *Journal of pharmaceutical sciences* **1997**, *86*, 1105-1110.

17. Li, J.; Angelow, S.; Linge, A.; Zhuo, M.; Yu, A.S., Claudin-2 pore function requires an intramolecular disulfide bond between two conserved extracellular cysteines. *American journal of physiology. Cell physiology* **2013**, *305*, C190-196.

18. Furuse, M.; Fujita, K.; Hiiragi, T.; Fujimoto, K.; Tsukita, S., Claudin-1 and -2: Novel integral membrane proteins localizing at tight junctions with no sequence similarity to occludin. *The Journal of cell biology* **1998**, *141*, 1539-1550.

19. Furuse, M.; Sasaki, H.; Fujimoto, K.; Tsukita, S., A single gene product, claudin-1 or -2, reconstitutes tight junction strands and recruits occludin in fibroblasts. *The Journal of cell biology* **1998**, *143*, 391-401.

20. Furuse, M.; Hata, M.; Furuse, K.; Yoshida, Y.; Haratake, A.; Sugitani, Y.; Noda, T.; Kubo, A.; Tsukita, S., Claudin-based tight junctions are crucial for the mammalian epidermal barrier: A lesson from claudin-1-deficient mice. *The Journal of cell biology* **2002**, *156*, 1099-1111.

21. Furuse, M.; Sasaki, H.; Tsukita, S., Manner of interaction of heterogeneous claudin species within and between tight junction strands. *The Journal of cell biology* **1999**, *147*, 891-903.

22. Furuse, M.; Furuse, K.; Sasaki, H.; Tsukita, S., Conversion of zonulae occludentes from tight to leaky strand type by introducing claudin-2 into madin-darby canine kidney i cells. *The Journal of cell biology* **2001**, *153*, 263-272.

23. Martin-Padura, I.; Lostaglio, S.; Schneemann, M.; Williams, L.; Romano, M.; Fruscella, P.; Panzeri, C.; Stoppacciaro, A.; Ruco, L.; Villa, A., *et al.*, Junctional adhesion molecule, a novel member of the immunoglobulin superfamily that distributes at intercellular junctions and modulates monocyte transmigration. *The Journal of cell biology* **1998**, *142*, 117-127.

24. Itoh, M.; Sasaki, H.; Furuse, M.; Ozaki, H.; Kita, T.; Tsukita, S., Junctional adhesion molecule (jam) binds to par-3: A possible mechanism for the recruitment of par-3 to tight junctions. *The Journal of cell biology* **2001**, *154*, 491-497.

25. Tsukita, S.; Furuse, M., [identification of two distinct types of four-transmembrane domain proteins, occludin and claudins: Towards new physiology in paracellular pathway]. *Seikagaku. The Journal of Japanese Biochemical Society* **2000**, *72*, 155-162.

26. Tsukita, S.; Furuse, M.; Itoh, M., Multifunctional strands in tight junctions. *Nature reviews. Molecular cell biology* **2001**, *2*, 285-293.

27. Stevenson, B.R.; Siliciano, J.D.; Mooseker, M.S.; Goodenough, D.A., Identification of zo-1: A high molecular weight polypeptide associated with the tight junction (zonula occludens) in a variety of epithelia. *The Journal of cell biology* **1986**, *103*, 755-766.

28. Haskins, J.; Gu, L.; Wittchen, E.S.; Hibbard, J.; Stevenson, B.R., Zo-3, a novel member of the maguk protein family found at the tight junction, interacts with zo-1 and occludin. *The Journal of cell biology* **1998**, *141*, 199-208.

29. Jesaitis, L.A.; Goodenough, D.A., Molecular characterization and tissue distribution of zo-2, a tight junction protein homologous to zo-1 and the drosophila discs-large tumor suppressor protein. *The Journal of cell biology* **1994**, *124*, 949-961.

30. Kosińska, A.; Andlauer, W., Modulation of tight junction integrity by food components. *Food Research International* **2013**.

31. Itoh, M.; Furuse, M.; Morita, K.; Kubota, K.; Saitou, M.; Tsukita, S., Direct binding of three tight junction-associated maguks, zo-1, zo-2 and zo-3, with the cooh termini of claudins. *Journal of Cell Biology* **1999**, *147*, 1351-1363.

32. Ebnet, K.; Schulz, C.U.; Meyer Zu Brickwedde, M.K.; Pendl, G.G.; Vestweber, D., Junctional adhesion molecule interacts with the pdz domain-containing proteins af-6 and zo-1. *The Journal of biological chemistry* **2000**, *275*, 27979-27988.

33. Anderson, J.M.; Van Itallie, C.M., Tight junctions: Closing in on the seal. *Current biology : CB* **1999**, *9*, R922-924.

34. Ikenouchi, J.; Furuse, M.; Furuse, K.; Sasaki, H.; Tsukita, S., Tricellulin constitutes a novel barrier at tricellular contacts of epithelial cells. *The Journal of cell biology* **2005**, *171*, 939-945.

35. Raleigh, D.R.; Marchiando, A.M.; Zhang, Y.; Shen, L.; Sasaki, H.; Wang, Y.; Long, M.; Turner, J.R., Tight junction-associated marvel proteins

marveld3, tricellulin, and occludin have distinct but overlapping functions. *Molecular biology of the cell* **2010**, *21*, 1200-1213.

36. Riazuddin, S.; Ahmed, Z.M.; Fanning, A.S.; Lagziel, A.; Kitajiri, S.; Ramzan, K.; Khan, S.N.; Chattaraj, P.; Friedman, P.L.; Anderson, J.M., *et al.*, Tricellulin is a tight-junction protein necessary for hearing. *American journal of human genetics* **2006**, *79*, 1040-1051.

37. Krug, S.M.; Amasheh, S.; Richter, J.F.; Milatz, S.; Gunzel, D.; Westphal, J.K.; Huber, O.; Schulzke, J.D.; Fromm, M., Tricellulin forms a barrier to macromolecules in tricellular tight junctions without affecting ion permeability. *Molecular biology of the cell* **2009**, *20*, 3713-3724.

38. Shin, K.; Fogg, V.C.; Margolis, B., Tight junctions and cell polarity. *Annual review of cell and developmental biology* **2006**, *22*, 207-235.

39. Ivanov, A.I.; Young, C.; Den Beste, K.; Capaldo, C.T.; Humbert, P.O.; Brennwald, P.; Parkos, C.A.; Nusrat, A., Tumor suppressor scribble regulates assembly of tight junctions in the intestinal epithelium. *The American journal of pathology* **2010**, *176*, 134-145.

40. Balda, M.S.; Matter, K., The tight junction protein zo-1 and an interacting transcription factor regulate erbb-2 expression. *The EMBO journal* **2000**, *19*, 2024-2033.

41. Anderson, J.M., Molecular structure of tight junctions and their role in epithelial transport. *News in physiological sciences : an international journal of physiology produced jointly by the International Union of Physiological Sciences and the American Physiological Society* **2001**, *16*, 126-130.

42. Vanmeer, G.; Simons, K., The function of tight junctions in maintaining differences in lipid-composition between the apical and the basolateral cell-surface domains of mdck cells. *Embo Journal* **1986**, *5*, 1455-1464.

43. Li, D.; Mrsny, R.J., Oncogenic raf-1 disrupts epithelial tight junctions via downregulation of occludin. *The Journal of cell biology* **2000**, *148*, 791-800.

44. Wang, W.; Jobbagy, Z.; Bird, T.H.; Eiden, M.V.; Anderson, W.B., Cell signaling through the protein kinases camp-dependent protein kinase, protein kinase cepsilon, and raf-1 regulates amphotropic murine leukemia virus envelope protein-induced syncytium formation. *The Journal of biological chemistry* **2005**, *280*, 16772-16783.

45. Aijaz, S.; D'Atri, F.; Citi, S.; Balda, M.S.; Matter, K., Binding of gef-h1 to the tight junction-associated adaptor cingulin results in inhibition of rho signaling and g1/s phase transition. *Developmental cell* **2005**, *8*, 777-786.

46. Barrios-Rodiles, M.; Brown, K.R.; Ozdamar, B.; Bose, R.; Liu, Z.; Donovan, R.S.; Shinjo, F.; Liu, Y.; Dembowy, J.; Taylor, I.W., *et al.*, High-

throughput mapping of a dynamic signaling network in mammalian cells. *Science* **2005**, *307*, 1621-1625.

47. Balda, M.S.; Matter, K., Tight junctions and the regulation of gene expression. *Biochimica Et Biophysica Acta-Biomembranes* **2009**, *1788*, 761-767.

48. Subauste, M.C.; Nalbant, P.; Adamson, E.D.; Hahn, K.M., Vinculin controls pten protein level by maintaining the interaction of the adherens junction protein beta-catenin with the scaffolding protein magi-2. *The Journal of biological chemistry* **2005**, *280*, 5676-5681.

49. Mostov, K.E.; Verges, M.; Altschuler, Y., Membrane traffic in polarized epithelial cells. *Current opinion in cell biology* **2000**, *12*, 483-490.

50. Guillemot, L.; Hammar, E.; Kaister, C.; Ritz, J.; Caille, D.; Jond, L.; Bauer, C.; Meda, P.; Citi, S., Disruption of the cingulin gene does not prevent tight junction formation but alters gene expression. *Journal of cell science* **2004**, *117*, 5245-5256.

51. Larre, I.; Lazaro, A.; Contreras, R.G.; Balda, M.S.; Matter, K.; Flores-Maldonado, C.; Ponce, A.; Flores-Benitez, D.; Rincon-Heredia, R.; Padilla-Benavides, T.*, et al.*, Ouabain modulates epithelial cell tight junction. *Proceedings of the National Academy of Sciences of the United States of America* **2010**, *107*, 11387-11392.

52. Dean, P.; Kenny, B., Intestinal barrier dysfunction by enteropathogenic escherichia coli is mediated by two effector molecules and a bacterial surface protein. *Molecular microbiology* **2004**, *54*, 665-675.

53. Hecht, G.; Pothoulakis, C.; LaMont, J.T.; Madara, J.L., Clostridium difficile toxin a perturbs cytoskeletal structure and tight junction permeability of cultured human intestinal epithelial monolayers. *The Journal of clinical investigation* **1988**, *82*, 1516-1524.

54. Maes, R.K.; Grooms, D.L.; Wise, A.G.; Han, C.; Ciesicki, V.; Hanson, L.; Vickers, M.L.; Kanitz, C.; Holland, R., Evaluation of a human group a rotavirus assay for on-site detection of bovine rotavirus. *Journal of clinical microbiology* **2003**, *41*, 290-294.

55. Sears, C.L., Molecular physiology and pathophysiology of tight junctions v. Assault of the tight junction by enteric pathogens. *American journal of physiology. Gastrointestinal and liver physiology* **2000**, *279*, G1129-1134.

56. The community summary report on food-borne outbreaks in the european union in 2007. *The EFSA Journal* **2009**, *271*.

57. Fact sheet no. 237. *WHO* **2007**, *march*.

58. Krugliak, P.; Hollander, D.; Schlaepfer, C.C.; Nguyen, H.; Ma, T.Y., Mechanisms and sites of mannitol permeability of small and large intestine in the rat. *Digestive diseases and sciences* **1994**, *39*, 796-801.

59. Lambert, D.; O'Neill, C.A.; Padfield, P.J., Depletion of caco-2 cell cholesterol disrupts barrier function by altering the detergent solubility and distribution of specific tight-junction proteins. *Biochemical Journal* **2005**, *387*, 553-560.

60. Van Itallie, C.M.; Holmes, J.; Bridges, A.; Gookin, J.L.; Coccaro, M.R.; Proctor, W.; Colegio, O.R.; Anderson, J.M., The density of small tight junction pores varies among cell types and is increased by expression of claudin-2. *Journal of cell science* **2008**, *121*, 298-305.

61. Racowsky, C.; Satterlie, R.A., Metabolic, fluorescent dye and electrical coupling between hamster oocytes and cumulus cells during meiotic maturation in vivo and in vitro. *Developmental biology* **1985**, *108*, 191-202.

62. Krug, S.M.; Gunzel, D.; Conrad, M.P.; Lee, I.F.M.; Amasheh, S.; Fromm, M.; Yu, A.S.L., Charge-selective claudin channels. *Barriers and Channels Formed by Tight Junction Proteins I* **2012**, *1257*, 20-28.

63. Gunzel, D.; Yu, A.S., Claudins and the modulation of tight junction permeability. *Physiological reviews* **2013**, *93*, 525-569.

64. Van Itallie, C.M.; Anderson, J.M., Molecular structure and regulation of tight junctions. *Gastrointestinal Transport* **2001**, *50*, 163-186.

65. Cereijido, M.; Robbins, E.S.; Dolan, W.J.; Rotunno, C.A.; Sabatini, D.D., Polarized monolayers formed by epithelial cells on a permeable and translucent support. *The Journal of cell biology* **1978**, *77*, 853-880.

66. Thomas, C.A., Jr.; Springer, P.A.; Loeb, G.E.; Berwald-Netter, Y.; Okun, L.M., A miniature microelectrode array to monitor the bioelectric activity of cultured cells. *Experimental cell research* **1972**, *74*, 61-66.

67. Clarke, L.L., A guide to ussing chamber studies of mouse intestine. *Am J Physiol-Gastr L* **2009**, *296*, G1151-G1166.

68. Alexander, F.; Price, D.; Bhansali, S., From cellular cultures to cellular spheroids: Is impedance spectroscopy a viable tool for monitoring multicellular spheroid (mcs) drug models? *IEEE reviews in biomedical engineering* **2012**.

69. Giaever, I.; Keese, C.R., A morphological biosensor for mammalian cells. *Nature* **1993**, *366*, 591-592.

70. Wegener, J.; Keese, C.R.; Giaever, I., Electric cell-substrate impedance sensing (ecis) as a noninvasive means to monitor the kinetics of cell spreading to artificial surfaces. *Exp Cell Res* **2000**, *259*, 158-166.

71. Stolwijk, J.A.; Hartmann, C.; Balani, P.; Albermann, S.; Keese, C.R.; Giaever, I.; Wegener, J., Impedance analysis of adherent cells after in situ electroporation: Non-invasive monitoring during intracellular manipulations. *Biosensors and Bioelectronics* **2011**, *26*, 4720-4727.

72. Benson, K.; Cramer, S.; Galla, H.-J., Impedance-based cell monitoring: Barrier properties and beyond. *Fluids and Barriers of the CNS* **2013**, *10*, 5.

73. McCaig, C.D.; Rajnicek, A.M.; Song, B.; Zhao, M., Controlling cell behavior electrically: Current views and future potential. *Physiological reviews* **2005**, *85*, 943-978.

74. Bernards, D.A.; Malliaras, G.G.; Toombes, G.E.S.; Gruner, S.M., Gating of an organic transistor through a bilayer lipid membrane with ion channels. *Appl Phys Lett* **2006**, *89*, -.

75. Boyle, E.C.; Brown, N.F.; Finlay, B.B., Salmonella enterica serovar typhimurium effectors sopb, sope, sope2 and sipa disrupt tight junction structure and function. *Cellular microbiology* **2006**, *8*, 1946-1957.

76. Ma, T.Y.; Nguyen, D.; Bui, V.; Nguyen, H.; Hoa, N., Ethanol modulation of intestinal epithelial tight junction barrier. *The American journal of physiology* **1999**, *276*, G965-974.

77. McLaughlin, J.; Padfield, P.J.; Burt, J.P.H.; O'Neill, C.A., Ochratoxin a increases permeability through tight junctions by removal of specific claudin isoforms. *American Journal of Physiology - Cell Physiology* **2004**, *287*, C1412-C1417.

78. Prozialeck, W.C.; Edwards, J.R.; Lamar, P.C.; Smith, C.S., Epithelial barrier characteristics and expression of cell adhesion molecules in proximal tubule-derived cell lines commonly used for in vitro toxicity studies. *Toxicology in Vitro* **2006**, *20*, 942-953.

79. Van Itallie, C.M.; Fanning, A.S.; Holmes, J.; Anderson, J.M., Occludin is required for cytokine-induced regulation of tight junction barriers. *Journal of cell science* **2010**, *123*, 2844-2852.

80. Wegener, J.; Abrams, D.; Willenbrink, W.; Galla, H.J.; Janshoff, A., Automated multi-well device to measure transepithelial electrical resistances under physiological conditions. *BioTechniques* **2004**, *37*, 590, 592-594, 596-597.

81. Kottra, G.; Haase, W.; Fromter, E., Tight-junction tightness of necturus gall-bladder epithelium is not regulated by camp or intracellular ca2+ .1. Microscopic and general electrophysiological observations. *Pflug Arch Eur J Phy* **1993**, *425*, 528-534.

82. Sun, T.; Swindle, E.J.; Collins, J.E.; Holloway, J.A.; Davies, D.E.; Morgan, H., On-chip epithelial barrier function assays using electrical impedance spectroscopy. *Lab on a chip* **2010**, *10*, 1611-1617.

83. BERGGREN; Magnus; RICHTER-DAHLFORS; Agneta, *Organic bioelectronics*. Wiley: Weinheim, ALLEMAGNE, 2007; Vol. 19, p 13.

84. Shim, N.Y.; Bernards, D.A.; Macaya, D.J.; DeFranco, J.A.; Nikolou, M.; Owens, R.M.; Malliaras, G.G., All-plastic electrochemical transistor for glucose sensing using a ferrocene mediator. *Sensors-Basel* **2009**, *9*, 9896-9902.

85. Yang, S.Y.; Defranco, J.A.; Sylvester, Y.A.; Gobert, T.J.; Macaya, D.J.; Owens, R.M.; Malliaras, G.G., Integration of a surface-directed microfluidic system with an organic electrochemical transistor array for multi-analyte biosensors. *Lab on a chip* **2009**, *9*, 704-708.

86. Someya, T.; Dodabalapur, A.; Gelperin, A.; Katz, H.E.; Bao, Z., Integration and response of organic electronics with aqueous microfluidics. *Langmuir : the ACS journal of surfaces and colloids* **2002**, *18*, 5299-5302.

87. Wong, J.Y.; Langer, R.; Ingber, D.E., Electrically conducting polymers can noninvasively control the shape and growth of mammalian cells. *Proceedings of the National Academy of Sciences of the United States of America* **1994**, *91*, 3201-3204.

88. Kim, D.H.; Richardson-Burns, S.; Povlich, L.; Abidian, M.R.; Spanninga, S.; Hendricks, J.L.; Martin, D.C., Soft, fuzzy, and bioactive conducting polymers for improving the chronic performance of neural prosthetic devices. In *Indwelling neural implants: Strategies for contending with the in vivo environment*, Reichert, W.M., Ed. Boca Raton (FL), 2008.

89. Guimard, N.K.; Gomez, N.; Schmidt, C.E., Conducting polymers in biomedical engineering. *Prog Polym Sci* **2007**, *32*, 876-921.

90. Wan, A.M.; Brooks, D.J.; Gumus, A.; Fischbach, C.; Malliaras, G.G., Electrical control of cell density gradients on a conducting polymer surface. *Chem Commun (Camb)* **2009**, 5278-5280.

91. Bolin, M.H.; Svennersten, K.; Nilsson, D.; Sawatdee, A.; Jager, E.W.H.; Richter-Dahlfors, A.; Berggren, M., Active control of epithelial cell-density gradients grown along the channel of an organic electrochemical transistor. *Advanced Materials* **2009**, *21*, 4379-+.

92. Bolin, M.H.; Svennersten, K.; Wang, X.J.; Chronakis, I.S.; Richter-Dahlfors, A.; Jager, E.W.H.; Berggren, M., Nano-fiber scaffold electrodes based on pedot for cell stimulation. *Sensor Actuat B-Chem* **2009**, *142*, 451-456.

93. Isaksson, J.; Kjall, P.; Nilsson, D.; Robinson, N.D.; Berggren, M.; Richter-Dahlfors, A., Electronic control of ca2+ signalling in neuronal cells using an organic electronic ion pump. *Nature materials* **2007**, *6*, 673-679.

94. Simon, D.T.; Kurup, S.; Larsson, K.C.; Hori, R.; Tybrandt, K.; Goiny, M.; Jager, E.H.; Berggren, M.; Canlon, B.; Richter-Dahlfors, A., Organic electronics for precise delivery of neurotransmitters to modulate mammalian sensory function. *Nature materials* **2009**, *8*, 742-746.

95. Ludwig, K.A.; Uram, J.D.; Yang, J.; Martin, D.C.; Kipke, D.R., Chronic neural recordings using silicon microelectrode arrays electrochemically deposited with a poly(3,4-ethylenedioxythiophene) (pedot) film. *J Neural Eng* **2006**, *3*, 59-70.

96. Kim, D.H.; Richardson-Burns, S.M.; Hendricks, J.L.; Sequera, C.; Martin, D.C., Effect of immobilized nerve growth factor on conductive polymers: Electrical properties and cellular response. *Adv Funct Mater* **2007**, *17*, 79-86.

97. Kim, D.H.; Abidian, M.; Martin, D.C., Conducting polymers grown in hydrogel scaffolds coated on neural prosthetic devices. *Journal of biomedical materials research. Part A* **2004**, *71*, 577-585.

98. Nyberg, T.; Inganäs, O.; Jerregård, H., Polymer hydrogel microelectrodes for neural communication. *Biomedical microdevices* **2002**, *4*, 43-52.

99. Yang, S.Y.; Kim, B.N.; Zakhidov, A.A.; Taylor, P.G.; Lee, J.K.; Ober, C.K.; Lindau, M.; Malliaras, G.G., Detection of transmitter release from single living cells using conducting polymer microelectrodes. *Adv Mater* **2011**, *23*, H184-188.

100. Blau, A.; Murr, A.; Wolff, S.; Sernagor, E.; Medini, P.; Iurilli, G.; Ziegler, C.; Benfenati, F., Flexible, all-polymer microelectrode arrays for the capture of cardiac and neuronal signals. *Biomaterials* **2011**, *32*, 1778-1786.

101. Khodagholy, D.; Doublet, T.; Gurfinkel, M.; Quilichini, P.; Ismailova, E.; Leleux, P.; Herve, T.; Sanaur, S.; Bernard, C.; Malliaras, G.G., Highly conformable conducting polymer electrodes for in vivo recordings. *Adv Mater* **2011**, *23*, H268-272.

102. Khodagholy, D.; Doublet, T.; Quilichini, P.; Gurfinkel, M.; Leleux, P.; Ghestem, A.; Ismailova, E.; Hervé, T.; Sanaur, S.; Bernard, C., *et al.*, In vivo recordings of brain activity using organic transistors. *Nature Communications* **2013**, *4*, 1575.

103. Khodagholy, D.; Doublet, T.; Gurfinkel, M.; Quilichini, P.; Ismailova, E.; Leleux, P.; Herve, T.; Sanaur, S.; Bernard, C.; Malliaras, G.G., Highly conformable conducting polymer electrodes for in vivo recordings. *Advanced Materials* **2011**, *23*, H268-+.

104. Lin, P.; Yan, F.; Yu, J.; Chan, H.L.; Yang, M., The application of organic electrochemical transistors in cell-based biosensors. *Adv Mater* **2010**, *22*, 3655-3660.

105. Bernards, D.A.; Malliaras, G.G., Steady-state and transient behavior of organic electrochemical transistors. *Adv Funct Mater* **2007**, *17*, 3538-3544.

106. Bernards, D.A.; Malliaras, G.G.; Toombes, G.E.S.; Gruner, S.M., Gating of an organic transistor through a bilayer lipid membrane with ion channels. *Appl Phys Lett* **2006**, *89*.

2 Chapter 2

Validation of the Organic Electrochemical Transistor

This first results chapter consists of the characterization of the Caco-2 cell line used to mimic the gastrointestinal tract, and its integration with the Organic Electrochemical Transistor. Once different parameters of the cell line were set with traditional techniques, the barrier tissue was integrated with the OECT. The barrier tissue was then attacked by different chemicals to destroy it. The results obtain with our transistor were compared with traditional methods to validate our technique as a new way to assess barrier tissue integrity. In the work shown in this chapter, I was in charge of the establishment of Caco-2 cell growth and characterization by immunofluorescence, measurement of the TER and permeability assays. I also performed the assays after exposure to toxic compounds. The parameters that I determined to obtain a fully differentiated barrier tissue were used for the OECT experiment as well as the protocol to test the chemical compounds.

This chapter corresponds to the following published articles:

L.H. Jimison, S.A. Tria, D. Khodagholy, M. Gurfinkel, E. Lanzarini, A. Hama, G.G. Malliaras, and R.M. Owens, "Measurement of barrier tissue integrity with an organic electrochemical transistor", Adv. Mater. 24, 5919 (2012)

S.A. Tria, L.H. Jimison, A. Hama, M. Bongo, and R.M. Owens, "Validation of the organic electrochemical transistor for in vitro toxicology", BBA - General Subjects 1830, 4381 (2013).

2.1 Introduction

The ability of organic electronic materials to interface with biological systems has been much vaunted of late, with examples showing the elegant use of these materials to deliver neurotransmitters *in vivo* [1], control cell adhesion [2,3] and migration [4] and measure neuronal activity *in vivo* [5,6].With the unique ability of organic electronic materials to conduct both electronic and ionic carriers, they act as an ideal platform for the integration of electronic and biological systems. The organic electrochemical transistor (OECT) has been recently employed as a sensor for DNA [7], enzymes [8] and cell attachement [9]. Here, we show for the first time the integration of OECTs with human cells for assessing barrier tissue layer integrity. We are able to measure minute variations in paracellular ionic flux induced by toxic compounds in real time, with unprecedented temporal resolution and extreme sensitivity. The ability to measure paracellular transport is important as it provides a wealth of information about barrier tissue function, and disruption or malfunction of the structures involved in transport through barrier tissue is often indicative of toxicity or disease. Development of this technology will have implications for toxicology, drug development, infectious disease diagnostics and basic research on the molecular biology and electrophysiology of barrier function.

Barrier tissues in multicellular organisms serve as essential functional interfaces, maintaining highly regulated fluid compartments by limiting the diffusion of ions, macromolecules and other cells, while selectively absorbing nutrients, electrolytes and water that sustain the host [10]. Examples of barrier tissue in the body include the intestinal epithelium, kidney epithelium and the blood brain barrier endothelium. Epithelial and endothelial cells generally exist in single layers and are joined to each other by specialized complexes that include the adherens junction and the tight junction (TJ)[11]. TJs restrict paracellular diffusion [12,13] by regulating the passage of molecules across the barrier as they selectively open and close in response to signals from inside and outside the cells. The degree of barrier tissue integrity serves as an indicator for disease state [14,15] and also of the appropriateness of a particular *in vitro* model for use in toxicology and drug screening. Accurate *in vitro* cell models are urgently required, as current *in vivo* methods for evaluating toxic compounds or drugs are expensive and time consuming. Efficient methods of characterization will help to validate and develop models as replacements for animal testing, an essential component of the European REACH regulation to handle toxicological profiling of more than 30 000 chemical substances imported into Europe. Currently, two main parameters are used for assessing the integrity of barrier tissue: permeability and trans-epithelial/endothelial electric resistance (TER or TEER). In general, a correlation between permeability of a cell layer and the TER exists, with tight cell layers exhibiting high TER and low permeability [10,12]. Permeability is typically measured by monitoring the flux of radiolabeled/fluorescence compounds across cells cultured on suspended porous filters (Transwell). TER can be measured with a

handheld epithelial volt-ohm meter. Unfortunately, data collection is associated with slow temporal resolution, poor measurement reproducibility and incompatibility with high throughput methods. Impedance spectroscopy can be employed to measure the capacitance and resistance of the cell layer in a more automated and reproducible fashion [16,17]. This technology has provided significant contributions in the field, but requires expensive equipment and still presents limitations in temporal resolution and sensitivity. Here, we present a method for monitoring in situ barrier tissue integrity using an organic electrochemical transistor (OECT). With the proposed device, we introduce a novel mechanism for sensing barrier tissue integrity achieved with simple device format, compatible with low cost solution-based fabrication [18]. The OECT presents an exciting new avenue for assessing barrier tissue cell layers, with their exquisitely tuned ionic transport systems [10]. The integration of barrier tissue with an OECT is illustrated in Figure 2.1a. PEDOT: PSS, a conducting polymer (CP) with demonstrated biocompatibility and stability [8,9], is used as the active material in the transistor channel. The cell layer is grown on a Transwell membrane and incorporated into the device prior to measurement. In order to understand the sensing mechanism of the device, it is necessary to briefly review the operating mechanism of an OECT. The OECT comprises a degenerately doped CP channel in contact with an electrolyte [6,19]. A gate electrode is immersed in the electrolyte, and source and drain contacts at either side of the transistor channel measure the drain current (I_D). On application of a positive gate voltage (V_G), cations from the electrolyte enter the channel, de-doping the CP and decreasing the drain current (I_D). The steady state I_D is linearly proportional to the total number of ions that have entered the polymer film, and the ionic flux determines the speed at which the transistor reaches steady state [20]. Thus, the OECT acts as a transducer of ionic signal to electronic current. A key difference in the use of a transistor as the sensing element, opposed to a conventional electrode[16,17,21], is the inherent amplification associated with the former, where small changes in the ionic flux are integrated and amplified in the drain current. It has been shown that the ionic current in an OECT can be modeled using a combination of linear circuit elements [20]. The modification of the OECT ionic circuit on the addition of barrier tissue is shown schematically in Figure 2.1b, with the cell layer represented as a resistor and capacitor in parallel [16]. The resistance of the cell layer (the TER) influences the ionic flux into the device: a higher TER will result in a lower ionic flux, and vice versa. Figure 2.1c shows the OECT I_D response to a square voltage pulse in the absence of a cell layer. The hypothesized effect of TER is illustrated in Figure 2.1d by subjecting the device to pulses of constant gate current (I_G): as I_G is decreased, the transient I_D response is slower. The influence of the cell layer on the ionic flux is thus reflected in I_D. The sensing mechanism presented here is in contrast to a previous application of an OECT as a whole cell sensor for measurement of cell adhesion and detachment[9]. With cells grown directly on the CP channel, authors demonstrated a change in steady state transistor performance as a function of cell coverage, attributed to electrostatic modification of the cell/CP interface. While this device was able to detect gross cell detachment, our device

is designed to dynamically address the health of a tissue layer that may be reversibly or temporarily damaged. Furthermore, the use of Transwell filters as the support for the cell layer renders our device completely compatible with existing barrier tissue characterization and toxicology techniques.

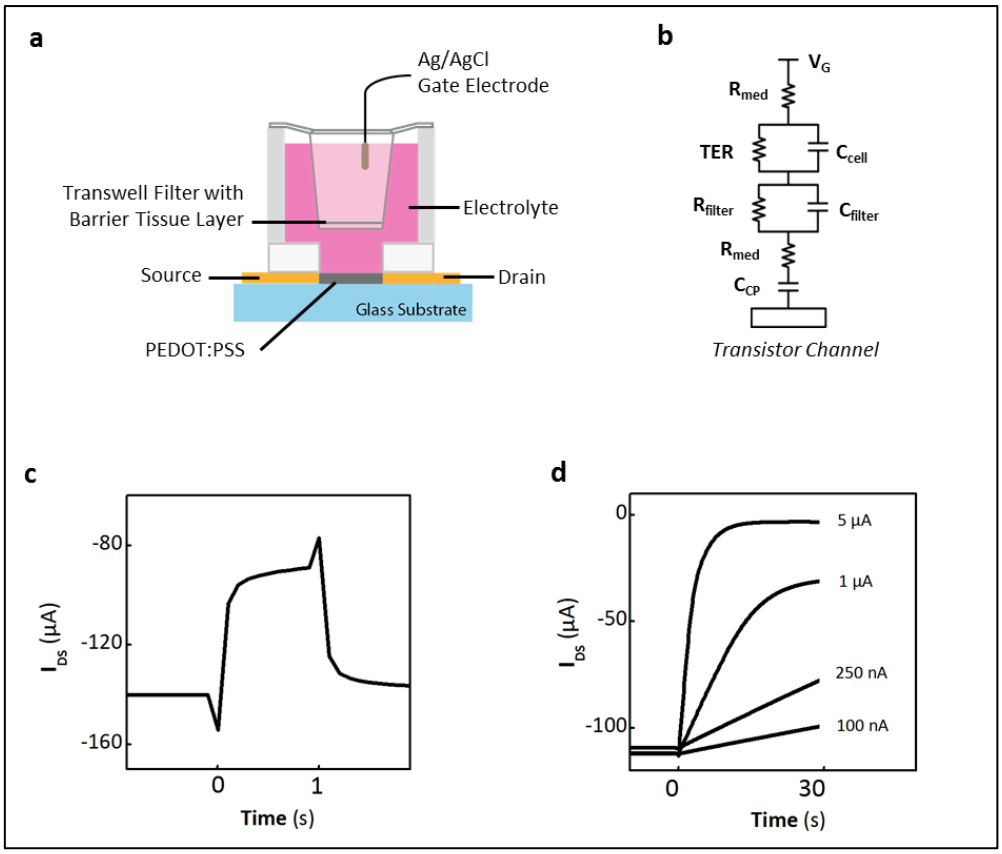

Figure 2.1: The integration of barrier tissue with an OECT. a) Device architecture. b) Equivalent circuit describing ionic transport between gate electrode and transistor channel. TER refers to the transepithelial resistance of the cell layer, Ccell refers to the capacitance of the cell layer, R_{filter} and C_{filter} refer to the resistance and capacitance of the porous filter, respectively, R_{med} refers to the resistance of the media, and C_{CP} refers to the capacitance at the CP and electrolyte layer. c) OECT I_D transient response to a V_G pulse. d) OECT transient I_D response to a 30 s pulse of constant I_G of varying magnitudes, as labeled. As with other experiments, V_D = –0.1.

2.2 Material and methods

2.2.1 Cell Culture :

Caco-2 cells were seeded at 5.10^4 cells/insert (1.1 cm^2). Cells were routinely maintained at 37°C in a humidified atmosphere of 5% CO_2, in DMEM (Advanced Dulbecco's Modified Eagle Medium, Reduced Serum 1X, Invitrogen) with 2 mM Glutamine (Glutamax-1, Invitrogen), 10% FBS (fetal bovine serum, Invitrogen) and Pen-strep (5000 [U/mL] penicillin–5000 [µg/mL] streptomycin,

Invitrogen). For all OECT and permeability experiments, Caco-2 cell layers were used at 21 days in culture, corresponding to a TER of 400–500 $\Omega.cm^2$ and an apparent permeability of 1.10^6 $cm.s^{-1}$, consistent with literature reports[22]. Cells were cultured on Transwell filters with a 0.4 μm^2 pore size and area of 1.1 cm^2. For OECT measurements only, cell layer area was reduced by a factor of ten using silicone on the back side of the filter, for purposes of increasing effective cell layer resistance.

2.2.2 Permeability Assays :

Prior to permeability measurements, cells were exposed to various concentrations of ethanol and H_2O_2 in complete DMEM for 24 h. The value of the apparent permeability (P app) was calculated according to the following relationship: P app =((Flux x V_{bas})/ t)(1/ C_o A) and Flux =100(LY_{bas} x V_{bas})/(LY_{api} xV_{api}), where LY_{bas} and LY_{api} are the concentration of Lucifer yellow in the basal and apical sides of the hanging porous filter, respectively, V_{bas} and V_{api} are the volume in the basal and apical sides, respectively, t is the time of incubation, C_o is the initial concentration of Lucifer yellow on the apical side and A is the area of the filter. At least two samples were measured for each condition.

2.2.3 Device Fabrication :

PEDOT:PSS (Heraeus, Clevios PH 1000) was used as the conducting polymer active layer. Ethylene glycol (Sigma Aldrich) was added in a volume ratio of 1:4 (ethylene glycol to PEDOT:PSS) to increase conductivity. Dodecylbenzenesulfonic acid (DBSA) (0.5 µL/mL) was added as a surfactant to improve fi lm formation, and 3-glycidoxypropyltrimethoxysilane (GOPS) (10 mg/mL) was added as a cross-linker to improve fi lm stability. Thermally evaporated gold source and drain contacts were defined via lift-off lithography. Channel dimensions were patterned using a parylene peel-off technique described previously [6,23], resulting in a PEDOT:PSS channel width of 1 mm. Following PEDOT deposition, devices were baked for 1 h at 140°C at atmospheric conditions. A PDMS well defined active area, resulting in a channel area of approximately 8 mm^2.

2.2.4 Device Measurements :

For OECT measurements, Ag/AgCl was used as the gate electrode and (DMEM) cell culture media was used as the electrolyte. All measurements were made with Keithley 2612 SourceMeter and customized Labview software. In all

cases, cell media (as described above) was used as the electrolyte. Measurements were performed at ambient temperature, but controls were conducted to ensure that temperature effects do not dominate changes in OECT response within the time required for measurements. H_2O_2 was added to the apical side of the cell filter, without changing media. Because larger amounts of EtOH were needed to achieve compositions of 10, 20, and 30%, half of the apical media was removed before introducing EtOH. In both cases, we confirmed that the act alone of addition/removal of liquid did not disrupt the barrier tissue layer. Throughout these experiments, measurement parameters were chosen to avoid exposing the cell layers to a voltage drop above 0.4 V, as high voltages have been shown to damage bilayer membranes[23]. Unless otherwise stated, OECT data was collected using the following parameters: V_{GS} =0.3 V, V_{DS} =0.1 V, V_{GS} on time =1 s, off time =29 s, duty cycle =3.33%. In some cases, OECT data is shown in the form of a normalized response (NR). NR is obtained by calculating ΔI_D /I0 (where ΔI_D refers to drain current modulation in response to the application of the gate voltage, and I 0 refers to the drain current when V_G is off) and subsequently normalizing the dataset to [0,1].

2.3 Results

To commence OECT validation, we characterized healthy, intact barrier tissue using immunofluorescence (Figure 2.2A), TER measurements (Figure 2.2B) (using CellZscope) and solute permeability assays (Figure 2.2C) (with respect to Lucifer Yellow). These results were compared to barrier tissue assessment using an OECT (Fig. 2D). Immunofluorescence staining of junctional proteins, although not a technique that is compatible with high throughput screening, is still the reference technique for assessing barrier tissue integrity since it allows localization of key proteins known to be essential for the barrier properties of the tight junction. In the immunofluorescence experiments, cells were stained for occludin and claudin, two of the proteins present in the tight junction complex. A clear colocalization of occludin and claudin can be seen in (Figure 2.2A, panels 2 and 3, respectively) while the cell nucleus stained with DAPI is also visible (Figure 2.2A panels 1). In differentiated cell layers, these proteins are localized around the cellular periphery. Cells grown on filters were also used for LY permeability assays shown in Figure 2.2B. A control filter without cells shows an apparent permeability of $3.11 \pm 0.33\times10^{-4}$ $cm\cdot s^{-1}$,while a filter with cells shows an apparent permeability of $1.78 \pm 0.08\times10^{-8}$ $cm\cdot s^{-1}$ consistent with literature reports [24,25]. For measurement of TER, cells were seeded on filters and cultured in the CellZscope instrument for a period of 21 days. Data shown in Fig. 2C show the evolution of the TER over time, starting from $20.57 \pm 0.14 \Omega\cdot cm^2$ for a bare filter and plateauing at $457.71 \pm 71.82 \Omega\cdot cm^2$ over the course of 21 days.

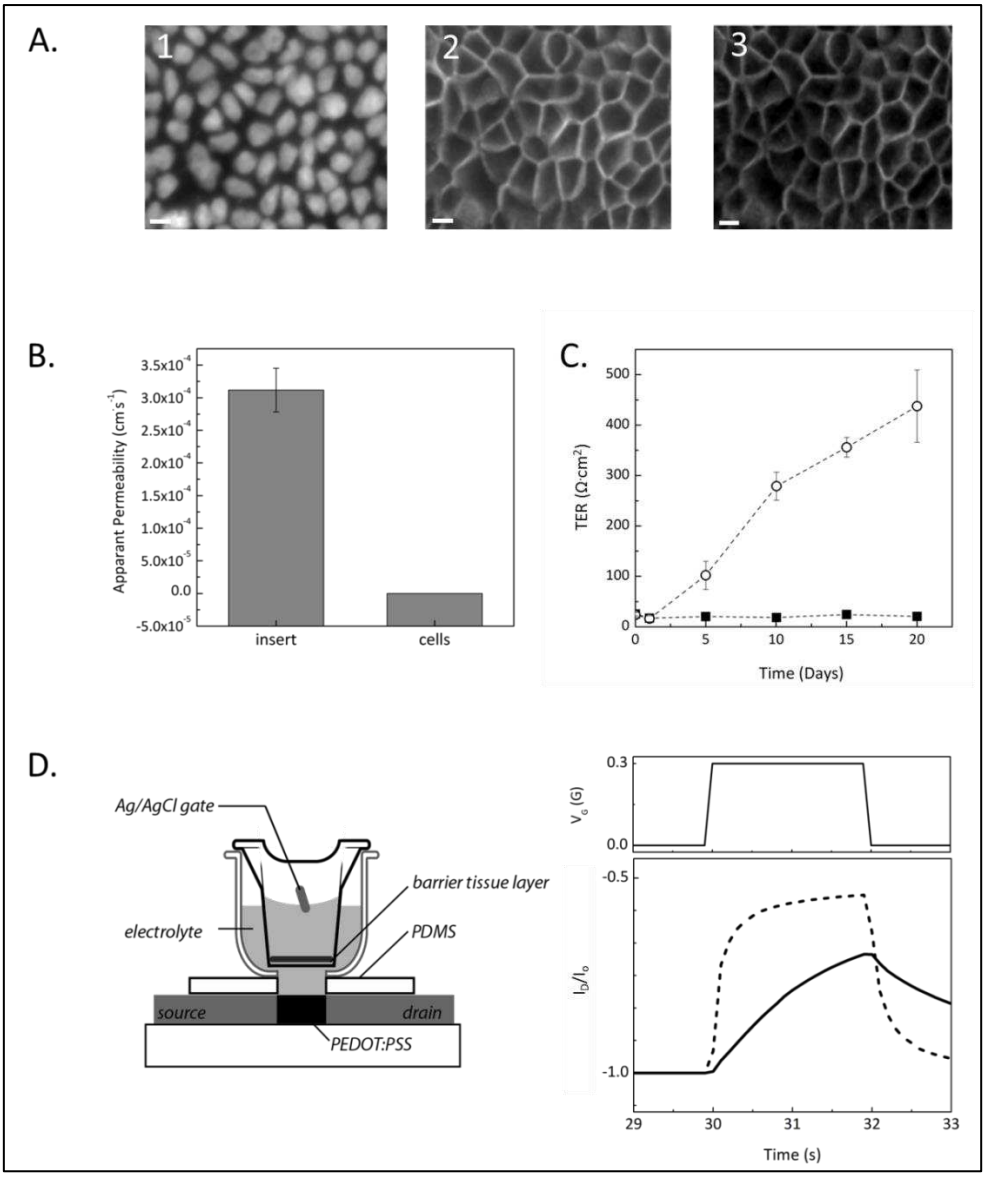

Figure 2.2: Comparison of different methods used for assessing barrier tissue integrity. (A) Immunofluorescence images of Caco-2 cells grown on inserts for 21 days. The nuclei were stained with DAPI (1). Cells were also stained with antibodies against tight junction proteins occludin (2) and claudin-1 (3). (B) The apparent permeability of a filter alone and a filter with differentiated Caco-2 cells was determined by adding Lucifer Yellow solution on top of the insert and measuring the fluorescence of each compartment of the insert after 1 h. Data represent mean value ± standard deviation of experiments made in duplicate. (C) TER of Caco-2 cells and the filter alone were continuously monitored over 21 days using the CellZscope. Each point represents the mean ± standard deviation from different experiments, with a minimum of three inserts for each point. (D) Illustration of the integration of cells grown on a filter with an OECT (left). Example of a typical OECT response with and without cells (right): the drain current (I_D) response to a gate voltage pulse (top). The OECT response in the presence of cells is shown with the solid black line, while the OECT response in the presence of insert alone is shown with a dashed line (bottom).

Having established the baseline parameters for intact barrier tissue, we used the same experimental conditions (Caco-2 cells grown on Transwell filters for 21 days) to perform assays with the OECT.

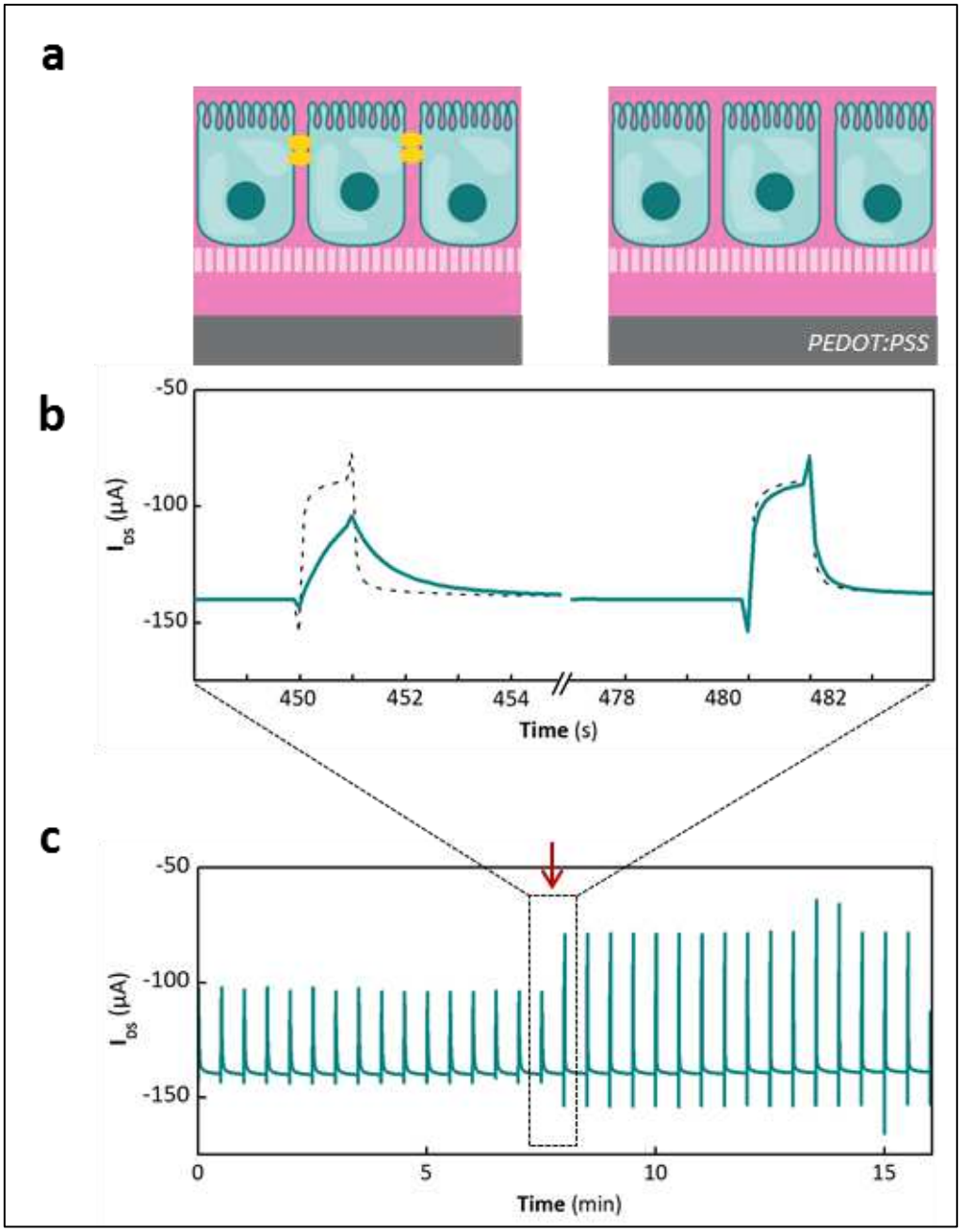

Figure 2.3: Monitoring barrier tissue integrity with an OECT. a) Cartoon showing polarized Caco-2 cells with tight junctions (left) and without (right), sitting on a porous cell culture membrane, above a PEDOT:PSS transistor channel. Tight junctions are shown in yellow. b) OECT I_D transient response with cells before (left) and after (right) the addition of 100 mM H_2O_2, (solid lines). OECT I_D response in the absence of cells is overlaid (dashed lines). c) In situ OECT response to periodic square V_{GS} pulses. As indicated, data here correspond to the same measurement as shown in (b), but for an expanded time scale. The red arrow indicates the point of H_2O_2 introduction. The immediate change in OECT response to the addition of H_2O_2 is evident by the drastic change in Δ_{ID}.

Figure 2.3a shows a cartoon monolayer of polarized Caco-2 cells with tight junction protein complexes (left) and without (right). In Figure 2.3b (left), we demonstrate that in the presence of cells with TJs, the barrier properties slow the OECT I_D response time, compared to the I_D response when no cells are present. To induce a change in tissue layer integrity, hydrogen peroxide (H_2O_2), a reactive oxygen species known to disrupt TJs [26], was introduced. The disruption of barrier tissue integrity results in an increase in ionic transport across the cell layer and therefore a faster I_D response (Figure 2.3b, right). Control experiments were carried out to confirm that what we observe is not a parasitic effect of H_2O_2 reacting with the gate electrode or the polymer channel (Supporting Information).

By comparing the data obtained from the OECT (Fig. 2D) with these other methods (Fig. 2A, B and C) we rigorously ensured that the change of curve shape observed with the OECT corresponds to a localization of tight junction proteins around the cellular periphery, a low flux of Lucifer Yellow, and finally a high electrical resistance (CellZscope).

The OECT has potential as a method for the measurement of compound toxicology *in vitro* and also for diagnostics. To confirm this potential we performed toxicology studies using the three traditional methods presented here. We then compared data from traditional methods against data from the OECT, investigating the ability of the OECT to not only measure the presence of intact barrier tissue, but also detect damage to barrier tissue. We chose toxins previously demonstrated to affect paracellular permeability of the gastrointestinal barrier. Our goal was to choose simple compounds, known to affect different components of the tight junction, which could be added in the apical media compartment of the cell culture well. Both ethanol and H_2O_2 have been previously demonstrated to affect paracellular permeability of the gastrointestinal barrier, although with distinct molecular mechanisms. Ethanol exposure is known to damage the gastrointestinal mucosal surface, proposedly through mucosal injury, changes to epithelial membrane integrity, and disruption of the tight junction barrier [27], with a concomitant dose-dependent drop in Caco-2 epithelial resistance and increase in paracellular permeability [28]. The effect of ethanol has been reported to be mediated via an effect on ZO-1, as ethanol treatment resulted in a progressive loss of ZO-1 in the cellular periphery and formation of large gaps between adjacent cells [28]. There have also been reports of changes in occludin localization [29]. Low non-cytotoxic doses (10%) have been shown to cause functional opening of the Caco-2 intestinal epithelial TJ barrier while high concentrations of ethanol (40%) are thought to cause functional damage of the gastrointestinal epithelial barrier by direct cytotoxic effect on the epithelial cells. Reactive Oxygen Species (ROS; such as H_2O_2) are rapidly metabolized in tissues by antioxidant defense systems under normal conditions. However, an excessive generation of oxidants and/or a defect in antioxidant defense mechanisms may lead to tissue injury such as inflamed mucosa of inflammatory bowel disease (IBD) and or loss of intestinal barrier function. ROS can be produced by toxins, mycoplasma, bacteria and xenobiotics [30] and may mediate their effects by phosphorylation

and regulation of TJ protein–protein interactions [31]. Reversible phosphorylation on Ser, Thr and Tyr residues on the TJ proteins occludin and claudin upon exposure to hydrogen peroxide has also been demonstrated [32], possibly leading to a decrease of the interaction of these proteins with ZO-1, ZO-2 and ZO-3 [33]. To assess the effects of both ethanol and H_2O_2 on Caco-2 cell barrier tissue integrity, we first carried out immunofluorescence of these cells treated with both toxic compounds.

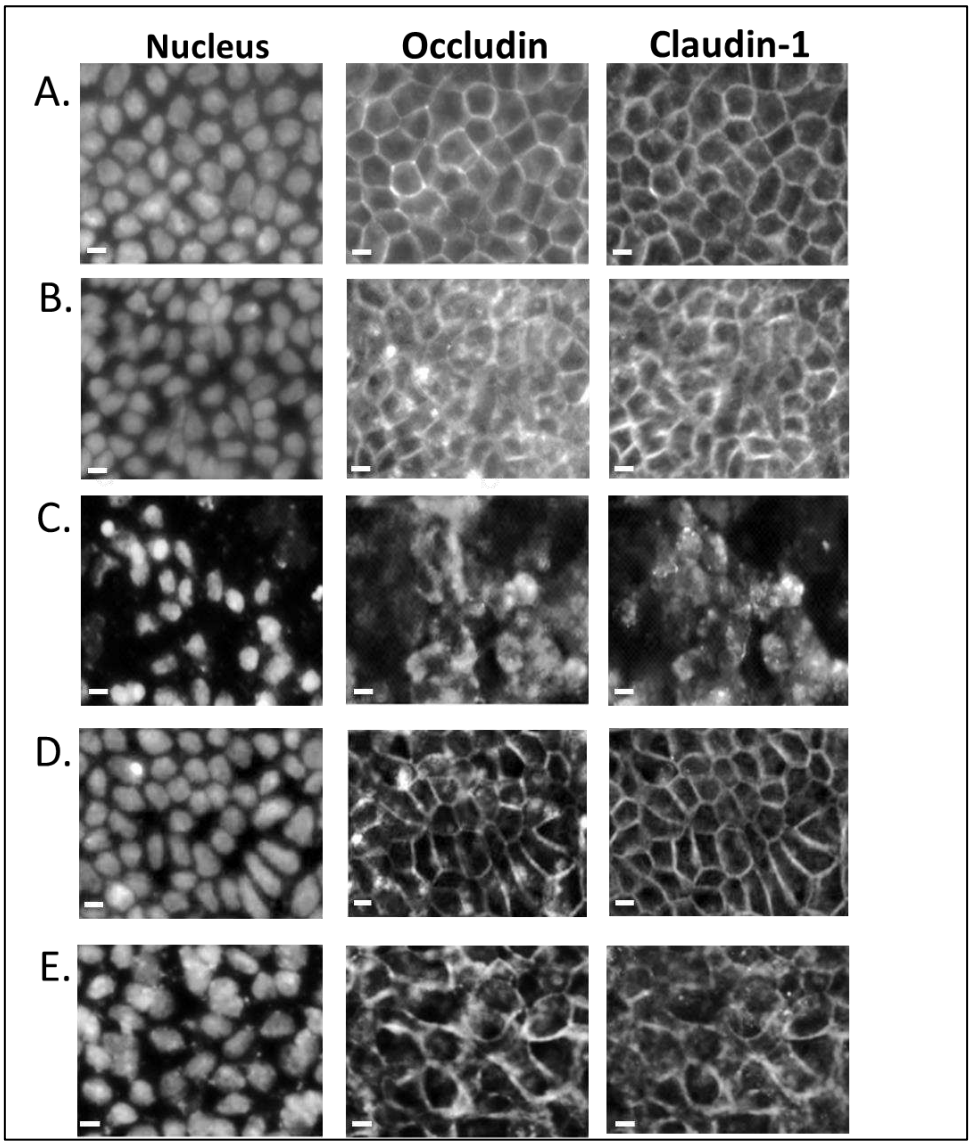

Figure 2.4: Immunofluorescence of tight junction proteins upon exposure to ethanol and H_2O_2. Monolayers were exposed to various concentrations of ethanol and H_2O_2 for 24 h and then stained with antibodies against tight junction proteins. Immunofluorescence image of a control cell monolayer with no exposure to toxic compounds (A). Immunofluorescences images of cells exposed to 5% ethanol (B), 20% ethanol (C), 5 mM H_2O_2 (D), and 20 mM H_2O_2 (E). The cells were then treated with antibodies against occludin, Claudin-1 and nuclei were stained with DAPI. The scale bar is 10 µm.

Figure 2.4 shows immunofluorescence images taken using antibodies against occludin and claudin-1. The nucleus was stained with DAPI. In all cases, immunofluorescence was carried out after 24 h of exposure to the toxic compound. Panel A shows control samples (no toxic compound added) for comparison. As before, a clear localization of both occludin and claudin-1 is visible around the periphery of the cells. Panels B and C show cells after the addition of ethanol at 5% and 20%, respectively. On addition of 5% ethanol, it can be seen that localization of occludin, and to a lesser extent claudin, is not as clearly present at the cellular periphery as in the control. In addition, the slightly diffuse nature of the staining indicates that there may be a delocalization towards the cytoplasm. In the presence of 20% ethanol, we see a complete disorganization of the cell structures, and indeed loss of the continuity of the cell layer. This is in agreement with other studies showing diffuse arrangement or absence of occludin upon exposure to 0.1–10% ethanol, although these results are often hard to compare due to vastly different experimental conditions (including age of cell layers, exposure media, exposure time, etc. [29,34]). Panels D and E show the effect of addition of 5 mM and 20 mM H_2O_2 on cell layers. On the addition of 5 mM H_2O_2, there is a slightly diffuse and delocalized nature to the staining of occludin, while claudin remains relatively unchanged and the cell layers appear intact. However, the addition of 20 mM results in irregular staining of occludin, claudin and indeed of the nucleus, and a deformation in the cell contour, possibly due to changes in the cell cytoskeleton. Again, comparisons with other studies from literature confirm for concentrations of 20 μM to 10 mM H_2O_2 the observation of occludin redistribution [31,35,36], as well as delocalization of claudin-1 [37]. It should be noted that although some studies show a faster effect with lower doses of H_2O_2, these cells were incubated in PBS–BSA rather than complex media, the latter mitigating the effect of the peroxide on the cells. Another oxidant, NH_4Cl, has additionally been shown to result in dispersion of ZO-1 and Claudin-1 from the cellular periphery [42].

Following the immunofluorescence assays, Caco-2 cells were assessed for their permeability to Lucifer Yellow, again after exposure to both ethanol and H_2O_2. Figure 2.5 shows permeability assays carried out on cells again grown on filters. Figure 2.5A shows the effect after 24 h of exposure to ethanol. The addition of 5% and 10% ethanol results in little or no change, with apparent permeability values of $6.98\pm0.22\times10^{-7}$ and $9.61\pm 0.21\times10^{-7}$ $cm\cdot s^{-1}$, respectively, compared to the control value of $7.77\pm0.76\times10^{-7}$ $cm\cdot s^{-1}$. Addition of 20% and 30% EtOH results in significant disruption of the barrier function of the cells with an apparent permeability increase of 32-fold ($2.14\pm2.50\times10^{-5}$ $cm\cdot s^{-1}$) and 371-fold ($2.48\pm0.033\times10^{-4}$ $cm\cdot s^{-1}$) compared to the control, the latter value corresponding to a permeability akin to that observed with a filter alone. These data are confirmed in previous reports using radiolabeled mannitol, which show increases in mannitol permeability after exposure to ethanol for both Caco-2 cells [28] and MDCK II cells (a canine kidney epithelial cell line) [38], and increases in LY apparent permeability on exposure to ethanol for Caco-2 cells [39].

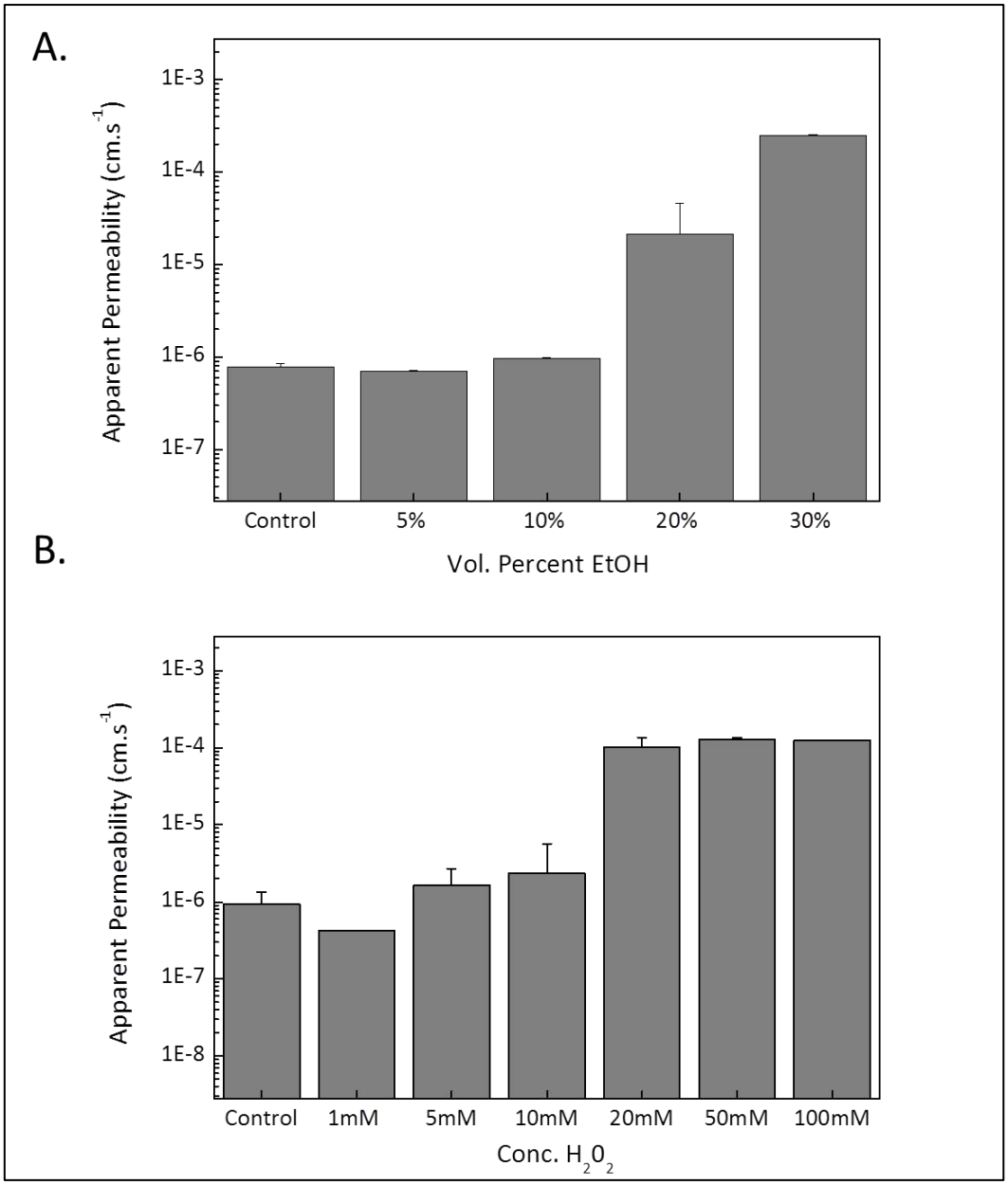

Figure 2.5: Permeability assays of cells upon exposure to ethanol or H_2O_2. Monolayers were exposed to various concentrations of ethanol (A) and H_2O_2 (B) for 24 h. Lucifer Yellow, the permeability marker, was added to the apical side of the monolayer and fluorescence was measured after incubation for 1 h at 37 °C in a humidified CO2 incubator. Data represent mean value + standard deviation of experiments made in duplicate.

A similar trend is observed on addition of H_2O_2 (Figure 2.5B). Exposure to 1 mM H_2O_2 results in a slight decrease in permeability to $4.20 \pm 0.03 \times 10^{-7}$ $cm \cdot s^{-1}$ compared to the control $9.45 \pm 3.90 \times 10^{-7}$ $cm \cdot s^{-1}$. The addition of 5 mM and 10 mM H_2O_2 results in a small increase in the permeability to $1.66 \pm 1.01 \times 10^{-6}$ and $2.36 \pm 3.32 \times 10^{-6}$ $cm \cdot s^{-1}$, respectively. However, concentrations of 20 mM and above show permeabilities similar to the filter alone with no cells (3.11

± 0.33×10^{-4} $cm\cdot s^{-1}$). Previous studies assessing caco-2 cells after exposure to H_2O_2 also show increases in permeability of Mannitol [3H] [26] and LY [39].

The final assay carried out for validation was to assess the effect of ethanol and H_2O_2 by measuring the effect on the transepithelial resistance. Cells grown on inserts were placed inside the CellZscope and exposed to ethanol and H_2O_2 and monitored in situ. The CellZscope is an apparatus that permits real time scanning of cell layer impedance.

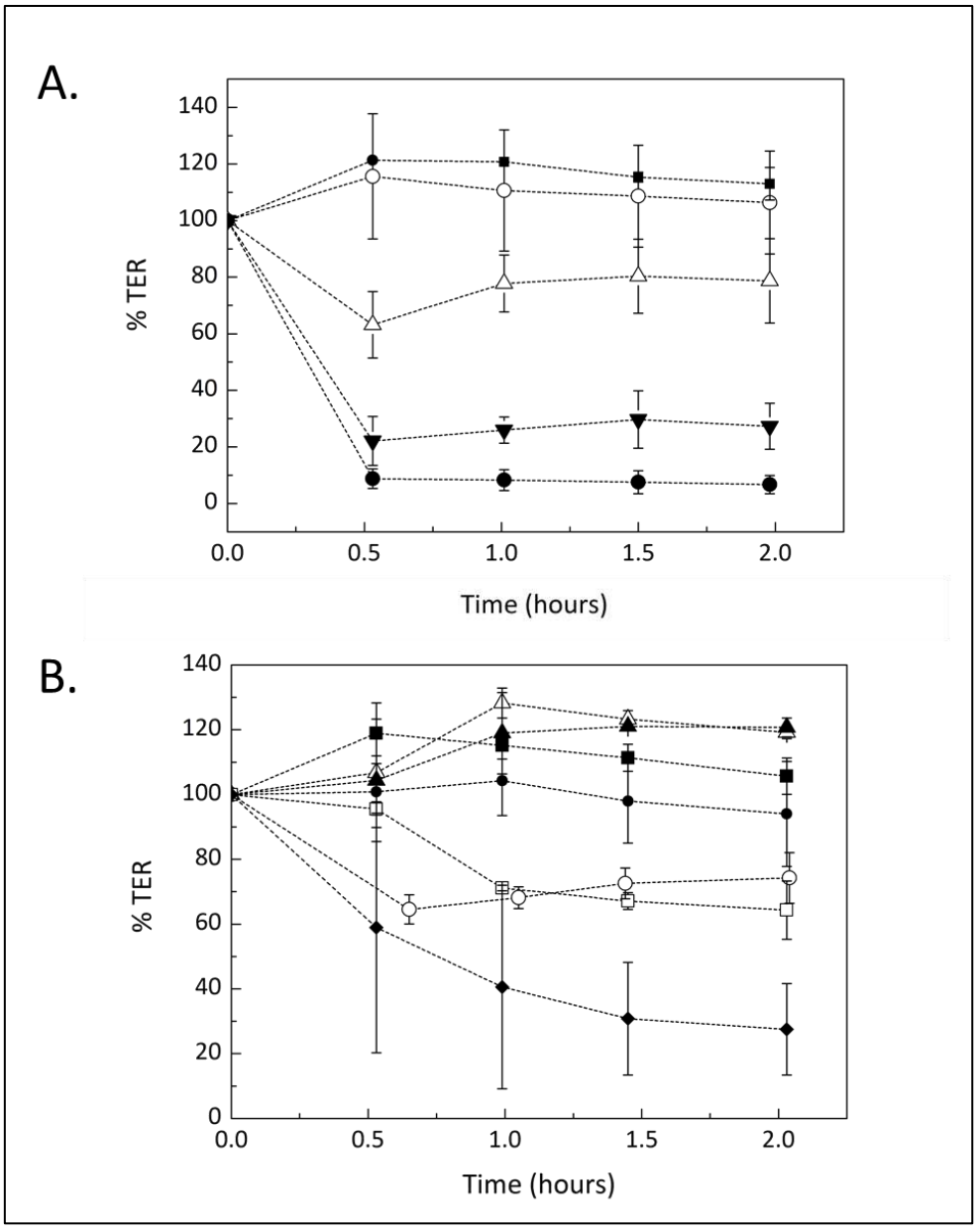

Figure 2.6: % TER value upon exposure to ethanol or H_2O_2. Monolayers were exposed to different concentrations of ethanol (A) or H_2O_2 (B). Each concentration was tested in duplicate. TER was measured continuously using the CellZscope. Data shown is the normalized value. Panel A shows the TER values of cells exposed to 0% (filled rectangle), 5% (open circle), 10% (open triangle), 20% (filled triangle) and 30% ethanol (filled circle). Panel B shows TER values of cells exposed to 0 mM (filled rectangle), 1 mM (closed circle), 5 mM (open triangle), 10 mM (filled triangle), 20 mM (open circle) 50 mM (open rectangle) and 100 mM H_2O_2 (filled diamond).

Using an appropriate equivalent circuit model, the collected data can be fit and values for individual components, including TER, can be extracted [16]. The CellZscope models the two stainless steel electrodes as constant phase elements (CPE), the media as a resistor, the cell layer as a capacitor and resistor in parallel, and the porous filter as a capacitor and filter in parallel. It uses a least squares fitting scheme to extract quantitative values for all of the circuit components. Data were taken for 24 h, however we have chosen to focus on the first 2 h of measurement (which is sufficient for measurement stabilization) as shown in Figure 2.6. In the case of exposure to ethanol (Figure 2.6A), we observed decreases in TER at concentrations of 10, 20 and 30 % resulting in reduction of TER of approximately 20%, 75% and 90% of initial values after 2 h. For both the control and the addition of 5% ethanol, there was a slight increase in TER, followed by a decrease to initial levels. It is not clear what causes this fluctuation in TER, however it has been demonstrated previously by Moyes et al. [40] using a Millicell system for measurement of TER. In the case of exposure to 10% ethanol, the apparent sensitivity limit, the signal remained at approximately 80% of the initial value for a period of about 5 h but then gradually recovered to control levels after approximately 10 h, demonstrating the reversibility of this toxic effect at this concentration (data not shown). Figure 2.6B shows the results obtained after exposure to H_2O_2. On addition of 5 mM, 10 mM and 20 mM H_2O_2, TER remained similar to the control for the 2 h measurement period shown. The addition of 1 mM resulted in a slow decrease to approximately 70% of the initial value, followed by a slight increase. The addition of 50 mM and 100 mM resulted in sharp decreases in TER within the period shown. It is not clear why there is a non-continuous trend (decrease in TER at 1 mM, increase at 5, 10, 20 mM, decrease at 50 and 100 mM). One advantage of the CellZscope setup is that it can be used for continuous measurements in an incubator. Therefore we were able to carry out measurements for 24 h to determine if these trends were maintained at later time points. Following exposure of H_2O_2 for 24 h (data not shown), we observed an increase in the TER to initial levels for cells exposed to 1 mM indicating a recovery of the barrier properties. For 5 and 10 mM the increase in TER was maintained. The TER for cells exposed to 20 mM decreased steadily until approximately 5 h post exposure, when it reached a TER equivalent to 50% of the initial value. It is interesting that the opposite trend is observed with the permeability assay. At 24 h we observed a slight decrease in permeability at 1 mM H_2O_2, but slight increases in permeability at 5 mM and 10 mM. As with the other techniques, data from literature shows similar trends on exposure to H_2O_2 using the Millicell measurement system [41], although as before, experimental conditions vary significantly [26,35,36].

Having established the performance of the three 'traditional methods' for assessing barrier tissue integrity upon exposure to both ethanol and H_2O_2, we proceeded to compare them against the OECT as a means to measure damage to barrier tissue integrity.

A key advantage of our sensor compared to common characterization methods is the ability to measure the response of the cell layer to a destructive

species with such high temporal resolution. Figure 2.7b shows the in situ OECT response on addition of H_2O_2. In previous reports, effects of H_2O_2 on Caco-2 barrier integrity were observed after 30 to 60 min [26], whereas we show an effect within 30 s. Detection of such an immediate response has enormous potential for toxicology purposes. In addition to high temporal resolution, we also observe high sensitivity.

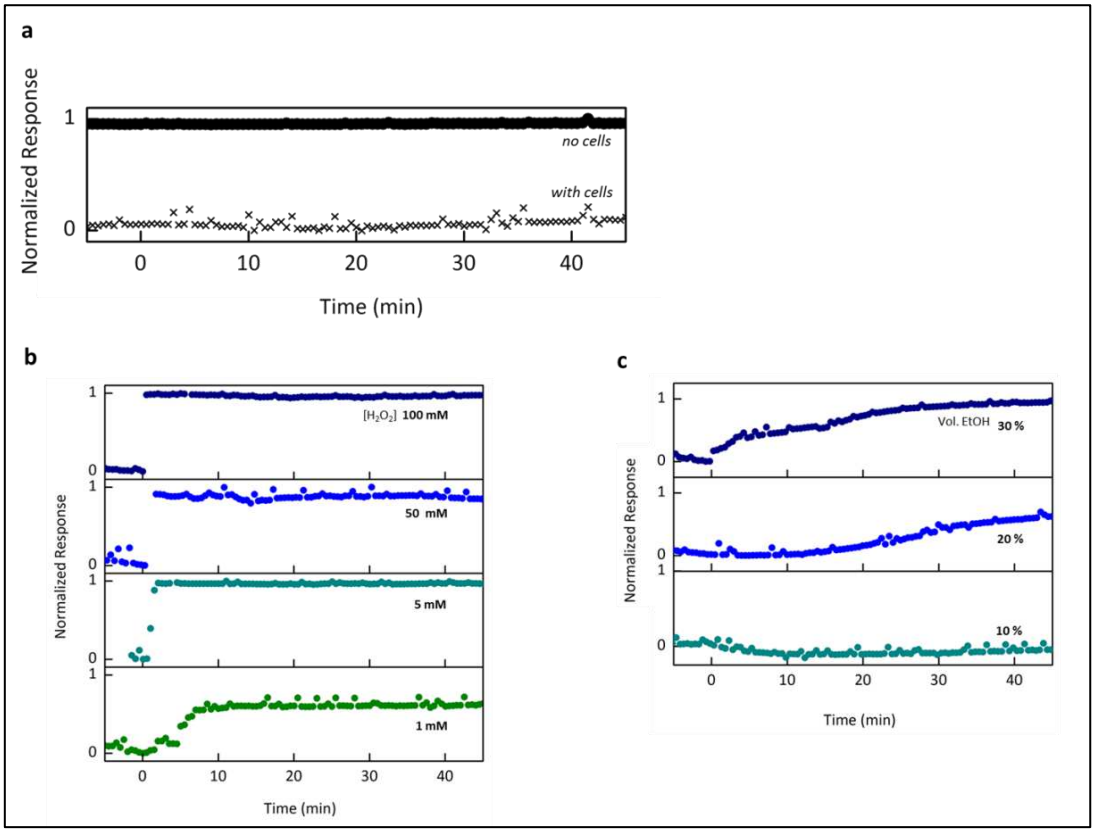

Figure 2.7: In situ OECT response and sensitivity. a) In situ normalized response of the OECT with barrier tissue on introduction of 100, 50, 5, and 1 mM H_2O_2, as labeled. H_2O_2 was introduced at t = 0. Here, NR = 0 corresponds to full barrier properties of a confluent monolayer and a NR = 1 correspond to a cell layer with no barrier properties. b) NR controls corresponding to the OECT alone, with no cells (•), and a control corresponding to OECT with cells, but no added destructive species (×). c) NR of OECT with barrier tissue on introduction of ethanol (EtOH) at volume concentrations of 30, 20, and 10%, as labeled. Ethanol was introduced at t = 0.

Figure 2.7 shows the normalized response of the OECT in the absence of toxic compound (A), and on exposure to different concentrations of H_2O_2 (B) and ethanol (C). As indicated in the materials and methods section, data are shown in the form of a normalized response (NR). NR is obtained by calculating $\Delta I_D / I_0$ and subsequently normalizing the dataset to [0,1]. Thus in Figure 2.7A, 0 represents an intact barrier, while 1 represents a fully disrupted cell layer (or OECT in the absence of cells). In the current generation of device, since we are operating at room temperature, experiments were carried out for 1 h only. This was to ensure that temperature would the control cells had a stable response for the measurement period, remaining at a normalized value of 1 throughout. When cells were incubated with 10% ethanol (Figure 2.7c), we

observe only a partial disruption of the barrier function. On exposure to 20% ethanol, total disruption of the barrier was achieved in a gradual manner over the course of 1 h. The addition of 30% ethanol results in almost total disruption after approximately 40 min. For both 20% and 30% ethanol, a clear effect, corresponding to at least a 50% increase in the normalized response, is visible within 25 and 35 min using the OECT, akin to the CellZscope measurements where a clear effect is visible at 30 min for both concentrations. The effect of H_2O_2 as monitored by the OECT is shown in Figure 2.7b. On exposure to 1 mM H_2O_2, barrier disruption proceeded gradually over the course of 10 min, at which point it stabilized for the remainder of the measurement. In contrast, on addition of concentrations ranging from 5 to 100 mM, complete disruption was observed within 30 s. For both ethanol and H_2O_2, control experiments were conducted to ensure that the changes measured in the OECT response were due to changes in the cell layer, rather than direct interaction of the OECT and the disrupting species [25]. OECT data match very well with data gathered using the other techniques, showing similar levels of sensitivity for ethanol and a higher sensitivity for H_2O_2 than the other techniques as measured in our laboratory. The OECT response to H_2O_2 shows a strict correlation between increasing dose of the toxic compound and increased disruption of barrier tissue. This is in contrast to the CellZscope and the solute permeability assay where the trends are in fact opposite for lower doses and in addition reflect a non-monotonic trend. An additional point to note is the speed with which the response is obtained, particularly in the case of exposure to H_2O_2, where disruption was observed at all concentrations (except 1 mM) from one pulse to the next. In the case of 1 mM we assume that we are at or near the limit of sensitivity for this generation of device as we have intermediate data between the fully intact (NR=0) and fully open (NR=1). Indeed upon addition of 1 mM H_2O_2 incomplete disruption was observed. To compare the speed of the response, we can consider the time required to achieve a 50% increase in signal for the OECT with a 50% decrease in signal for the CellZscope. For the CellZscope, even at the highest concentration, it takes approximately 45 min to reach a 50% decrease in signal, while for the OECT, with the lowest concentration attempted (1 mM) this 50% increase is achieved within approximately 7 min. It should be noted that perhaps in contrast to the CellZscope, the OECT has been optimized to allow sensitive detection of minute breaches in intact barrier tissue, but in turn, lacks sensitivity at the other end of this range, unable to detect differences in barrier tissue properties below a certain integrity threshold. In this sense, the current OECT sensor is ideal for early time point diagnostics and toxin detection, but less suited for studying cell coverage evolution.

2.4 Conclusions

The goal of the work presented here was to validate the OECT against current techniques that are used to measure barrier tissue integrity. Of the traditional techniques, immunofluorescence provides the only way to clearly visualize protein arrangement and cell layer integrity, but it is a static method that is time and labor consuming and requires the use of multiple antibodies (and therefore multiple samples) for a complete measurement. With the immunofluorescence staining, however, it is possible to discern disorganization in the tight junction proteins (by immunofluorescence) after exposure to 5% ethanol, a lower concentration than for any of the other methods tested. Permeability assays provide a robust means to study changes in translayer solute flux, and are particularly useful in the context of drug absorption. Unfortunately, these assays are not well suited for dynamic measurements. And since permeability measurements are conducted with respect to a certain tracer molecule, data are size and charge specific. For these reasons, permeability assays are most valuable when combined with TER measurements; together, painting a more complete picture of the barrier properties of the cell layer. It should be emphasized that although TER and solute flux are both related to barrier tissue integrity, they describe different functional and structural components of the barrier and do not always change in parallel [48]. In this study, nonetheless, for the compounds chosen, we show that trends observed using the OECT correlate very well with the Lucifer Yellow permeability assay, albeit more rapidly and with higher sensitivity. Both the OECT and the CellZscope allow for dynamic monitoring of TER that is not possible with immunofluorescence or permeability assays. The OECT compares very favorably to the CellZscope, and could be viewed in the short term as a complementary technology more suitable in some situations, or in the longer term as an organic electronic based alternative to expensive electrical impedance spectroscopy equipment. The quick action detected with the OECT on addition of H_2O_2 was more difficult to observe with the CellZscope. In addition, the response with the Cellzscope was somewhat complex in nature, without a strict dependency between increase in dose and decrease in TER. This may reflect the fact that there are multiple effects occurring on multiple timescales being observed by the Cellzscope, while the OECT may be measuring a simpler, earlier effect. We demonstrated that the OECT was able to detect not only faster events, but also more subtle breaches of barrier integrity caused by lower H_2O_2 concentrations. Disruption of barrier tissue by ethanol was more gradual in nature and the evolution could be followed by CellZscope and OECT alike. We postulate that the different nature of the signal shown between ethanol and H_2O_2 may be linked to the different mechanism of action of these compounds in inducing damage to barrier tissue. Of all the toxic compounds tested in our laboratory to date (manuscripts in preparation) we observe that the OECT measures changes in TER with sensitivity greater or equal to traditional methods, accompanied with increased temporal resolution. We believe that the increased temporal resolution is due to the fact that the

OECT is more sensitive to subtle breaches in barrier tissue. Further optimization of circuit geometry and OECT channel characteristics for the purpose of increased sensitivity is ongoing. A greater advantage of the OECT based sensor, however, may lie in the fabrication: these devices, based on conducting polymers, can be made with low cost processing techniques such as ink jet printing and spray coating, with active areas designed to conform to flexible substrates with unique form factors. Indeed, we have previously demonstrated the fabrication of an 'all-plastic' OECT, where PEDOT:PSS served as both the transistor channel and the electrical leads [49]. In addition to cost related aspects, solution processing allows facile modification of device architecture to suit particular applications or satisfy various cell-culture related constraints, such as the need for multiple chambers for *in vitro* cocultures, or smaller/larger/flexible form factors. Work is also in progress to develop an OECT in a format suitable for carrying out measurements within an incubator to allow the performance of longer term experiments under appropriate conditions for cell culture. Supported by the data presented in the work, we believe that the OECT is a competitive method for barrier tissue assessment in regards to both function and versatility.

2.5 References

1. Simon, D.T.; Kurup, S.; Larsson, K.C.; Hori, R.; Tybrandt, K.; Goiny, M.; Jager, E.H.; Berggren, M.; Canlon, B.; Richter-Dahlfors, A., Organic electronics for precise delivery of neurotransmitters to modulate mammalian sensory function. *Nature materials* **2009**, *8*, 742-746.

2. Bolin, M.H.; Svennersten, K.; Wang, X.J.; Chronakis, I.S.; Richter-Dahlfors, A.; Jager, E.W.H.; Berggren, M., Nano-fiber scaffold electrodes based on pedot for cell stimulation. *Sensor Actuat B-Chem* **2009**, *142*, 451-456.

3. Wan, A.M.; Brooks, D.J.; Gumus, A.; Fischbach, C.; Malliaras, G.G., Electrical control of cell density gradients on a conducting polymer surface. *Chem Commun (Camb)* **2009**, 5278-5280.

4. Gumus, A.; Califano, J.P.; Wan, A.M.D.; Huynh, J.; Reinhart-King, C.A.; Malliaras, G.G., Control of cell migration using a conducting polymer device. *Soft Matter* **2010**, *6*, 5138-5142.

5. Abidian, M.R.; Ludwig, K.A.; Marzullo, T.C.; Martin, D.C.; Kipke, D.R., Interfacing conducting polymer nanotubes with the central nervous system: Chronic neural recording using poly (3,4-ethylenedioxythiophene) nanotubes. *Advanced Materials* **2009**, *21*, 3764-3770.

6. Khodagholy, D.; Doublet, T.; Gurfinkel, M.; Quilichini, P.; Ismailova, E.; Leleux, P.; Herve, T.; Sanaur, S.; Bernard, C.; Malliaras, G.G., Highly conformable conducting polymer electrodes for *in vivo* recordings. *Advanced Materials* **2011**, *23*, H268-+.

7. Yan, F.; Mok, S.M.; Yu, J.J.; Chan, H.L.W.; Yang, M., Label-free DNA sensor based on organic thin film transistors. *Biosens Bioelectron* **2009**, *24*, 1241-1245.

8. Zhu, Z.T.; Mabeck, J.T.; Zhu, C.; Cady, N.C.; Batt, C.A.; Malliaras, G.G., A simple poly(3,4-ethylene dioxythiophene)/poly(styrene sulfonic acid) transistor for glucose sensing at neutral ph. *Chem Commun (Camb)* **2004**, 1556-1557.

9. Lin, P.; Yan, F.; Yu, J.; Chan, H.L.; Yang, M., The application of organic electrochemical transistors in cell-based biosensors. *Adv Mater* **2010**, *22*, 3655-3660.

10. Balda, M.S.; Whitney, J.A.; Flores, C.; Gonzalez, S.; Cereijido, M.; Matter, K., Functional dissociation of paracellular permeability and transepithelial electrical resistance and disruption of the apical-basolateral intramembrane diffusion barrier by expression of a mutant tight junction membrane protein. *The Journal of cell biology* **1996**, *134*, 1031-1049.

11. Balda, M.S.; Gonzalezmariscal, L.; Contreras, R.G.; Maciassilva, M.; Torresmarquez, M.E.; Sainz, J.A.G.; Cereijido, M., Assembly and sealing of tight junctions - possible participation of g-proteins, phospholipase-c, protein-kinase-c and calmodulin. *Journal of Membrane Biology* **1991**, *122*, 193-202.

12. Prozialeck, W.C.; Edwards, J.R.; Lamar, P.C.; Smith, C.S., Epithelial barrier characteristics and expression of cell adhesion molecules in proximal tubule-derived cell lines commonly used for *in vitro* toxicity studies. *Toxicology in Vitro* **2006**, *20*, 942-953.

13. Shen, L.; Weber, C.R.; Turner, J.R., The tight junction protein complex undergoes rapid and continuous molecular remodeling at steady state. *Journal of Cell Biology* **2008**, *181*, 683-695.

14. Balkovetz, D.F.; Katz, J., Bacterial invasion by a paracellular route: Divide and conquer. *Microbes and infection / Institut Pasteur* **2003**, *5*, 613-619.

15. Larre, I.; Lazaro, A.; Contreras, R.G.; Balda, M.S.; Matter, K.; Flores-Maldonado, C.; Ponce, A.; Flores-Benitez, D.; Rincon-Heredia, R.; Padilla-Benavides, T.*, et al.*, Ouabain modulates epithelial cell tight junction. *Proceedings of the National Academy of Sciences of the United States of America* **2010**, *107*, 11387-11392.

16. Wegener, J.; Abrams, D.; Willenbrink, W.; Galla, H.J.; Janshoff, A., Automated multi-well device to measure transepithelial electrical resistances under physiological conditions. *BioTechniques* **2004**, *37*, 590, 592-594, 596-597.

17. Wegener, J.; Keese, C.R.; Giaever, I., Electric cell-substrate impedance sensing (ecis) as a noninvasive means to monitor the kinetics of cell spreading to artificial surfaces. *Experimental cell research* **2000**, *259*, 158-166.

18. Shim, N.Y.; Bernards, D.A.; Macaya, D.J.; DeFranco, J.A.; Nikolou, M.; Owens, R.M.; Malliaras, G.G., All-plastic electrochemical transistor for glucose sensing using a ferrocene mediator. *Sensors-Basel* **2009**, *9*, 9896-9902.

19. White, H.S.; Kittlesen, G.P.; Wrighton, M.S., Chemical derivatization of an array of 3 gold microelectrodes with polypyrrole - fabrication of a molecule-based transistor. *Journal of the American Chemical Society* **1984**, *106*, 5375-5377.

20. Bernards, D.A.; Malliaras, G.G., Steady-state and transient behavior of organic electrochemical transistors. *Adv Funct Mater* **2007**, *17*, 3538-3544.

21. Sun, T.; Swindle, E.J.; Collins, J.E.; Holloway, J.A.; Davies, D.E.; Morgan, H., On-chip epithelial barrier function assays using electrical impedance spectroscopy. *Lab on a chip* **2010**, *10*, 1611-1617.

22. Artursson, P., Epithelial transport of drugs in cell culture. I: A model for studying the passive diffusion of drugs over intestinal absorptive (caco-2) cells. *Journal of pharmaceutical sciences* **1990**, *79*, 476-482.

23. DeFranco, J.A.; Schmidt, B.S.; Lipson, M.; Malliaras, G.G., Photolithographic patterning of organic electronic materials. *Organic Electronics* **2006**, *7*, 22-28.

24. Artursson, P.; Palm, K.; Luthman, K., Caco-2 monolayers in experimental and theoretical predictions of drug transport. *Advanced drug delivery reviews* **2001**, *46*, 27-43.

25. Yee, S., *In vitro* permeability across caco-2 cells (colonic) can predict *in vivo* (small intestinal) absorbtion in man-fact or myth. *Pharmaceutical research* **1997**, *14*, 763-766.

26. Rao, R.; Baker, R.D.; Baker, S.S., Inhibition of oxidant-induced barrier disruption and protein tyrosine phosphorylation in caco-2 cell monolayers by epidermal growth factor. *Biochemical pharmacology* **1999**, *57*, 685-695.

27. Volpe, D.A.; Asafu-Adjaye, E.B.; Ellison, C.D.; Doddapaneni, S.; Uppoor, R.S.; Khan, M.A., Effect of ethanol on opioid drug permeability through caco-2 cell monolayers. *AAPS J* **2008**, *10*, 360-362.

28. Ma, T.Y.; Nguyen, D.; Bui, V.; Nguyen, H.; Hoa, N., Ethanol modulation of intestinal epithelial tight junction barrier. *The American journal of physiology* **1999**, *276*, G965-974.

29. Moyes, S.M.; Morris, J.F.; Carr, K.E., Culture conditions and treatments affect caco-2 characteristics and particle uptake. *International journal of pharmaceutics* **2010**, *387*, 7-18.

30. Banan, A.; Choudhary, S.; Zhang, Y.; Fields, J.Z.; Keshavarzian, A., Oxidant-induced intestinal barrier disruption and its prevention by growth factors in a human colonic cell line: Role of the microtubule cytoskeleton. *Free radical biology & medicine* **2000**, *28*, 727-738.

31. Jepson, M.A., Disruption of epithelial barrier function by h202: Distinct responses of caco-2 and madin-darby canine kidney (mdck) strains. *Cell Mol Biol (Noisy-le-grand)* **2003**, *49*, 101-112.

32. Rao, R.K.; Baker, R.D.; Baker, S.S.; Gupta, A.; Holycross, M., Oxidant-induced disruption of intestinal epithelial barrier function: Role of protein tyrosine phosphorylation. *The American journal of physiology* **1997**, *273*, G812-823.

33. Basuroy, S.; Dunagan, M.; Sheth, P.; Seth, A.; Rao, R.K., Hydrogen peroxide activates focal adhesion kinase and c-src by a phosphatidylinositol 3 kinase-dependent mechanism and promotes cell migration in caco-2 cell monolayers. *American journal of physiology. Gastrointestinal and liver physiology* **2010**, *299*, G186-195.

34. Elamin, E.; Jonkers, D.; Juuti-Uusitalo, K.; van Ijzendoorn, S.; Troost, F.; Duimel, H.; Broers, J.; Verheyen, F.; Dekker, J.; Masclee, A., Effects of

ethanol and acetaldehyde on tight junction integrity: *In vitro* study in a three dimensional intestinal epithelial cell culture model. *PloS one* **2012**, *7*, e35008.

35. Basuroy, S.; Seth, A.; Elias, B.; Naren, A.P.; Rao, R., Mapk interacts with occludin and mediates egf-induced prevention of tight junction disruption by hydrogen peroxide. *The Biochemical journal* **2006**, *393*, 69-77.

36. Sheth, P.; Samak, G.; Shull, J.A.; Seth, A.; Rao, R., Protein phosphatase 2a plays a role in hydrogen peroxide-induced disruption of tight junctions in caco-2 cell monolayers. *The Biochemical journal* **2009**, *421*, 59-70.

37. Gonzalez, J.E.; DiGeronimo, R.J.; Arthur, D.E.; King, J.M., Remodeling of the tight junction during recovery from exposure to hydrogen peroxide in kidney epithelial cells. *Free radical biology & medicine* **2009**, *47*, 1561-1569.

38. Fisher, S.J.; Swaan, P.W.; Eddington, N.D., The ethanol metabolite acetaldehyde increases paracellular drug permeability *in vitro* and oral bioavailability in vivo. *The Journal of pharmacology and experimental therapeutics* **2010**, *332*, 326-333.

39. Catalioto, R.M.; Festa, C.; Triolo, A.; Altamura, M.; Maggi, C.A.; Giuliani, S., Differential effect of ethanol and hydrogen peroxide on barrier function and prostaglandin e(2) release in differentiated caco-2 cells: Selective prevention by growth factors. *Journal of pharmaceutical sciences* **2009**, *98*, 713-727.

40. Moyes, S.M.; Morris, J.F.; Carr, K.E., Roles of pre-treatment time and junctional proteins in caco-2 cell microparticle uptake. *International journal of pharmaceutics* **2011**, *407*, 21-30.

41. Nemeth, E.; Halasz, A.; Barath, A.; Domokos, M.; Galfi, P., Effect of hydrogen peroxide on interleukin-8 synthesis and death of caco-2 cells. *Immunopharmacology and immunotoxicology* **2007**, *29*, 297-310.

3 Chapter 3:

Optimization of sensor towards high-throughput screening

This chapter is dedicated to the optimization of the OECT and the use of a calcium chelator to damage the barrier tissue. In this chapter, like the previous one, I performed the immunofluorescence, permeability assays and measurement of the TER. During this work, I learned how to set up the OECT experiment and have some trial with OECT experiment.

This chapter corresponds to articles the following published article:

S. A. Tria, L.H. Jimison, A. Hama, M. Bongo, and R.M. Owens, "Sensing of EGTA Mediated Barrier Tissue Disruption with an Organic Transistor", Biosensors 3, 44 (2013).

As supplementary information a protocol is available as an article in press:

S. A. Tria, M Ramuz, L.H. Jimison, A. Hama and R.M. Owens, Sensing of Barrier Tissue Disruption with an Organic Electrochemical Transistor, Journal of Visualized Experiments, in press.

3.1 Introduction

Understanding and controlling the barrier function of epithelial tissue is of great importance for pharmaceutical research and drug development, as well as having applications in diagnostics and fundamental research. Manipulating barrier function is primarily applicable in targeted drug delivery, which involves the specific transport of a molecule across the lumen to the underlying tissue. Developing methods to achieve such transport is of particular relevance for drug delivery across gastrointestinal tissue. In some cases, an agent is used to temporarily increase permeability of the cell layer and allow passage of a drug [1]. Further, drug delivery assays require adequate *in vitro* cell models to assess drug transport. *In vitro* models for barrier tissue are also necessary to assess the effects of toxins or pathogens, for the purpose of both diagnostics and the study of diseases. Regardless of application, the goal of *in vitro* models is to mimic *in vivo* barrier tissue behavior.

Barrier tissue generally consists of tightly packed layers of epithelial cells. Individual cells are joined to one another by junctional proteins, which act as cell-cell seals [2]. In addition, the cells are anchored to underlying tissues. The anchoring provides an asymmetric architecture to the barrier, in which the apical side is exposed to the lumen, and the basal side is attached to the basal lamina [3,4]. This architecture provides selective transport across the barrier, which can be modulated to increase the passage of nutrients via transient opening of the apical junction [5,6]. The apical junction is composed of two distinct junctions; the tight junction (TJ), found closest to the apical side, and the adherens junction (AJ), found underneath the TJ [7]. These junctions comprise complexes of intracellular and transmembrane proteins. The major proteins involved in TJs are claudins [8], occludins [9] and ZO-1 [10,11], while AJs consist primarily of E-cadherin and catenin [12]. Beneath the apical junction are additional junctional complexes known as desmosomes, which contribute to cell integrity [13]. The integrity of junctional protein complexes, and hence the integrity of barrier tissue, is known to be affected by outside stimuli. In particular, the function of some proteins such as cadherins, are sensitive to the concentration of extracellular calcium. Cadherins, found in both the adherens junction and the desmosome contain multiple calcium binding domains [14]. When insufficient calcium is present, cadherins are not able to form homo or heterojunctions with adjacent cells [15]. As a consequence, the proteins are internalized, leading to an opening of the paracellular pathway. Other tight junction associated proteins that require the presence of calcium include G proteins, protein kinase C and calmodulin [16]. Hence, decreases in extracellular calcium concentration can lead to disassembly of TJs. In fact, a calcium switch assay is often used to study TJ reformation after removal and then replacement of calcium [16].

In this study, we use Caco-2 cells grown on permeable transwell filters. When cultured in this format, these cells are known to form polarized monolayers with an apical brush border, similar to that found in the human

colon [17]. More specifically, differentiated monolayers of Caco-2 cells create a barrier similar to that observed *in vivo*. Confluent monolayers of Caco-2 cells are widely used by the pharmaceutical industry to evaluate the absorption of oral drugs: the fraction of drug absorption can be directly correlated with the apparent permeability of the drug molecule across the cell layer [18]. The dependence of barrier integrity of the Caco-2 cells on calcium concentration has been confirmed [19], with the internalization of TJ and AJ proteins occurring when calcium concentrations decrease to micromolars levels [20]. As discussed above, disruption of junctional protein complexes leads to opening of the intercellular junction. To mimic this effect *in vitro*, we exposed Caco-2 monolayers to EGTA (Ethylene glycol-bis(beta-aminoethylether)-N,N,N',N'-tetra acetic acid), a specific calcium chelator. EGTA has been shown previously to have dramatic effects on paracellular permeability and transepithelial resistance (TER) [1, 21]. In particular, E-cadherin was found delocalized from the cell periphery after treatment with EGTA [22, 23]. To monitor the barrier integrity of epithelial tissue on exposure to EGTA, we use a recently introduced method based on an organic electrochemical transistor (OECT) [24, 25]. We validate the OECT results with traditional characterization techniques, including immunofluorescence staining of junctional adhesion proteins, permeability assays and measurement of transepithelial resistance (TER).

3.2 Material and Methods

3.2.1 Cell Culture.

Caco-2 cells from ATCC were seeded at a density of 5×10^4 cells/insert (1.1 cm^2). Cells were routinely maintained at 37 °C in a humidified atmosphere of 5% CO2, in DMEM (Advanced DMEM Reduced Serum Medium 1×, Invitrogen) with 2 mM Glutamine (Glutamax™-1, Invitrogen), 10% FBS (Fetal Bovine Serum, Invitrogen) and Pen-strep (5,000 (U/mL) Penicillin-5000 (µg/mL) Streptomycin, Invitrogen). For all experiments, Caco-2 cell layers were used after 3 weeks in culture, corresponding to a TER of 400–500 $\Omega \cdot cm^2$ and a maximum apparent permeability of 1×10^{-6} $cm \cdot s^{-1}$, consistent with literature reports [26]. Cells were cultured on transwell filters with a 0.4 μm^2 pore size and area of 1.1 cm^2. For OECT measurements only, 24 transwell filters were used. Cells were exposed various concentrations of EGTA, from a stock solution of 0.6 M EGTA in DI water, pH adjusted to 7.4 with 1 M Tris-HCl. EGTA was added to the basal side of the cell filter, without changing media. Controls confirmed that the act of addition/removal of basal solution alone did not disrupt the barrier tissue layer.

3.2.2 Immunofluorescence.

After exposure to EGTA, Caco-2 cells grown on filters were fixed with 3–4% paraformaldehyde in PBS pH 7.4, for 15 min at room temperature. Permeabilization was performed using 0.25% Triton in PBS, for 10 min at room temperature and with a blocking step consisting of 1% BSA in PBST (0.05% Tween 20 in PBS), for 30 min at room temperature. Mouse monoclonal anti-E-cadherin and rabbit polyclonal anti-claudin-1 and anti occludin were used at 5 µg/mL (Invitrogen), in 1% BSA in PBST for 1h at room temperature. Monolayers were then incubated for 1h at room temperature with the secondary antibodies Alexa Fluor 488 goat anti-mouse IgG and Alexa Fluor 568 goat anti-rabbit (Molecular Probes). Finally, the cells were incubated for 5 min at room temperature with Fluoroshield with DAPI (Sigma Aldrich), mounted and examined with a fluorescent microscope.

3.2.3 Permeability Assays.

After exposure to EGTA, a permeability marker (Lucifer Yellow) was added to the apical side of the monolayer and fluorescence was measured after 1 h incubation at 37 °C in a humidified CO2 incubator. The value of the apparent permeability (Papp) was calculated according to the following relationship: $Papp = ((Flux \times V_{bas})/t) \times (1/C_o \times A)$ and $Flux = 100 \times (LY_{bas} \times V_{bas})/(LY_{api} \times V_{api})$, where LY_{bas} and LY_{api} are the concentration of Lucifer Yellow in the basal and apical sides of the hanging porous filter, respectively, V_{bas} and V_{api} are the volume in the basal and apical sides, respectively, t is the time of incubation, Co is the initial concentration of Lucifer Yellow (LY) on the apical side and A is the area of the filter. At least two samples were measured for each condition.

3.2.4 CellZscope Measurements.

The CellZscope (Nanoanalytics) measures the impedance of barrier-forming cell cultures grown on permeable membranes and provides the transepithelial electrical resistance as output. Impedance of cell layers grown on filters as previously described, were measured in complete DMEM. During EGTA exposure, TER values were measured continuously.

3.2.5 OECT Fabrication.

The conducting polymer formulation consisted of PEDOT:PSS (Heraeus, Clevios PH 1000), supplemented with ethylene glycol (Sigma Aldrich, 0.25 mL

for 1 mL PEDOT:PSS solution), dodecylbenzenesulfonic acid (DBSA, 0.5 µL/mL), and 3-glycidoxypropyltrimethoxysilane (GOPS) (10 mg/mL), the latter serving as a heat activated cross-linker to ensure film stability in aqueous solutions. Devices were fabricated on glass slides with channel dimensions defined using a parylene peel-off technique described previously [27,28]. In this technique, a parylene film is deposited on glass and subsequently patterned using conventional photolithography techniques. PEDOT:PSS is deposited on the glass/parylene pattern. When the patterned parylene is removed from the glass substrate via mechanical peeling, PEDOT:PSS is left on the glass in the negative spaces. This technique allows the patterning of sensitive materials, in that it avoids exposure of the active layer (here, the conducting polymer) to harsh developers, solvents, or other etchants. Following PEDOT:PSS deposition, devices were baked for 1 h at 140 °C in atmospheric conditions. A PDMS well was added to confine the electrolyte and define the channel area. The OECTs in this study have a channel width of 2 mm and a channel length of approximately 6 mm, resulting in a channel area of approximately 12 mm^2. PEDOT:PSS lines extending from the well served as the source and drain contacts.

3.2.6 OECT Measurements.

For OECT measurements, Ag/AgCl served as the gate electrode. All measurements were made using a Keithley 2612 Source Meter and customized Labview software. Cell media (as described above) was used as the electrolyte. Measurements were performed at ambient temperature, but controls were conducted to ensure that temperature effects do not dominate changes in OECT response within the time required for measurements. Measurement parameters were chosen to avoid exposing the cell layers to a voltage drop above 0.5 V, as high voltages have been shown to damage bilayer membranes [29]. OECT data were collected using the following parameters: V_{DS} = –0.2 V, V_{GS} = 0.3 V, V_{GS} on time = 2 s, off time = 28 s. Data are shown in the form of a normalized response of the OECT. The magnitude of modulation of drain current on application of a gate voltage pulse (ΔI_D) is divided by the baseline current Io. The resulting $\Delta I_D/Io$ dataset (unitless) is normalized to a [0,1] scale for easier data visualization and device to device comparison. Included in each measurement, but not shown, is a baseline of $\Delta I_D/Io$ after cell layer removal, to aid in the assignment of NR = 1. In this way, NR = 1 refers to no barrier properties, and NR = 0 refers to full barrier properties of the cell layer (although not full suppression of OECT modulation [24]).

3.3 Result and discussion

Barrier tissue cells grown on 24 well filters were integrated with an OECT as illustrated in Figure 3.1. A transwell filter hosting the cell layer is placed within an electrolyte well, between the Ag/AgCl gate electrode and the PEDOT:PSS channel.

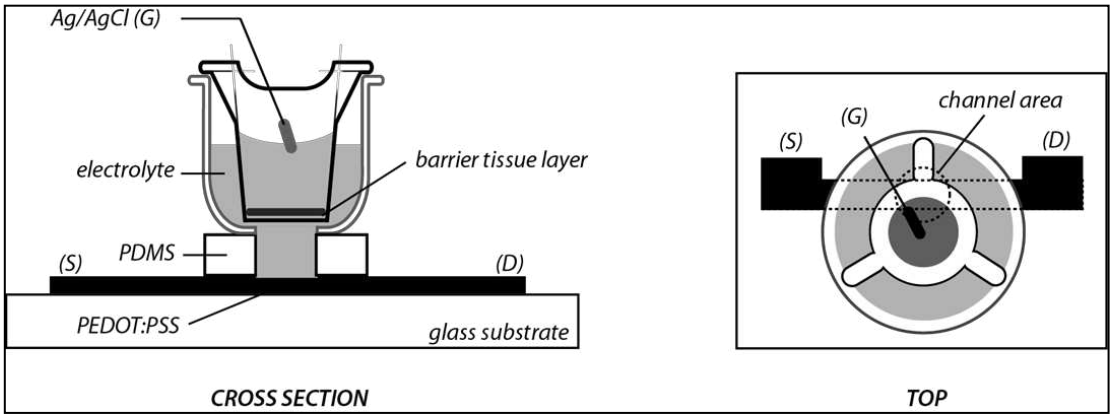

Figure 3.1: Illustration of organic electrochemical transistor (OECT) barrier tissue sensor. S, D, and G refer to the source, drain and gate electrodes. The channel area refers to the portion of PEDOT:PSS that is in contact with the electrolyte, and is defined by the PDMS well.

3.3.1 OECT Measurement of EGTA Mediated Barrier Tissue Disruption

In an OECT, the drain current (I_D) between the source and drain electrodes is modulated by the application of a gate voltage. The mechanism for current modulation relies on the electrochemical doping and dedoping of a degenerately doped conducting polymer film in contact with an electrolyte [30,31]. A positive gate voltage induces a flux of positive ions into the transistor channel, dedoping the polymer film and reducing conductivity. On release of this potential, the ions leave the film and the original doping level, and hence conductivity, is restored. The I_D transient response to a square gate voltage pulse is directly correlated with the magnitude of ionic flux into the conducting polymer. In the present device architecture, the barrier properties of the cell layer modify this ionic flux. Thus, monitoring the I_D response to square V_G pulses, shown in Figure 3.2 as normalized response (NR), yields information about the barrier properties of the cells with respect to ions in the electrolyte. Figure 3.2a shows the OECT normalized response as a function of time in the presence and absence of a cell layer. As illustrated in Figure 3.2a, operation of the OECT with no cell layer corresponds to NR = 1, which is associated with a high ionic flux through the electrolyte and into the polymer channel. When intact barrier tissue is present, the ionic flux is reduced, and NR = 0. Figure 3.2b shows the OECT response in the presence of barrier tissue on addition of varying concentrations of EGTA. On introduction of 1 mM EGTA to the

basolateral side of the transwell filter, we observe negligible changes in the normalized response of the OECT, indicating little or no disruption of barrier properties. There is perhaps a slight, transient increase in TER, which returns to baseline levels after 15 min. It is possible that there is a very slight decrease in ion flux. This has been observed with other compounds at low concentrations and may be explained by a tightening of the ion permeable TJ pores due to subtoxic exposure of certain chemicals [32]. Increases in TER have also been observed with an increase in permeability upon overexpression of occludin, illustrating functional decoupling of these two parameters [33].

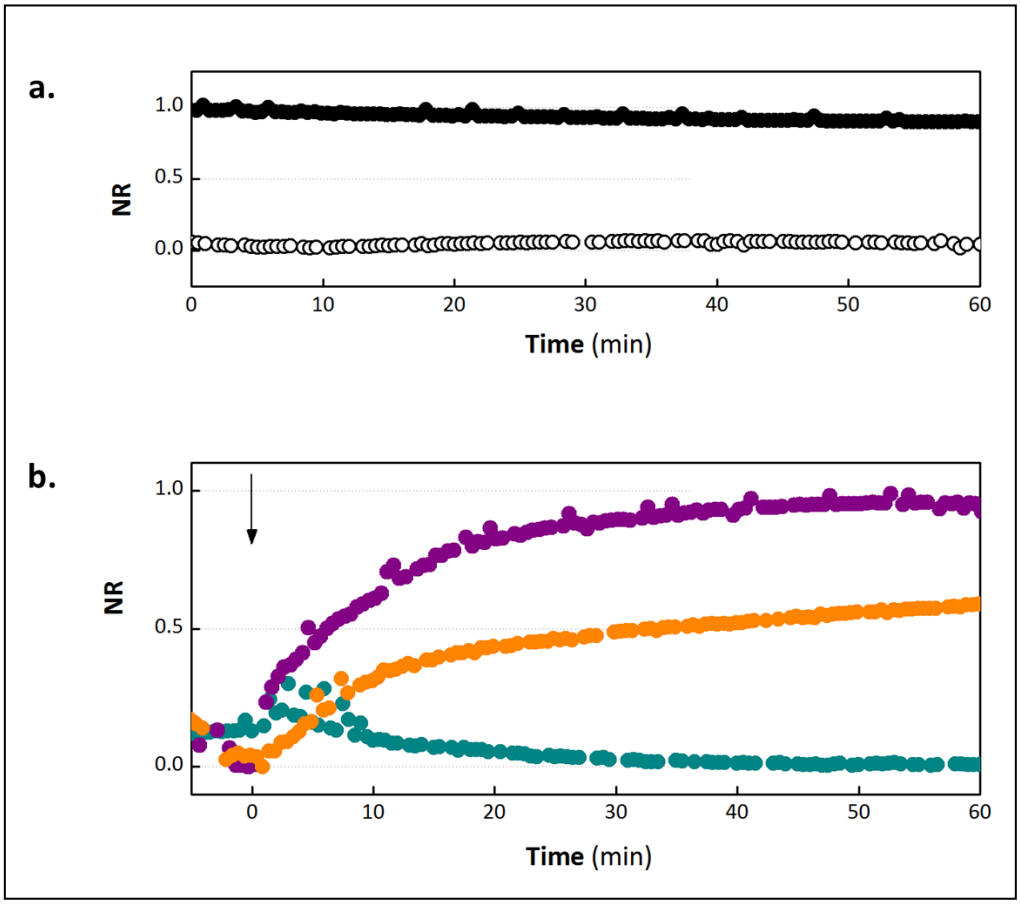

Figure 3.2: Normalized response of the OECT. (a) Control NR of OECT with cells (white) and without cells (black), with no exposure to ethylene glycol-bis(beta-aminoethylether)-*N*,*N*,*N*′,*N*′-tetra acetic acid (EGTA). (b) *In situ* monitoring of NR on addition of 1 mM (dark cyan), 10 mM (orange) and 100 mM (violet) EGTA. EGTA is added at time = 0, as indicated by the arrow.

On addition of 10 and 100 mM EGTA, we observe a concentration dependent reduction in NR, indicating increasing barrier disruption for higher concentrations of EGTA, with the presence of 100 mM EGTA destroying barrier integrity within 45 min. These experiments were carried out for 60 min only due to concerns that extended exposure of the cells to room temperature conditions would induce a change in barrier tissue properties [34]. It should be noted that in all experiments carried out in this study, EGTA was added directly to the cell medium. We anticipate that the use of EGTA in complete DMEM, as opposed to a calcium free buffer, will somewhat mitigate the effect of EGTA.

However, as changes in both media and ionic composition are known to affect TER, we wanted to ensure that we saw effects due to calcium chelation alone. As a consequence, it is not surprising that we measure no effect on addition of 1 mM EGTA, as the calcium concentration in complete DMEM is approximately 1–2 mM and EGTA chelates calcium at a ratio of 1:1. In the case of 10 mM EGTA, the signal appears to become saturated but at an NR of slightly greater than 0.5. It is possible that this signal would continue to rise slowly, however we have previously observed a similar situation with low concentrations of hydrogen peroxide [24], where the signal reaches an intermediate level and then does not increase. This could represent a partial opening of the TJ or an inhomogeneous chelation of the calcium across the barrier tissue layer. An important feature of the OECT is the time in which breaches in barrier tissue integrity are detected. In the case of 100 mM EGTA, a 50% increase in NR is observed within 5 min, and the NR plateaus at a value slightly less than 1.0. We believe that the OECT can detect barrier tissue damage more rapidly because it is sensitive to more subtle breaches in barrier tissue integrity. The improved sensing speed has been observed on addition of a variety of toxic compounds (manuscripts in preparation). Of note, while the device is more sensitive to subtle barrier damage, the sensitivity is expected to suffer at the other extreme, suggesting that the present OECT is a poor sensor for the formation of barrier tissue and gross cell death/detachment.

3.3.2 Validation of EGTA Effect Using Immunofluorescence Staining of Junctional Proteins

Figure 3.3 shows the immunofluorescence staining of adherens and tight junction proteins carried out after 2h of exposure to EGTA using antibodies against E-cadherin, occludin and claudin-1. Cell nuclei were stained with DAPI. Control staining on Caco-2 cells without EGTA exposure shows that there is at least partial colocalization of E-cadherin with both occludin (Figure 3.3a) and claudin (Figure 3.3b), and that all three proteins are present at the cell peripheries. The colocalization of E-cadherin with occludin and claudin-1 is indicative of normal maturation and polarization of the cell layer as the presence of AJs are necessary to recruit TJs on the apical side to form apical junction complexes, resulting in an alignment of the AJs and TJs [35]. In the case of occludin the staining is slightly diffuse, the control included. This may partly be because immunofluorescence was carried out on filters rather than on coverslips, leading to slight warping of the substrate. On exposure to 1 mM EGTA, the proteins remain colocalized, with negligible difference compared to the control. On the addition of 10 mM EGTA, delocalization of proteins from the periphery is observed, indicating that the apical junctional complexes have been compromised. E-cadherin is considerably more diffuse in the sample exposed to 10 mM EGTA compared to the control. On exposure of 100 mM EGTA, E-cadherin, occludin and claudin-1 are present, but no longer localized

at the cell borders. Previous studies have demonstrated that a 30 min treatment of 4 mM EGTA added to DMEM on the apical and basal side results in the displacement of occludin to the intracellular compartment [36], while a study which exposed Caco-2 cells to EGTA in media without calcium for 20 min [37] showed a normal localization of occludin with aberrant localization of claudin-1.

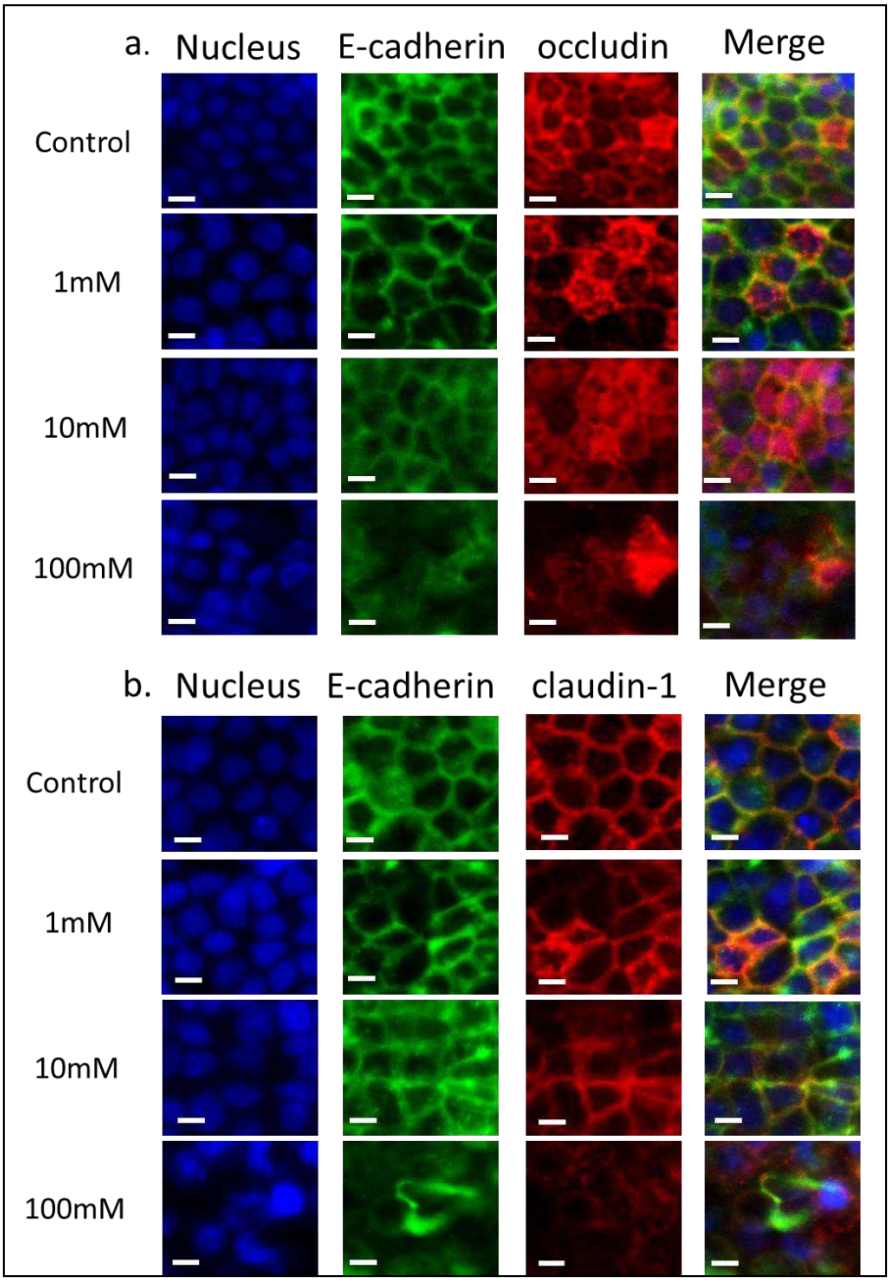

Figure 3.3: Immunofluorescence of proteins in the apical junction upon exposure to EGTA. Monolayers were exposed to various concentrations of EGTA for 2 h and then stained with antibodies against apical junction proteins. In panel a: DAPI (blue), E-cadherin (green) and occludin (red); in panel b: DAPI (blue), E-cadherin (green) and claudin-1 (red). Cells were exposed to 0, 1, 10 and 100 mM EGTA from top to bottom. The scale bar is 10 µm.

3.3.3 Validation of EGTA Effect Using CellZscope Measurement of TER and Permeability Assays

Figure 3.4a shows the effect of EGTA on TER, as measured with the CellZscope. As seen with the OECT, exposure to 1 mM EGTA shows a slight change in TER with respect to the control. On exposure of 10 mM EGTA for two and half hours, the mean TER is reduced to approximately 20% of the initial value. On addition of 100 mM EGTA, the reduction in TER is faster, stabilizing at 10% of the initial value. To directly compare the rate of sensing with the OECT, a useful parameter to consider is the time taken to reach a 50% decrease in TER. As mentioned above, the OECT detects a 50% change (increase in NR) within approximately 5 min. In the case of the CellZscope, this change takes approximately 15 min. The time taken to reach a minimum TER value with 100 mM EGTA was 1.5–2 h, compared to 45 min with the OECT. It was previously demonstrated by the EVOM (epithelial Volt-Ohm meter) technique that in the presence of 1 mM EGTA on both sides of the monolayer, a rapid drop in TER value was observed in 10 min [38]. The discrepancy between these results and what we present here can be explained by the increased potency of EGTA when presented to both the apical and basal sides, further exaggerated by the use of a calcium free buffer [23].

Figure 3.4b shows results of permeability assays carried out on Caco-2 monolayers after 2 h of EGTA exposure. The addition of 1 mM EGTA leads to a permeability of $(1.08 \pm 0.81) \times 10^{-6}$ cm·s^{-1}, a slight increase compared to the control permeability of $(8.81 \pm 7.94) \times 10^{-7}$ cm·s^{-1}. The addition of 10 mM EGTA leads to an increase in permeability to $(6.30 \pm 1.95) \times 10^{-6}$ cm·s^{-1}, while treatment with 100 mM EGTA results in a permeability of $(1.64 \pm 0.14) \times 10^{-5}$ cm·s^{-1}, 18 times larger than the control value. For comparison, a filter alone typically has a permeability of 1×10^{-4} cm·s^{-1}. Previous studies of Caco-2 permeability have demonstrated a mild increase on exposure of 2 mM EGTA in Krebs buffer, with a more marked increase at 20 mM EGTA (up to 4 hour exposure) [23].

Measurement of permeability, although a valuable parameter, must be considered carefully as the permeability measured is molecule-specific (depending on charge and size). Therefore, care must be taken when comparing these data with other parameters that describe barrier tissue integrity, such as TER. In general, a direct correlation between the solute permeability of a cell layer and the TER exist; tight cell layers exhibit high electrical resistance and low permeability, although there are certain conditions where these two parameters can be decoupled [39]. In fact, if the slight increase in permeability can be taken as statistically significant, it is in agreement with literature demonstrating that increases in TER can sometimes be accompanied by increases in permeability (discussed above), thus illustrating decoupling of these two parameters. This can be explained in part by the fact that TER is a parameter that describes an instantaneous snapshot of ion flux through claudin

based pores in epithelial tissue layers [40], while permeability is a parameter that describes the transport of larger molecules, most likely through a different pathway, one theory being that larger molecules go through barrier tissue layers via dynamic opening and closing of tight junction strands. For this reason, permeability is a parameter that must be measured over longer time periods, e.g., 1 h. As indicated above, the permeability of Lucifer Yellow was measured after incubation of this compound for 1 hour (after 2 h exposure to EGTA). Therefore, for a fairer comparison, the latter time points should be considered for TER measurements. In the case of the results shown here, a clear increase in permeability is observed with 10 mM and 100 mM EGTA, in line with the trends observed with the OECT and the CellZscope.

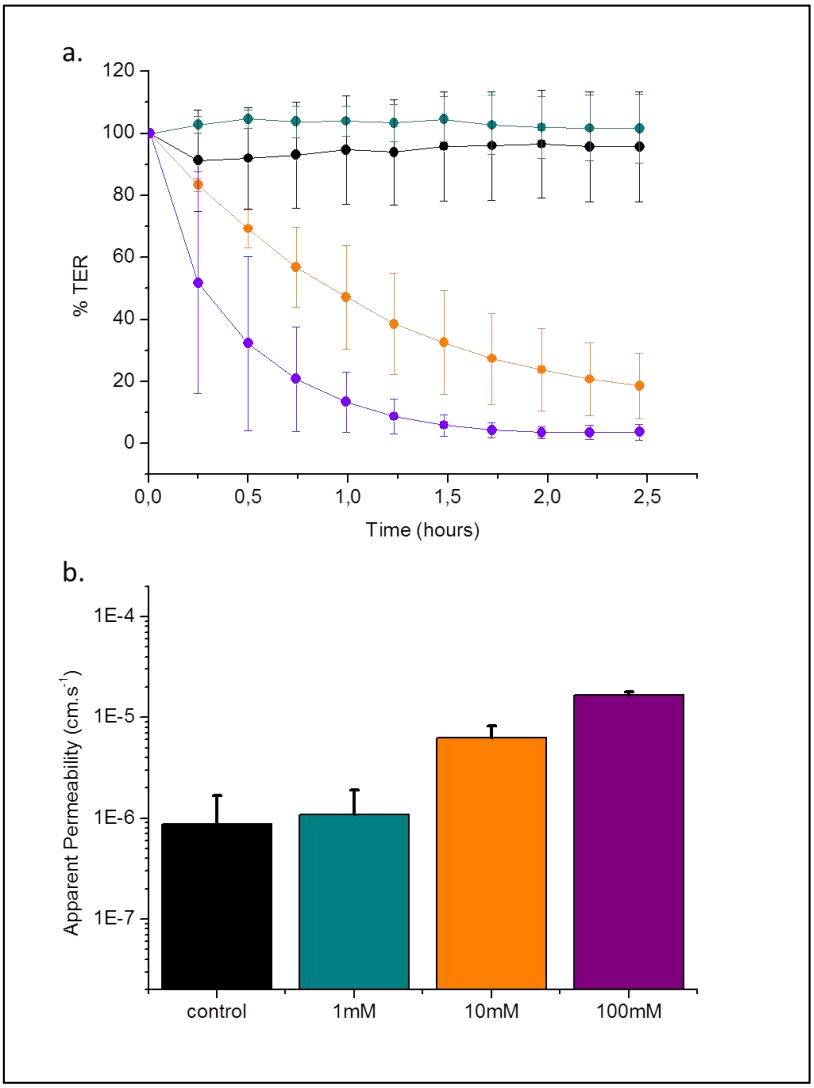

Figure 3.4: % TER value and permeability assays of cells upon exposure to EGTA. Monolayers were exposed to various concentrations of EGTA for 2.5 h. Panel a shows normalized TER value + standard deviation upon exposure to 0 mM (black), 1 mM (dark cyan), 10 mM (orange) and 100 mM EGTA (violet) for 2.5 h. During the experiment, measurements were taken continuously. Panel b shows the apparent permeability after exposure to EGTA. Data represents mean value + standard deviation of experiments made in duplicate.

3.4 Conclusions

In this study, we integrate cells with OECTs and demonstrate that the presence of a cell layer modulates the OECT transient response. Upon a decrease of extracellular calcium concentration due to the presence of EGTA, the OECT rapidly senses the breach in the epithelial cell layer in a concentration dependent manner. We validated these results by comparison with traditional techniques such as immunofluorescence, TER measurement and a Lucifer Yellow permeability assay, and found that the data correlates with the results obtained using the OECT. The OECT was able to detect EGTA-induced breaches in epithelial layers with equal sensitivity to the three techniques tested. Of the traditional techniques, only TER measurements (CellZscope) allow dynamic monitoring of barrier tissue integrity. Importantly, the OECT was found to be able to detect EGTA-induced breaches in epithelial layers with increased temporal resolution compared to the CellZscope. The OECT appears to be uniquely sensitive to subtle breaches in barrier tissue integrity, and measures with an extremely fine temporal resolution. We previously showed that the OECT was capable of measuring disruption of barrier tissue caused by exposure to hydrogen peroxide with 30 s [24]. Currently, the device probes the barrier tissue for a duration of 2 s, followed by a 28 off time, to realize a 30 s temporal resolution. The off time of the device serves two purposes: to give the cells adequate time to recover from the voltage pulse, and to allow for the recovery of the PEDOT:PSS film, bringing the drain current back to a baseline value. Duty cycle, and pulse duration could be optimized to observe more dynamic behavior if desired, with the limiting parameter being recovery of baseline current. For sake of comparison, the CellZscope requires 40 s to collect an impedance scan, which puts a hard limit on its temporal resolution.

The CellZscope has an additional advantage in that it has been developed for use in an incubator, allowing continuous, real time monitoring of barrier tissue properties. Although the current prototype of the OECT allows dynamic measurement, it is limited to operation at room temperature. Work is ongoing to transition the OECT to an in situ measurement system to allow integration of traditional cell culture materials and electronics into an incubator to allow longer term measurements and further to streamline the operation for medium to high throughput testing. Future optimization of the OECT device for sensitivity is ongoing; the device is also being adapted for use with additional cell lines to create new tools in different diagnostic applications. In addition, we intend to capitalize on the advantages in low cost fabrication and ease of device design facilitated by the use of conducting polymers towards the goal of high throughput, disposable sensing and diagnostics.

3.5 References

1. Boulenc, X.; Marti, E.; Joyeux, H.; Roques, C.; Berger, Y.; Fabre, G. Importance of the paracellular pathway for the transport of a new bisphosphonate using the human Caco-2 monolayers model. *Biochem. Pharmacol.* **1993**, *46*, 1591–1600.

2. Farquhar, M.G.; Palade, G.E. Junctional complexes in various epithelia. *J. Cell Biol.* **1963**, *17*, 375–412.

3. Gaillard, J.L.; Finlay, B.B. Effect of cell polarization and differentiation on entry of listeria monocytogenes into the enterocyte-like Caco-2 cell line. *Infec. Immunity* **1996**, *64*, 1299–1308.

4. Anderson, J.M.; Balda, M.S.; Fanning, A.S. The structure and regulation of tight junctions. *Curr. Opin. Cell Biol.* **1993**, *5*, 772–778.

5. Anderson, J.M. Molecular structure of tight junctions and their role in epithelial transport. *News Physiol. Sci.* **2001**, *16*, 126–130.

6. Anderson, J.M.; van Itallie, C.M. Tight junctions: Closing in on the seal. *Curr. Biol.* **1999**, *9*, R922–R924.

7. Guttman, J.A.; Finlay, B.B. Tight junctions as targets of infectious agents. *Biochim. Biophys. Acta* **2009**, *1788*, 832–841.

8. Colegio, O.R.; van Itallie, C.M.; McCrea, H.J.; Rahner, C.; Anderson, J.M. Claudins create charge-selective channels in the paracellular pathway between epithelial cells. *Am. J. Physiol. Cell Physiol.* **2002**, *283*, C142–C147.

9. Matter, K.; Balda, M.S. Occludin and the functions of tight junctions. *Int. Rev. Cytol.* **1999**, *186*, 117–146.

10. Anderson, J.M.; Stevenson, B.R.; Goodenough, D.A.; Mooseker, M.S. Molecular characterization of z0-1, a peripheral membrane-protein of the tight junction. *J. Cell Biol.* **1986**, *103*, A71.

11. Fanning, A.S.; van Itallie, C.M.; Anderson, J.M. Zonula occludens-1 and-2 regulate apical cell structure and the zonula adherens cytoskeleton in polarized epithelia. *Mol. Biol. Cell* **2012**, *23*, 577–590.

12. Baum, B.; Georgiou, M. Dynamics of adherens junctions in epithelial establishment, maintenance, and remodeling. *J. Cell Biol.* **2011**, *192*, 907–917.

13. Kowalczyk, A.P.; Bornslaeger, E.A.; Norvell, S.M.; Palka, H.L.; Green, K.J. Desmosomes: Intercellular adhesive junctions specialized for attachment of intermediate filaments. *Int. Rev. Cytol.* **1999**, *185*, 237–302.

14. Angst, B.D.; Marcozzi, C.; Magee, A.I. The cadherin superfamily: Diversity in form and function. *J. Cell Sci.* **2001**, *114*, 629–641.

15. Nagar, B.; Overduin, M.; Ikura, M.; Rini, J.M. Structural basis of calcium-induced e-cadherin rigidification and dimerization. *Nature* **1996**, *380*, 360–364.

16. Balda, M.S.; Gonzalez-Mariscal, L.; Contreras, R.G.; Macias-Silva, M.; Torres-Marquez, M.E.; Garcia-Sainz, J.A.; Cereijido, M. Assembly and sealing of tight junctions: Possible participation of G-proteins, phospholipase C, protein kinase C and calmodulin. *J. Membrane Biol.* **1991**, *122*, 193–202.

17. Sambuy, Y.; De Angelis, I.; Ranaldi, G.; Scarino, M.L.; Stammati, A.; Zucco, F. The Caco-2 cell line as a model of the intestinal barrier: Influence of cell and culture-related factors on Caco-2 cell functional characteristics. *Cell Biol. Toxicol.* **2005**, *21*, 1–26.

18. Artursson, P.; Karlsson, J. Correlation between oral drug absorption in humans and apparent drug permeability coefficients in human intestinal epithelial (Caco-2) cells. *Biochem. Biophys. Res. Commun.* **1991**, *175*, 880–885.

19. Artursson, P.; Magnusson, C. Epithelial transport of drugs in cell culture. II: Effect of extracellular calcium concentration on the paracellular transport of drugs of different lipophilicities across monolayers of intestinal epithelial (Caco-2) cells. *J. Pharm. Sci.* **1990**, *79*, 595–600.

20. Ivanov, A.I.; Nusrat, A.; Parkos, C.A. Endocytosis of epithelial apical junctional proteins by a clathrin-mediated pathway into a unique storage compartment. *Mol. Biol. Cell* **2004**, *15*, 176–188.

21. Artursson, P. Epithelial transport of drugs in cell culture. I: A model for studying the passive diffusion of drugs over intestinal absorptive (Caco-2) cells. *J. Pharm. Sci.* **1990**, *79*, 476–482.

22. Raiman, J.; Tormalehto, S.; Yritys, K.; Junginger, H.E.; Monkkonen, J. Effects of various absorption enhancers on transport of clodronate through Caco-2 cells. *Int. J. Pharm.* **2003**, *261*, 129–136.

23. Collares-Buzato, C.B.; McEwan, G.T.; Jepson, M.A.; Simmons, N.L.; Hirst, B.H. Paracellular barrier and junctional protein distribution depend on basolateral extracellular Ca2+ in cultured epithelia. *Biochim. Biophys. Acta* **1994**, *1222*, 147–158.

24. Jimison, L.H.; Tria, S.A.; Khodagholy, D.; Gurfinkel, M.; Lanzarini, E.; Hama, A.; Malliaras, G.G.; Owens, R.M. Measurement of barrier tissue integrity with an organic electrochemical transistor. *Adv. Mater.* **2012**, *24*, 5919–5923.

25. Tria, S.A.; Jimison, L.H.; Hama, A.; Bongo, M.; Owens, R.M. Validation of the organic electrochemical transistor for *in vitro* toxicology. *BBA-Gen. Subjects* **2012**, http://dx.doi.org/ 10.1016/j.bbagen.2012.12.003.

26. Weber, C.R.; Shen, L.; Wu, L.; Wang, Y.; Turner, J.R. Occludin is required for tumor necrosis factor (TNF)-mediated regulation of tight junction (TJ) barrier function. *Gastroenterology* **2011**, *140*, S64.

27. DeFranco, J.A.; Schmidt, B.S.; Lipson, M.; Malliaras, G.G. Photolithographic patterning of organic electronic materials. *Org. Electron.* **2006**, *7*, 22–28.

28. Khodagholy, D.; Gurfinkel, M.; Stavrinidou, E.; Leleux, P.; Herve, T.; Sanaur, S.; Malliaras, G.G. High speed and high density organic electrochemical transistor arrays. *Appl. Phys. Lett.* **2011**, *99*, 163304:1–163304:3.

29. Bernards, D.A.; Malliaras, G.G.; Toombes, G.E.S.; Gruner, S.M. Gating of an organic transistor through a bilayer lipid membrane with ion channels. *Appl. Phys. Lett.* **2006**, *89*, 053505:1–053505:3.

30. Bernards, D.A.; Malliaras, G.G. Steady-state and transient behavior of organic electrochemical transistors. *Adv. Funct. Mater.* **2007**, *17*, 3538–3544.

31. White, H.S.; Kittlesen, G.P.; Wrighton, M.S. Chemical derivatization of an array of three gold microelectrodes with polypyrrole: Fabrication of a molecule-based transistor. *J. Am. Chem. Soc.* **1984**, *106*, 5375–5377.

32. Moyes, S.M.; Morris, J.F.; Carr, K.E. Roles of pre-treatment time and junctional proteins in Caco-2 cell microparticle uptake. *Int. J. Pharm.* **2011**, *407*, 21–30.

33. Balda, M.S.; Whitney, J.A.; Flores, C.; Gonzalez, S.; Cereijido, M.; Matter, K. Functional dissociation of paracellular permeability and transepithelial electrical resistance and disruption of the apical-basolateral intramembrane diffusion barrier by expression of a mutant tight junction membrane protein. *J. Cell Biol.* **1996**, *134*, 1031–1049.

34. Armitage, W.J.; Juss, B.K.; Easty, D.L. Response of epithelial (mdck) cell junctions to calcium removal and osmotic stress is influenced by temperature. *Cryobiology* **1994**, *31*, 453–460.

35. Miyoshi, J.; Takai, Y. Molecular perspective on tight-junction assembly and epithelial polarity. *Adv. Drug Deliv. Rev.* **2005**, *57*, 815–855.

36. Sheth, P.; Samak, G.; Shull, J.A.; Seth, A.; Rao, R. Protein phosphatase 2A plays a role in hydrogen peroxide-induced disruption of tight junctions in Caco-2 cell monolayers. *Biochem. J.* **2009**, *421*, 59–70.

37. Rothen-Rutishauser, B.; Riesen, F.K.; Braun, A.; Gunthert, M.; Wunderli-Allenspach, H. Dynamics of tight and adherens junctions under egta treatment. *J. Membrane Biol.* **2002**, *188*, 151–162.

38. Ma, T.Y.; Tran, D.; Hoa, N.; Nguyen, D.; Merryfield, M.; Tarnawski, A. Mechanism of extracellular calcium regulation of intestinal epithelial tight junction permeability: Role of cytoskeletal involvement. *Microsc. Res. Technique* **2000**, *51*, 156–168.

39. Balda, M.S.; Whitney, J.A.; Flores, C.; Gonzalez, S.; Cereijido, M.; Matter, K. Functional dissociation of paracellular permeability and

transepithelial electrical resistance and disruption of the apical-basolateral intramembrane diffusion barrier by expression of a mutant tight junction membrane protein. *J. Cell Biol.* **1996**, *134*, 1031–1049.

40. Van Itallie, C.M.; Fanning, A.S.; Bridges, A.; Anderson, J.M. Zo-1 stabilizes the tight junction solute barrier through coupling to the perijunctional cytoskeleton. *Mol. Biol. Cell* **2009**, *20*, 3930–3940.

3.6 Appendix

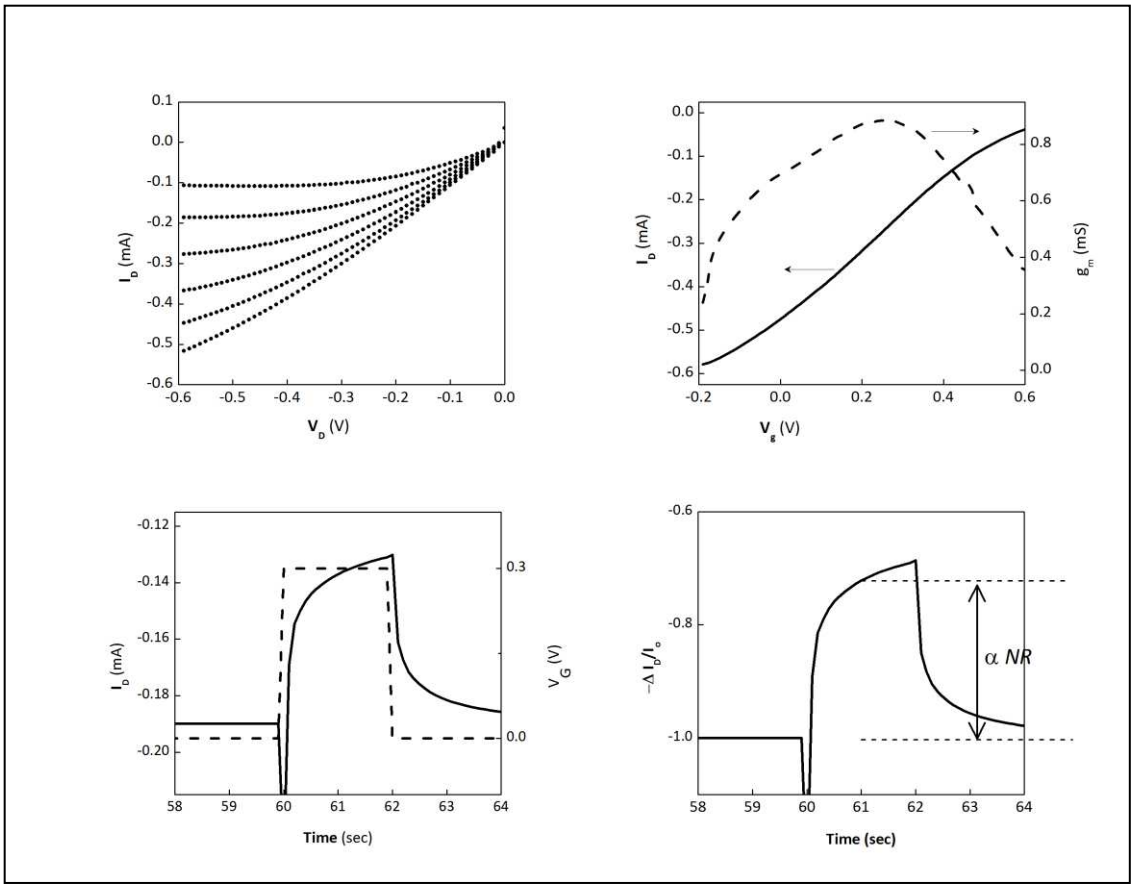

Figure S1. OECT Characteristics (no cells present.) (A) Output characteristics of the OECT used for barrier tissue sensing. (B) Transfer characteristics (solid line) and transconductance (dashed) for V_D = –0.6 V. The transconductance peaks near V_G = 0.3 V, the operating V_G of the OECT in sensing measurements. (C) I_D transient response (solid) to a square V_G pulse (dashed). (D) Normalized modulation, $\Delta I_D/I_o$, for the same V_G pulse shown in (C). The dashed lines indicate the value extracted from data. Extracted values are subsequently normalized to a [0,1] dataset to obtain normalized response (NR). $\Delta I_D/I_o$ values collected prior to sensing (no cells present) are used to define the upper extreme (NR = 1), while $\Delta I_D/I_o$ values collected immediately after cells are introduced is used to define the lower extreme (NR = 0).

4 Chapter 4:

Dynamic monitoring of *Salmonella typhimurium* infection of polarised epithelia using organic transistors

The work presented in this chapter was achieved to demonstrate the potential of the OECT to become a new technique for long term, multiplexed measurement of barrier tissue under physiological conditions. To reach this goal, I first characterize the growth of bacteria. Then, I realized the last part of the OECT fabrication which consists of the PDMS and holder gluing as well as wiring. In parallel, I did the cell culture to prepare cell culture inserts needed for the experiment, and prepared the bacterial cultures. I first tested the effect of invasive and non-invasive Salmonella typhimurium on Caco-2 cells by immunofluorescence, permeability assays and measurement of the TER after 4h exposure. Then I carried out the OECT experiment with the new setup developed in our lab.

This chapter corresponds to an article under review in Advanced Healthcare Materials.

4.1 Introduction

Epithelial tissues play a number of important roles including compartmentalisation, protection, selective absorption and transport [1]. Measurement of ion flow across epithelial tissue (generally termed the transepithelial resistance (TER); the inverse of the sum of ion permeabilities) is an accepted *in vitro* method for assessing the integrity of epithelia. The structures between adjacent cells in an epithelial layer that control ion flux are known as tight junctions, multi-protein complexes containing over 40 proteins including ZO-1, occludin and claudins [2,3]. Occludin and claudin are transmembrane proteins containing extracellular loops that form a seal between adjacent cells, assisted by a number of submembrane scaffold proteins such as ZO-1. Also intimately involved is the perijunctional actin cytoskeleton which binds to ZO-1, thus stabilising the tight junction [4]. The tightness of this seal is dependent on the composition of the proteins in the complex, particularly the claudins [5,6]. Steady-state ion flux via the paracellular pathway goes either through the pore pathway formed by transmembrane tight junction proteins, or via the non-pore pathway, postulated to be caused by dynamic breaking and resealing of tight junction strands[6]. The distinction between these pathways is often disregarded in literature and indeed in practice, and permeability is measured using tracer molecules which pass through the non-pore pathway, and thus cannot be considered an accurate assessment of the function of the pore pathway [2]. An accurate assessment of barrier tissue integrity must take into account both pathways, and so necessitates a direct measurement of ion flux. Measurements of ion flux are also label-free and directly measure a property of the cell layer, rather than indirectly measuring permeability of tracer molecules which does not always correlate with changes in permeability to ions [7].

Although one of the primary functions of the epithelium is to block pathogens and toxins from entry, many enteric pathogens have evolved to disrupt epithelial barriers through a variety of different mechanisms including direct targeting of tight junctions or hijacking of tight junction proteins by the pathogens as receptors [8,9]. One example is *Salmonella typhimurium,* one of the leading causes of food-borne illness [8]. Symptoms of enteric disease such as inflammation and diarrhoea are thought to result primarily from tight junction disruption [10]. A number of techniques are used to investigate epithelial barrier function following infection of the epithelia with enteric pathogens, including measurement of TER, permeability assays, or most frequently immunofluorescence images showing changes in co-localisation of tight junction proteins [8,11-15]. Due in large part to limitations in technology, the vast majority of these reports are either static images, or isolated measurements with a large degree of inhomogeneity [16].The tight junction has been demonstrated via FRAP (fluorescence recovery after photobleaching) to undergo continuous and rapid remodelling, suggesting a dynamic structure that changes rapidly upon exposure to extracellular stimuli on the scale of

seconds to minutes [17]. Therefore, a dynamic method for assessing changes in ion flux, that samples rapidly, is required to be able to distinguish between healthy, functioning epithelia, and those disrupted due to the effects of toxins and pathogens.

With the effort to reduce the numbers of animals used in toxicology and in diagnostics, comes the necessity not only for the development of physiologically relevant *in vitro* models, but also for relevant technology which can accurately assess them in a low cost, high-throughput and dynamic manner.Electronic impedance spectroscopy (EIS) has emerged as a technology to monitor toxicology of cells *in vitro* [18,19]. However, in many cases the devices are best suited to monitoring cell coverage or wound healing assays and are not adapted for measuring subtle changes in ionic flux [20]. One device that has been adapted for dynamic monitoring of changes in TER is the CellZscope [21], however in its current format it is not amenable to low-cost, high-throughput toxicology.

Organic electronic devices, over the last decade, have shown considerable promise in interfacing with biological systems due to advantages in terms of processing, flexibility and low-cost production [22,23]. In particular, the organic electrochemical transistor (OECT) is a device that has been shown to be particularly suited for measurement of the electrical properties of cells both *in vitro* and *in vivo* [16,24] ,providing a very efficient transduction of ionic signals to electronic ones [25,26]. In this work, we take advantage of the facile processing and stable operation of the OECT under physiological conditions, to dynamically monitor polarised epithelia *in situ*. We show simultaneous operation of multiple transistors to dynamically assess *Salmonella typhimurium* infection of an *in vitro* model of the human intestinal epithelium, both during long term operation of the device, as well as a focus on early time points, made possible due to rapid sampling. Finally, we show that the device operates stably in cell culture medium, but can also detect the presence of pathogens in complex matrices such as full-fat milk, of particular relevance for diagnostics.

4.2 Experimental Section

4.2.1 OECT Fabrication.

The conducting polymer formulation consisted of PEDOT:PSS (Heraeus, Clevios PH 1000), supplemented with ethylene glycol (Sigma Aldrich, 0.25 mL for 1 mL PEDOT:PSS solution),4,dodecylbenzenesulfonic acid (DBSA, 0.5 µL/mL), and 3-glycidoxypropyltrimethoxysilane (GOPS) (10 mg/mL). On a clean glass substrate (75 mm x 25 mm), gold source and drain contacts were patterned via lift-off lithography and then thermally evaporated. Photoresist S1813 (MicroChem Corp.) was spin coated at 3000 rpm for 30 s on the glass substrate. Patterns were defined by photolithography (Chrome mask and Mask Aligner). MF-319 was used as developer. Then, 5 nm and 100 nm of Chromium

and gold respectively, were evaporated. Finally, the photoresist was lifted-off in an acetone bath for 1 hour, which left the substrate with the source and drain Au contacts only. PEDOT:PSS channel dimensions were patterned using a parylene peel-off technique described previously [25,28], resulting in a PEDOT:PSS channel width and length of 6 mm and 1 mm, respectively. Following PEDOT:PSS deposition, devices were baked for 1 hour at 140°C under atmospheric conditions. A PDMS well defined the active area, resulting in a channel area of 6 mm^2.

4.2.2 Electronics

All measurements were done using a Ag/AgCl pellet as gate electrode (Harvard apparatus) and cell media (as described below) was the electrolyte. Experiments were performed in a humidified incubator at 37°C, 5% CO_2. Measurement parameters were chosen to avoid exposing the cell layers to a voltage drop above 0.5V, as high voltages have been shown to damage bilayer membranes [48]. The recording of the OECTs was performed using a National Instruments (NI) PXIe-1062Q system. A 4-channel source-measurement unit NI PXIe-4145 was used to bias and measure simultaneously up to 4 transistor channels. Each device is connected to an independent channel of the source-measurement system. All the channels are triggered through the built-in architecture of the system and are addressable individually. Both gating parameters such as time and voltage of the pulse, and acquisition parameters like the sampling frequency, can be set separately for each transistor. In the experiments presented here, the current in the channel was measured at V_{ds}=-0.2V and each channel was sampled at 60Hz. The gate voltage was applied using a NI PXI-6289 modular instrument. A 2s pulse was applied on the gate every 30s, at V_g=0.3V. All the measurements were triggered through the built-in PXI architecture. The recorded signals were saved and analyzed using customized LabVIEW software.

4.2.3 Data analysis

Data analysis was performed using a customized Matlab program to isolate and fit the time constant for each pulse. The time constant is extracted by performing a least-square fit of the data from each pulse current response to **Equation 1**.

$$I_d = \alpha\left\{\left[1-e^{\frac{-(t-t_o)}{\tau}}\right]+\left[1-e^{\frac{-(t-t')}{\tau'}}\right]\right\} \quad \text{Eq. 1}$$

Where α is a constant scaling term describing the magnitude of the current response, t_o is time at which the pulse starts, and τ is the time constant discussed above. Equation 1 is found to fit the experimental data well, both with and without cells (Figure 4.S2). The second exponential term, described by a time offset and time constant t' and τ' is incorporated to describe the long time evolution of the drain current, likely associated with the OECT not the barrier tissue. The contribution from the second, slow exponential does not vary significantly over the time-scale of the experiment. Similar relative results are attained whether or not the second exponential is used, but result in poor fits to the entire pulse duration (Figure 4.S2).

A background is subtracted by taking into account the time response with no cells and after scratch. The data are then normalized using the following equation: $NR = (\tau_{no\ cells} - \tau)/ (\tau_{no\ cells} - \tau_{cells})$, where τ_{cells} refers to Tau value in response to the application of the gate voltage of a barrier forming monolayer, and $\tau_{no\ cells}$ refers to Tau value in response to the application of the gate voltage of no barrier, with the dataset subsequently normalized to a to [0,1] scale.

4.2.4 Cell Culture.

Caco-2 cells from ECACC (catalogue no. 86010202) were seeded at a density of 1.5 x 10^4 cells/insert. Cells were routinely maintained at 37°C in a humidified atmosphere of 5% CO_2, in DMEM (Advanced DMEM Reduced Serum Medium 1X, Invitrogen) with 2 mM Glutamine (Glutamax™-1, Invitrogen), 10% FBS (Fetal Bovine Serum, Invitrogen) and Pen-strep (5000 [U/mL] Penicillin – 5000 [µg/mL] Streptomycin, Invitrogen). For all experiments, Caco-2 cell layers were used after 3 weeks in culture, corresponding to a minimum TER of 400Ω·cm² and a maximum apparent permeability of 1 x 10^{-6} cm·s^{-1}, consistent with literature reports [49]. Cells were cultured on Transwell filters (Millipore) with a 0.4 µm pore size and area of 0.33 cm².

4.2.5 Bacterial Growth.

Salmonella typhimurium strain 12023 and the non-invasive prgH mutant were provided by Prof. Sansonetti of the Pasteur Institute, and were grown in LB media. The prgH mutant is an established strain which is unable to invade epithelial cells [50]. After an overnight incubation at 37°C with shaking, the bacteria were diluted 1:100 in fresh LB and grown for 3.5 h to reach mid-exponential phase for all experiments.

4.2.6 Bacterial quantitation.

Basal media were collected at 30 and 60 minutes post infection. The media and serial dilutions were plated in triplicate on LB agar plates and incubated overnight at 37°C. The bacteria were quantified by counting the number of colony-forming units per milliliter (CFU/mL).

4.2.7 Infection of polarised epithelia with S. typhimurium.

The day prior to the experiment, cell culture media was exchanged for DMEM without antibiotics. The number of bacteria for each multiplicity of infection (MOI) were calculated according to the relation $OD_{600nm}=6x10^8$ bacteria/mL. Bacteria were added on the apical side of the monolayer without changing media.

For the experiments in milk, before the experiment, apical media was changed for microfiltered full-fat milk and ionic flux measured for 1 hour to ensure a stable signal. Bacteria were then added to the apical side of the monolayer.

4.2.8 Immunofluorescence.

Cells were infected as above for specified timepoints and then fixed with 3-4% paraformaldehyde in PBS pH 7.4, for 15 min at room temperature. Permeabilization was performed using 0.25% Triton in PBS, for 10 min at room temperature and with a blocking step consisting of 1% BSA in PBST (0.05% Tween 20 in PBS), for 30 min at room temperature. Mouse monoclonal anti-ZO-1 and rabbit polyclonal anti-Claudin-1 were used at 5 µg/mL (Invitrogen), in 1% BSA in PBST for 1 hr at room temperature. Monolayers were then incubated for 1 hr at room temperature with the secondary antibodies Alexa Fluor 488 goat anti-mouse IgG and Alexa Fluor 568 goat anti-rabbit (Molecular Probes). Cells were stained for F-actin using Phallotoxin (Invitrogen) for 20 min. Finally, the cells were incubated for 5 min at room temperature with Fluoroshield with DAPI (Sigma Aldrich), mounted and examined with a fluorescent microscope.

4.2.9 CellZscope measurements.

The CellZscope (Nanoanalytics) measures the frequency dependent impedance of barrier-forming cell cultures grown on permeable membranes

and provides the transepithelial electrical resistance (TER) as output. Impedance of cell layer was measured in complete DMEM.

4.3 Results

4.3.1 Multiplexed OECTs for long-term monitoring of integrity of polarised epithelia

We previously integrated the OECT with epithelia and demonstrated the possibility of measuring intact barrier function, followed by monitoring of the effect of simple toxins such as hydrogen peroxide [16], with unmatched temporal resolution [1,27]. These devices were adequate for straightforward toxicology, operated at room temperature.

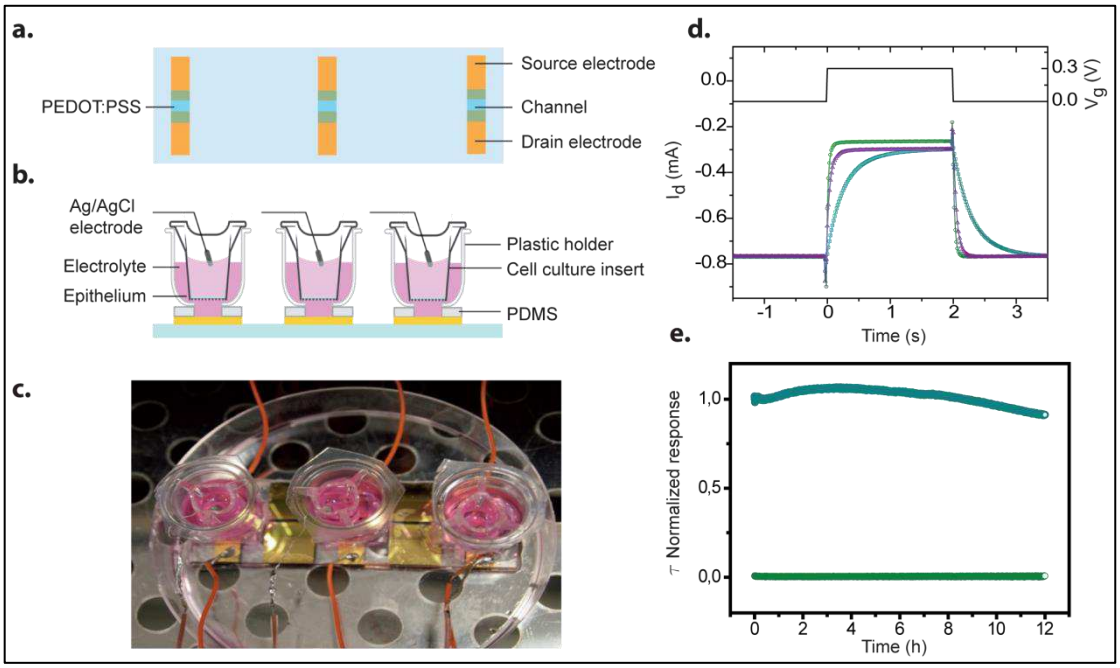

Figure 4.1: Layout, set-up and characterization of OECT integrated with polarized epithelia. (a) Layout of three OECT devices fabricated on a single glass slide. (b) Cartoon of the 3 OECTs fabricated on the same glass slide integrated with Caco-2 cells grown on Transwell filters. (c) Picture of the multiplex device shown on a Petri dish inside the cell-culture incubator. The cell culture insert is shown suspended in the plastic holder affixed to the glass slide. The Ag/AgCl gate electrode is shown immersed in the apical media, while source and drain cables are attached to their respective positions on the glass slide. (d) OECT current response (green) to a square gate pulse (VGS=0.3V), OECT with cells (blue) and OECT with cells after scratch (purple). (e) Normalized response of OECT alone (green) and OECT with cells (blue) for long term device operation. Results shown are from representative devices.

Limitations of the device included a lack of device-to-device reproducibility when cells were integrated and a loss of cell layer integrity after approximately 90 minutes at room temperature, precluding testing of more complex toxins or pathogens. To improve reproducibility and move towards high-throughput formats, a multiplex device was adopted, as illustrated in Figure 4.1a, where three photolithographically defined PEDOT:PSS devices were fabricated on a single glass slide, thus improving considerably device-to-device reproducibility. We maintained the ease of integration with current cell-culturing protocols by culturing Caco-2 cells in a 24-well transwell filter, depicted in Figure 4.1b. To enable long-term measurement of the device under physiological conditions, the completed devices were placed inside a portable incubator (Figure 4.1c). The OECT itself has been shown to be a remarkably stable device, operating in media for up to 5 weeks [28]. Our goal herein was to demonstrate integration of the OECT with polarised epithelia for use in diagnostics. The operation of the OECT integrated with barrier tissue has been described previously [16]. Briefly, on application of a positive gate voltage (V_G), cations from the electrolyte drift into the conducting polymer channel thus dedoping it, resulting in a decrease in the source-drain current (I_{DS}). The transient response of the device describes the ion flux between the gate electrode and channel of the OECT, and is therefore sensitive to the rate at which ions traverse the barrier tissue layer. Application of a gate voltage pulse is illustrated in Figure 4.1d, along with the transient response to the gate pulse an OECT alone, OECT + cells, OECT + cells after scratch (where the cell layer is deliberately disrupted by scratching the barrier tissue layer with a needle). The response from the OECT alone and the response from the OECT + cells after scratch are virtually superimposable, while a clear difference can be noted in the OECT + cells. For data analysis of long term measurements, a single parameter, the exponential time constant associated with the initial transient response to a constant gate voltage pulse, was chosen to monitor the barrier tissue integrity over time (see Methods and Figure 4.S1 for details). The use of the time constant, τ, is preferred over our previous use of normalized pulse (mid-modulation), as it is a more direct measure of the transient ion flux, is independent of pulse length, and shows lower noise over long term measurements.

For long-term device operation, the transient response of the OECT + cells should remain stable. A plot of the normalised response of the time constant for long term device operation is shown in Figure 4.1e, where 0 is the OECT alone, and 1 is the OECT + cells, showing that a stable baseline is maintained for approximately 10 hours of continuous device operation, after which, the barrier properties of the monolayer seem to deteriorate. In agreement with literature [29,30], we have found that there is a toxic effect of the Ag/AgCl electrode over longer time periods (≥ 10 hours). This effect was seen even when the electrode is not in active use, simply passively present in the media (Figure 4.S1). For acute toxicology or diagnostics purposes, an operation time of up to 10 hours is more than sufficient, and Ag/AgCl shows superior performance than other metallic electrode materials such as

platinum[31]. However, we are currently investigating other materials for the gate electrode that balance performance with lack of toxicity.

4.3.2 Kinetics of *Salmonella typhimurium* infection of polarised epithelial cells.

We set out to use the OECT to monitor real-time infection of a polarised epithelial cell model (Caco-2 cells) by the enteric pathogen *Salmonella typhimurium*. Infections were carried out in the multiplex set-up shown in Figure 4.1, under physiological conditions, with simultaneous recording possible of up to 4 devices. It should be noted that addition of a relatively simple multiplexer can allow operation of many more devices and even higher sampling resolution. Here, the measurement was done at a sampling rate of 60Hz, to accurately characterize the response time of the transistor to the applied pulse on the gate. For the infections we used both a WT (wild type) *Salmonella typhimurium* strain and a NI (non-invasive) mutant (see materials and methods for details). As illustrated in the cartoon in Figure 4.2a, the ability of *Salmonella typhimurium* to infect Caco-2 cells has been established, and is known to result in significant decreases in TER over a 6 hour period at a similar multiplicity of infection (MOI) [32]. Figure 4.2b shows the normalised response of the OECT upon infection with three different concentrations of bacteria (MOI: 10, 100, 1000; based on the initial seeding of the cells), over a 4 hour time period. In agreement with literature [33], the WT *Salmonella* provoked a dramatic increase in ionic flux across the cell monolayer, with a complete destruction of the barrier observed within 1 hour at MOI: 1000. In the case of the NI bacteria, only negligible changes were observed compared with the control.

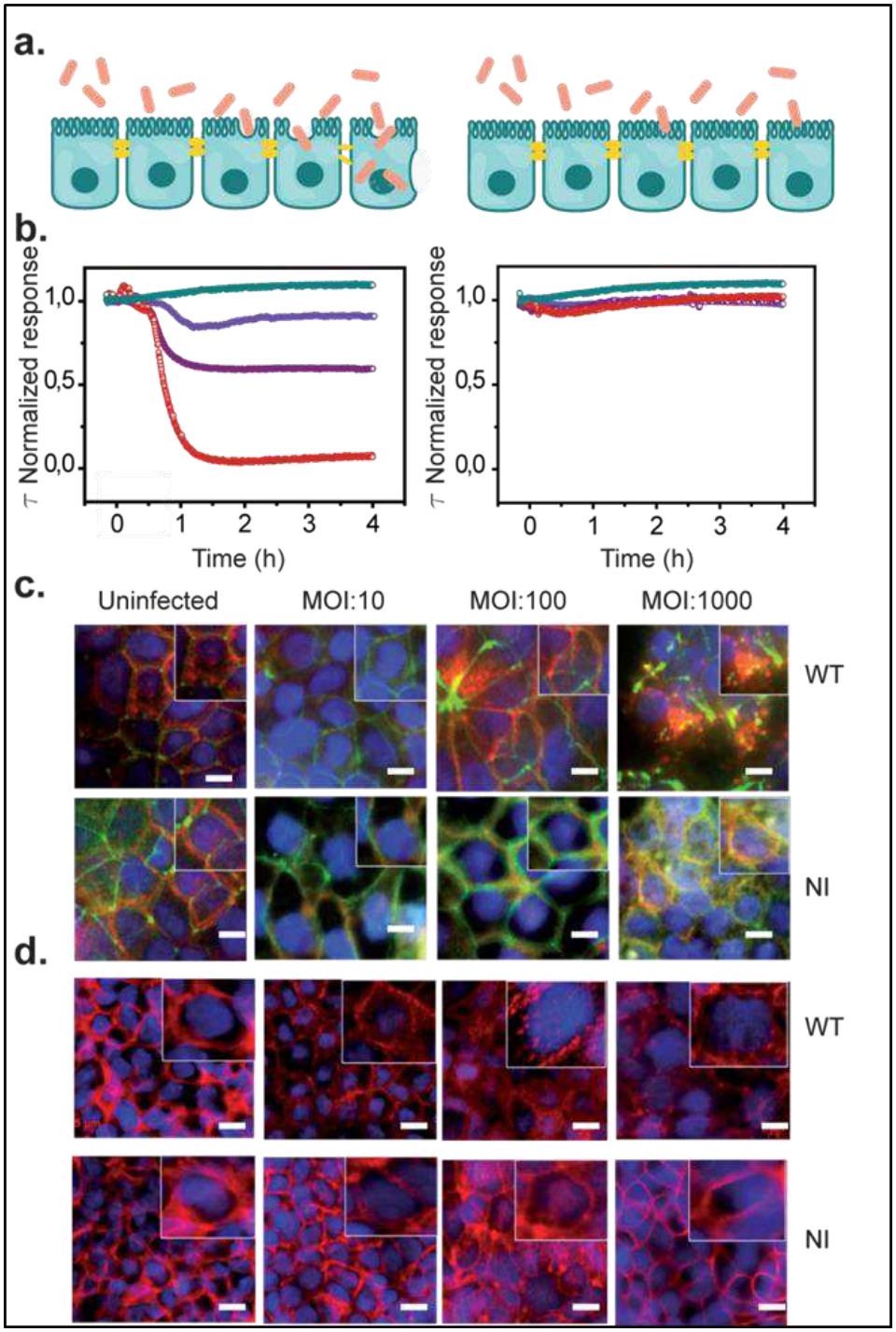

Figure 4.2: Kinetics of polarized epithelial monolayer infected with Salmonella typhimurium (a) Cartoon illustrating infection with WT (left) and NI Salmonella typhimurium (right). (b) Mean normalized response of the OECT in the presence of WT (left) and NI Salmonella typhimurium (right) at different MOI over 4h, bacteria were added at t=0. Non-infected represents OECT + cells with no added bacteria. (c) For clarity individual experiments are shown here, however mean data from multiple experiments with error bars is shown in the supplementary information (Figure 4.S3 and Figure 4.S4). (c) Immunofluorescence of tight junction proteins ZO-1 (green) and claudin-1 (red), and the nucleus (blue) after 4h infection with WT and NI Salmonella at different MOI. (d) Immunofluorescence of Actin cytoskeleton (red) and nucleus (blue) after 4h infection with WT and NI Salmonella at different MOI.

These observations were confirmed by immunofluorescence analysis of the tight junction proteins claudin-1 and ZO-1 (Figure 4.2c) showing complete destruction of the monolayer at MOI: 1000 with the WT bacteria. In agreement with the OECT data, at MOI:10 or 100, while some disorganisation of the tight junction proteins and changes to cell morphology is observable, the cell layer remains more or less intact, corresponding to a less than total disruption of the barrier function. It is well known that actin depolymerisation disrupts tight junction structure and barrier function[34]. *Salmonella's* ability to rearrange host actin is well documented, and indeed we demonstrate significant rearrangement of actin (Figure 4.2d), with characteristic punctate actin staining previously noted for the WT [35], but not for the NI.

4.3.3 Initial kinetics of *Salmonella typhimurium* infection of polarized epithelial monolayers

One of the key advantages of the device described here is the possibility to do rapid monitoring of multiple samples. In Figure 4.2 it is clear that even at the lowest MOI, the infection reaches steady state within the first hour. For this reason we focused on the first hour of infection (Figure 4.3a) to monitor the initial kinetics of infection of *Salmonella typhimurium.* In Figure 4.3a, a clear relation may be observed between the number of bacteria added and the dramatic decrease in the barrier properties of the epithelial layer within the first hour of infection. We show conclusively that the NI strain does not generate any changes in the ion flux across the epithelial cells, regardless of the MOI (Figure 4.3b). One interesting observation from the WT infection data is that there is a lag time of approximately 30 minutes before the onset of the increase in ion flux with the MOI of 10 and 100. In the case of the MOI:1000 an initial plateau appears to be reached rapidly, within the first 20-30 minutes, followed by a second increase leading to a complete breach of the barrier properties of the tissue within 1 hour. To determine whether this effect was related to bacterial replication, we determined the number of bacteria in the basolateral compartment of the device at 30 and 60 minutes post infection (Figure 4.3c).

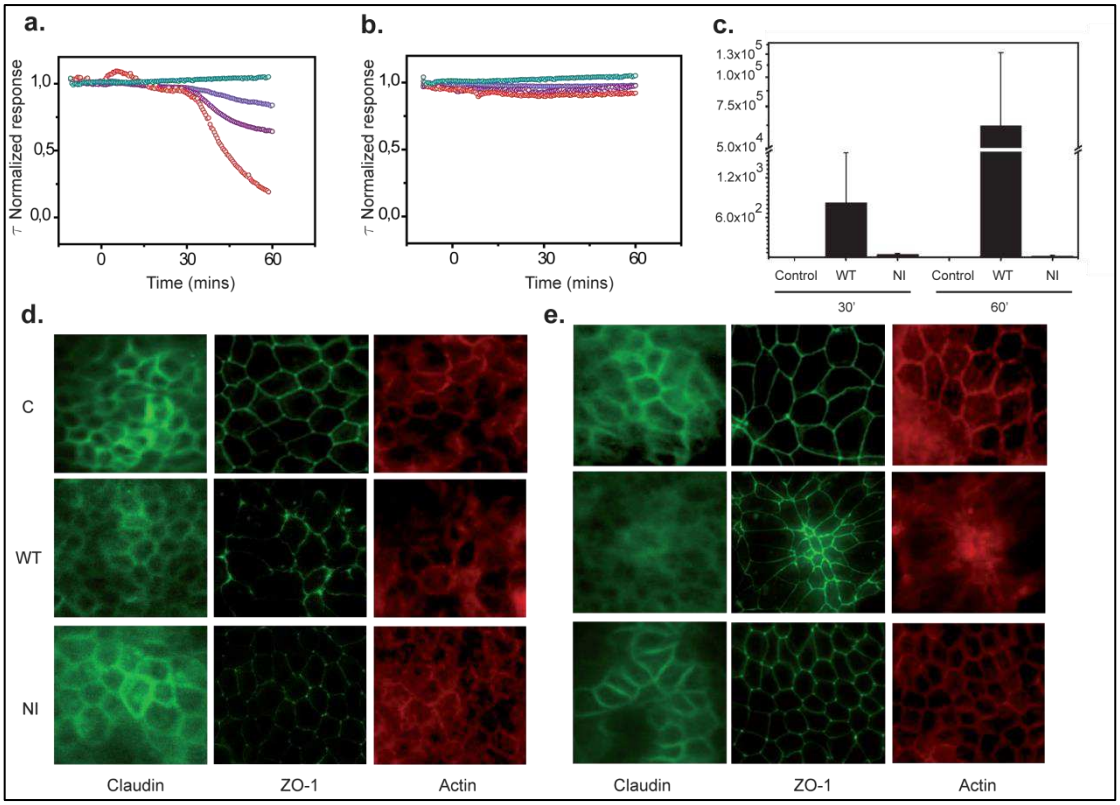

Figure 4.3: Initial kinetics of Salmonella typhimurium infection of polarized epithelial monolayers. (a) Mean normalized response of the OECT in the presence of WT Salmonella over the first hour of infection. (b) Mean normalized response of the OECT in the presence of NI Salmonella over the first hour of infection. (c) Number of bacteria present in the basolateral compartment of the epithelial monolayer 30min and 1h post infection. For clarity individual experiments are shown here, however mean data from multiple experiments with error bars is shown in the supplementary information (Figure 4.S3 and Figure 4.S4). (d) and (e) Immunofluorescence of tight junction protein ZO-1, claudin-1 and actin after (d) 30min and (e) 1h infection. Bacteria were added at t=0.

For the WT, the number of bacteria in the basolateral compartment went from approximately 1 x 10^3 CFU/mL at 30 minutes, to 1 x 10^5 CFU/mL at 60 minutes. We assert that the second, faster phase of increase in ion flux could be due to effects of the bacteria on the basolateral side, as it has been reported that *Salmonella typhimurium* can infect polarised epithelial cells via either the apical or basolateral sides[36]. Immunofluorescence analysis of the tight junction proteins showed clear ring-like structures of ZO-1, claudin -1, and actin in control and NI monolayers. In the WT samples there was a diffuse pattern of claudin-1 and ZO-1, and a constriction of actin, starting at 30 minutes, but plainly visible at 60 minutes.

4.3.4 Kinetics of *Salmonella typhimurium* infection in milk

Hitherto we have shown OECTs are promising tools for monitoring the kinetics of infection of epithelia in ideal cell culture environments, however real-life pathogen diagnostics present a number of additional challenges. Two major problems in diagnostics are specificity; being able to distinguish pathogenic strains from non-pathogenic strains, and, purification and amplification of the target molecule. Often, the sample is a complex matrix containing many different compounds including proteins, fats and other molecules which may interfere with downstream analysis [37,38]. It is clear from the data shown above that the OECT integrated with polarized epithelial cells is capable of distinguishing pathogens such as S. typhimurium from attenuated strains which are not invasion competent, and by corollary other non-pathogenic bacteria, and is thus pathogen-specific. To mimic a 'real' sample, we spiked a full-fat milk with WT S. typhimurium (MOI: 1000) to assess the effect of a complex matrix on the device operation. Although most analysis would not occur in undiluted milk, we did not dilute the milk, considering this a stringent test of our device (illustrated in Figure 4.4a). We demonstrate the maintenance of a stable baseline of the OECT over 9 hours with full fat milk in the apical compartment (Figure 4.4b). Upon addition of S. typhimurium to the milk, we detect a complete destruction of the barrier tissue properties within approximately 4.5 hours. This is a slower response than that seen for the same concentration of bacteria in cell culture medium, possibly due to an attenuating factor present in the milk or to a change in the bacterial replication kinetics. The same experiment was carried out using a commercially available EIS technique. It can be seen (Figure 4.4c) that the baseline signal is unstable when the device is operated with milk in the apical compartment, although the infection can be detected within approximately the same time-frame.

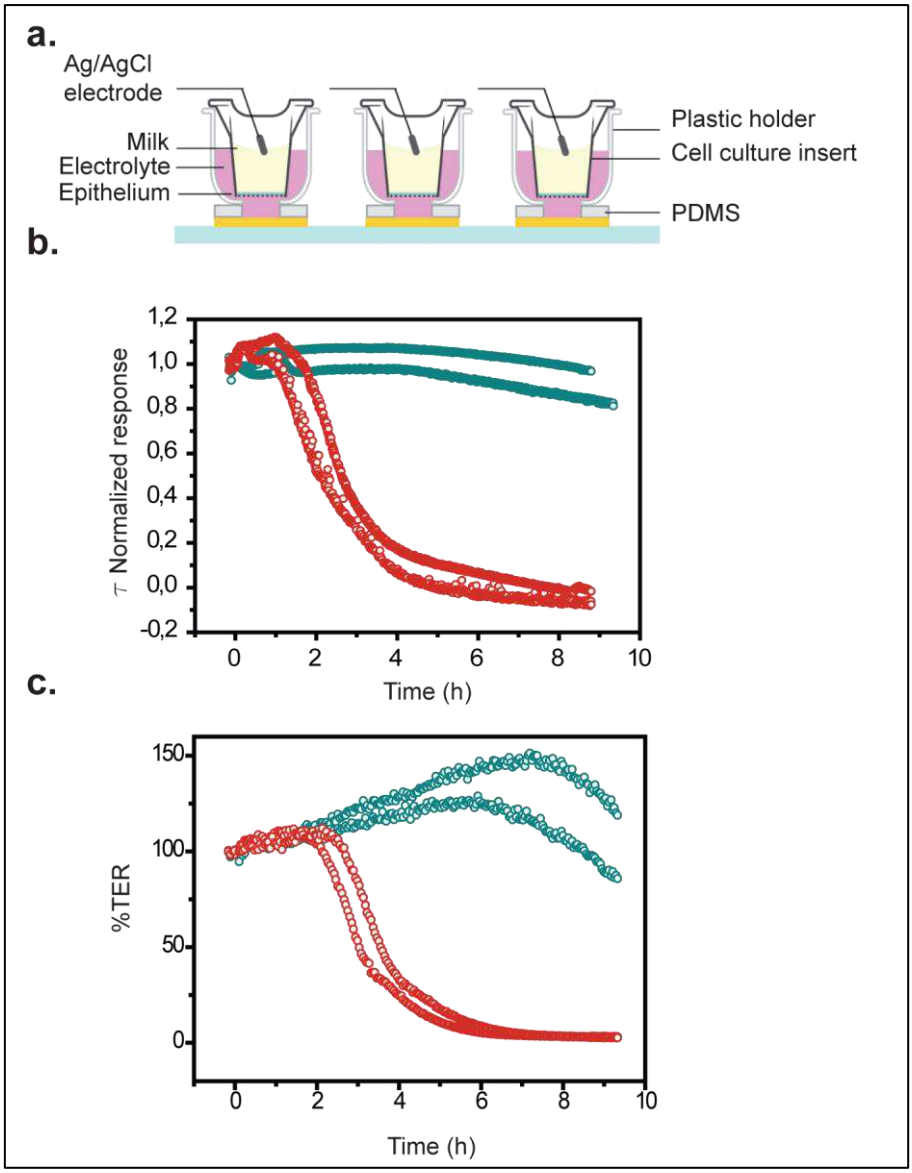

Figure 4.4: Kinetics of *Salmonella typhimurium* infection of polarized epithelial cells in milk. (a) Cartoon illustrating the integration of cells with OECT with milk in the apical side of the epithelial barrier. (b) Normalized response of the OECT in presence of milk and milk spiked with bacteria. WT *Salmonella typhimurium* bacteria were added at t=0, at an MOI: 1000. (c) Percentage of the initial TER value measured using a commercially available EIS technique (CellZscope, Nanoanalytics) upon exposure to milk and milk spiked with bacteria. WT *Salmonella typhimurium* bacteria were added at t=0, at an MOI: 1000.

4.4 Discussion

The development of new materials and related technologies has the potential to revolutionise fundamental and applied research in biomedical sciences. One example is the emergence of organic bioelectronics, which should not be thought of as a replacement for traditional electronic materials, but, in certain cases, has been shown to be uniquely suited to interfacing with niche applications in biomedical sciences. The OECT has been repeatedly shown over the last decade to be an excellent transducer of key biological processes [25,28,39-41]. Here, we show that the OECT can be integrated with a polarised epithelium and dynamically measure properties of the tissue in a multiplex fashion, under physiological conditions. Previously, studies reporting TER of infection of *S. typhimurium* or other enteric pathogens have tended to show TER measurements at isolated timepoints, with relatively little attention being paid to the initial infection, most likely due to limitations in technology. Few studies focussing on the first hour of infection [12]. One exception is the study by Jepson *et al*, where MDCK I cells were infected with *S. typhimurium* and conductance was measured in an Ussing-chamber type apparatus [42], a technique that requires a bulky apparatus that could be scaled up with difficulty [43]. We show the first example of a systematic dynamic study on the effect of *Salmonella typhimurium* infection of human epithelium. The OECT provides a detailed view of early events, allowing further investigation of the molecular events involved, using complementary techniques such as immunofluorescence and invasion assays.

We propose that the pathogen-specific diagnostic shown here holds great promise for food and water testing. This is particularly underlined by the excellent stability and long-term operation of our device, and further by its operation in milk. The majority of methods used for diagnosing the presence of a pathogen in a food or water sample rely on techniques such as PCR or ELISA. Such molecular diagnostics methods are capable of detecting very low levels of *Salmonella typhimurium,* however they generally require upstream purification and amplification steps, and often suffer from lack of specificity. Previously, studies have shown detection of *S. typhimurium* in milk[44], however, to our knowledge, this is the first report of the dynamics of infection of polarised epithelial cells with an enteric pathogen present in a complex matrix. The advantage of a live-cell based technique is that the disruption of ion flow in the cell layers will be due only to live pathogens and will not be affected by dead bacteria or background flora that often give false positives in current diagnostic methods[37]. The detection of *Salmonella typhimurium* in milk was found to be slower than in cell culture medium, possibly due to protective effects of milk proteins or sugars. Reduced levels of invasion of *Salmonella spp.* have been demonstrated in human milk [45,46], and in one additional study with certain bovine whey products [47].

4.5 Conclusions

A paradigm shift is slowly emerging in the study of barrier tissue with the realisation that the tissue is dynamic and undergoes changes very rapidly upon response to stimuli. To fully meet the needs of scientists studying barrier tissue for toxicological purposes, diagnostics and basic research, tools must be made available that provide an exact picture of the response of the tissue. We believe that our OECT-cell based device fulfils these requirements. Future requirements of the *in vitro* toxicology community will include a transition to 3D culture systems, with incorporated microfluidics, and importantly, in-line monitoring systems, something that seems infinitely possible given the progress reported here, and the literal flexibility of organic electronic devices. A further consideration is cost and capacity for high-throughput, again achievable with organic electronic devices which are amenable to large scale and low cost production.

4.6 Supplemental datas

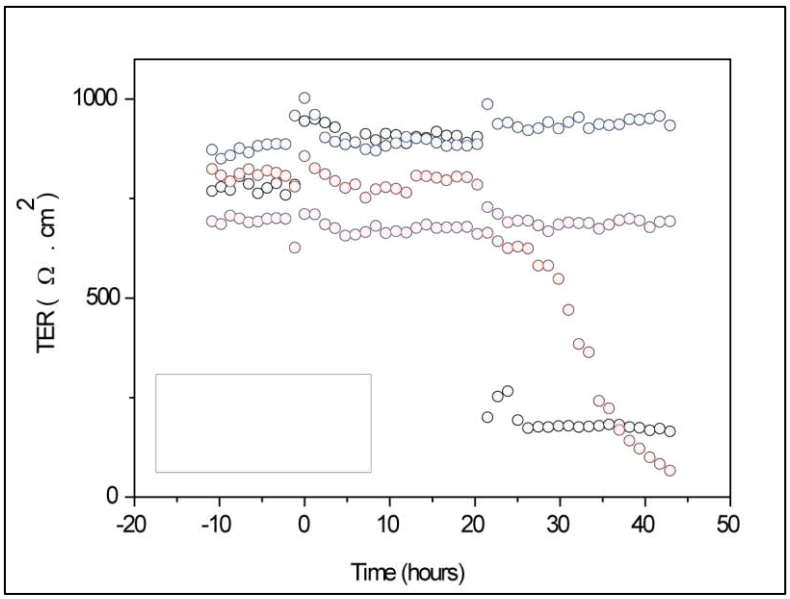

Figure 4.S1: Effect of Ag/AgCl electrode on barrier properties of polarized epithelia. TER values are shown as measured with the CellZscope. 3-week old Caco-2 cells grown on inserts were maintained in cell culture media and Ag/AgCl electrodes were added in the apical compartment at t=0.

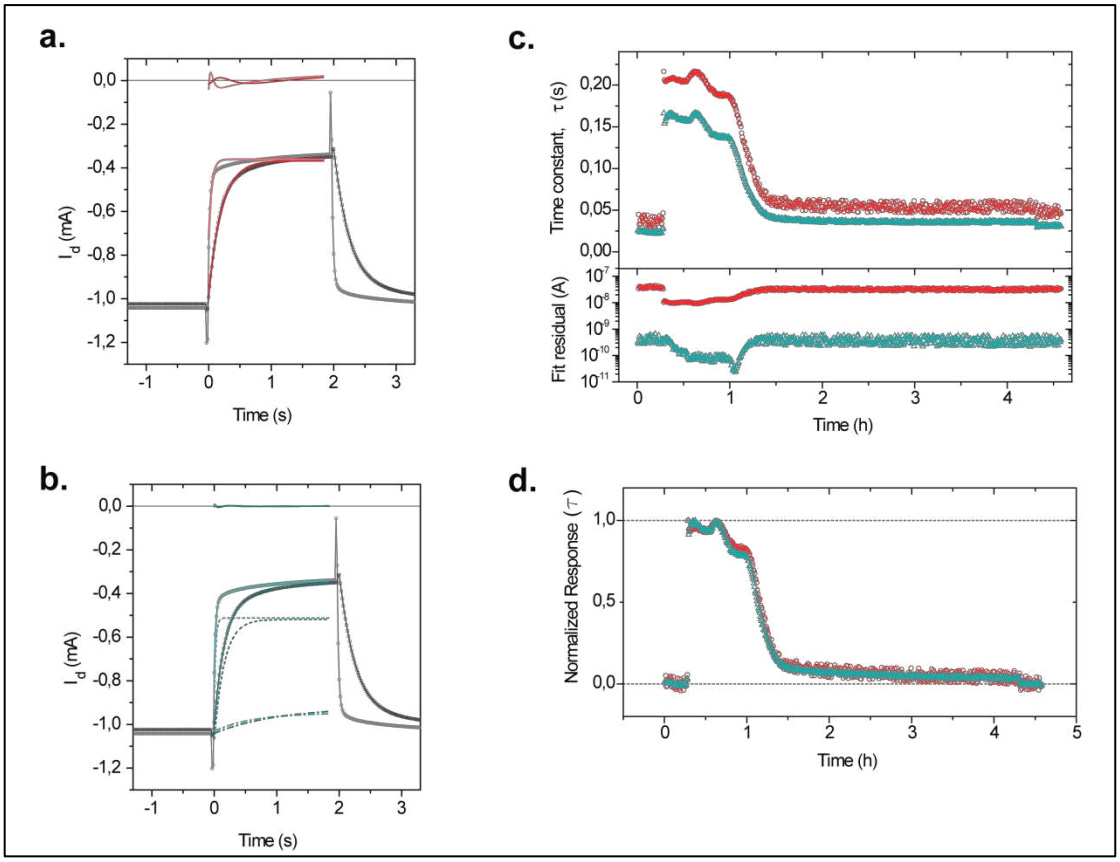

Figure 4.S2: Details of current pulse response curve fitting. a/b. Current pulse response data (grey/black) with (a) single exponential fit overlaid (red/pink), and (b) 2 exponential fit (dark/light cyan) in addition to the fit residuals. For the 2 exponential fits, the individual exponential components displayed: the initial exponential rise (dotted lines), used to extract the time constant, and the slow-varying exponential (dash-dot lines) which are similar regardless of the state of the barrier layer. c. The time course of the time constant extracted from fits, and the fit residual for MOI 1000 using single (red), and double (cyan) exponentials. d. The normalized response of the same data from c, top.

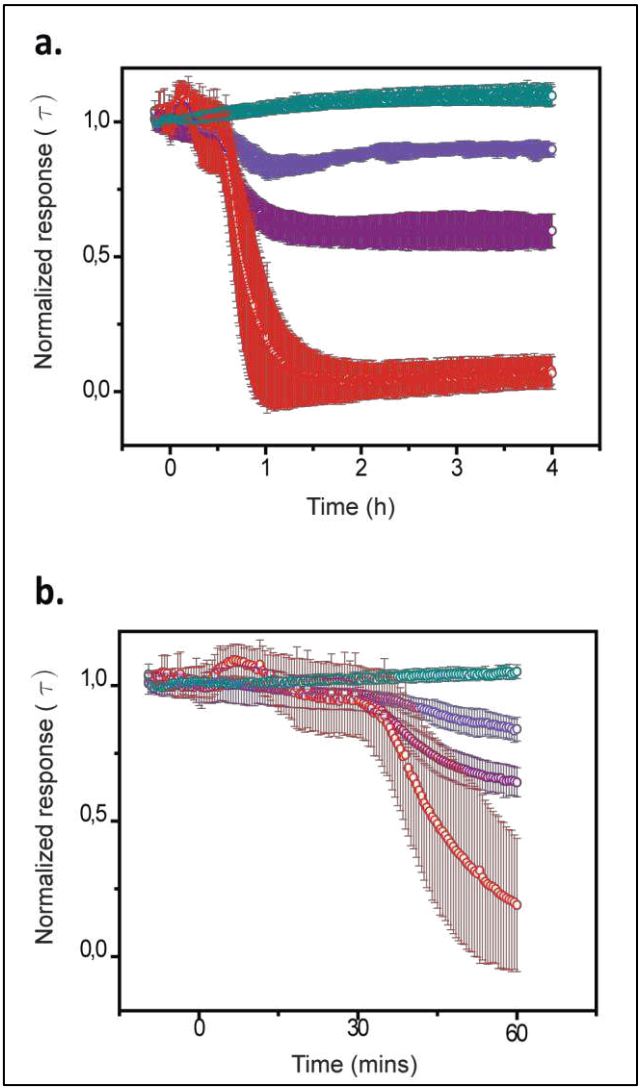

Figure 4.S3: Mean and standard deviation of the OECT normalized response in the presence of WT *Salmonella typhimurium*. a. Normalized response over 4h infection. b. Normalized response during the first hour of infection. Each curve represents the mean ± standard deviation from different experiments, with a minimum of three inserts for each point.

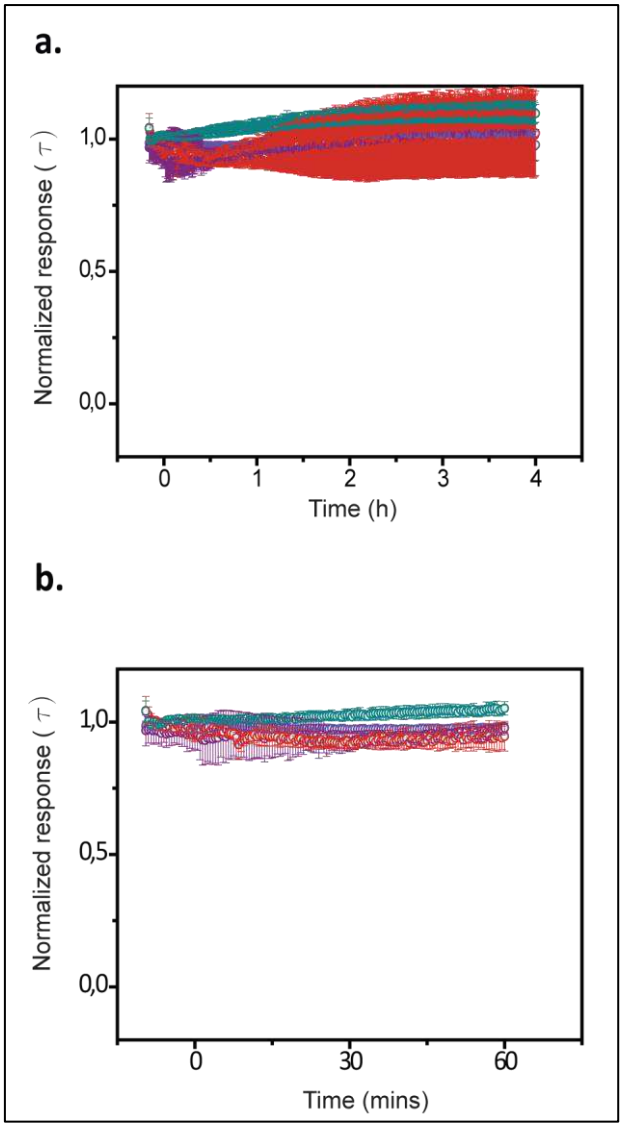

Figure 4.S4. Mean and standard deviation of the OECT normalized response in the presence of NI *Salmonella typhimurium*. a. Normalized response over 4h infection. b. Normalized response during the first hour of infection. Each curve represents the mean ± standard deviation from different experiments, with a minimum of three inserts for each point.

4.7 References

1. Tria, S.A.; Jimison, L.H.; Hama, A.; Bongo, M.; Owens, R.M., Validation of the organic electrochemical transistor for in vitro toxicology. *Biochimica et biophysica acta* **2012**.

2. Van Itallie, C.M.; Anderson, J.M., Molecular structure and regulation of tight junctions. *Gastrointestinal Transport* **2001**, *50*, 163-186.

3. Anderson, J.M.; Van Itallie, C.M., Physiology and function of the tight junction. *Cold Spring Harb Perspect Biol* **2009**, *1*, a002584.

4. Van Itallie, C.M.; Fanning, A.S.; Bridges, A.; Anderson, J.M., Zo-1 stabilizes the tight junction solute barrier through coupling to the perijunctional cytoskeleton. *Molecular biology of the cell* **2009**, *20*, 3930-3940.

5. Krug, S.M.; Gunzel, D.; Conrad, M.P.; Lee, I.F.M.; Amasheh, S.; Fromm, M.; Yu, A.S.L., Charge-selective claudin channels. *Barriers and Channels Formed by Tight Junction Proteins I* **2012**, *1257*, 20-28.

6. Gunzel, D.; Yu, A.S., Claudins and the modulation of tight junction permeability. *Physiological reviews* **2013**, *93*, 525-569.

7. Balda, M.S.; Whitney, J.A.; Flores, C.; Gonzalez, S.; Cereijido, M.; Matter, K., Functional dissociation of paracellular permeability and transepithelial electrical resistance and disruption of the apical-basolateral intramembrane diffusion barrier by expression of a mutant tight junction membrane protein. *The Journal of cell biology* **1996**, *134*, 1031-1049.

8. Guttman, J.A.; Finlay, B.B., Tight junctions as targets of infectious agents. *Biochimica et biophysica acta* **2009**, *1788*, 832-841.

9. Balkovetz, D.F.; Katz, J., Bacterial invasion by a paracellular route: Divide and conquer. *Microbes and infection / Institut Pasteur* **2003**, *5*, 613-619.

10. Schmitz, H.; Barmeyer, C.; Gitter, A.H.; Wullstein, F.; Bentzel, C.J.; Fromm, M.; Riecken, E.O.; Schulzke, J.D., Epithelial barrier and transport function of the colon in ulcerative colitis. *Epithelial Transport and Barrier Function* **2000**, *915*, 312-326.

11. Artursson, P., Epithelial transport of drugs in cell culture. I: A model for studying the passive diffusion of drugs over intestinal absorptive (caco-2) cells. *Journal of pharmaceutical sciences* **1990**, *79*, 476-482.

12. Finlay, B.B.; Gumbiner, B.; Falkow, S., Penetration of salmonella through a polarized madin-darby canine kidney epithelial cell monolayer. *The Journal of cell biology* **1988**, *107*, 221-230.

13. Katz, J.; Wu, J.H.; Michalek, S.M.; Balkovetz, D.F., Effect of porphyromonas gingivalis on epithelial cell adhesion complexes. *Journal of dental research* **2000**, *79*, 256-256.

14. Hoy, B.; Lower, M.; Weydig, C.; Carra, G.; Tegtmeyer, N.; Geppert, T.; Schroder, P.; Sewald, N.; Backert, S.; Schneider, G., *et al.*, Helicobacter pylori htra is a new secreted virulence factor that cleaves e-cadherin to disrupt intercellular adhesion. *EMBO Rep* **2010**, *11*, 798 - 804.

15. Dean, P.; Kenny, B., Intestinal barrier dysfunction by enteropathogenic escherichia coli is mediated by two effector molecules and a bacterial surface protein. *Molecular microbiology* **2004**, *54*, 665-675.

16. Jimison, L.H.; Tria, S.A.; Khodagholy, D.; Gurfinkel, M.; Lanzarini, E.; Hama, A.; Malliaras, G.G.; Owens, R.M., Measurement of barrier tissue integrity with an organic electrochemical transistor. *Adv Mater* **2012**.

17. Shen, L.; Weber, C.R.; Turner, J.R., The tight junction protein complex undergoes rapid and continuous molecular remodeling at steady state. *Journal of Cell Biology* **2008**, *181*, 683-695.

18. Giaever, I.; Keese, C.R., Monitoring fibroblast behavior in tissue culture with an applied electric field. *Proceedings of the National Academy of Sciences of the United States of America* **1984**, *81*, 3761-3764.

19. Giaever, I.; Keese, C.R., A morphological biosensor for mammalian cells. *Nature* **1993**, *366*, 591-592.

20. Benson, K.; Cramer, S.; Galla, H.-J., Impedance-based cell monitoring: Barrier properties and beyond. *Fluids and Barriers of the CNS* **2013**, *10*, 5.

21. Wegener, J.; Abrams, D.; Willenbrink, W.; Galla, H.J.; Janshoff, A., Automated multi-well device to measure transepithelial electrical resistances under physiological conditions. *BioTechniques* **2004**, *37*, 590, 592-594, 596-597.

22. Lin, P.; Yan, F., Organic thin-film transistors for chemical and biological sensing. *Advanced Materials* **2012**, *24*, 34-51.

23. Svennersten, K.; Larsson, K.C.; Berggren, M.; Richter-Dahlfors, A., Organic bioelectronics in nanomedicine. *Biochimica et biophysica acta* **2011**, *1810*, 276-285.

24. Lin, P.; Yan, F.; Yu, J.; Chan, H.L.; Yang, M., The application of organic electrochemical transistors in cell-based biosensors. *Adv Mater* **2010**, *22*, 3655-3660.

25. Khodagholy, D.; Doublet, T.; Quilichini, P.; Gurfinkel, M.; Leleux, P.; Ghestem, A.; Ismailova, E.; Hervé, T.; Sanaur, S.; Bernard, C., *et al.*, In vivo recordings of brain activity using organic transistors. *Nature Communications* **2013**, *4*, 1575.

26. Jimison, L.H.; Rivnay, J.; Owens, R.M., Conducting polymers to control and monitor cells. In *Organic electronics*, Wiley-VCH Verlag GmbH & Co. KGaA: 2013; pp 27-67.

27. Tria, S.; Jimison, L.; Hama, A.; Bongo, M.; Owens, R., Sensing of egta mediated barrier tissue disruption with an organic transistor. *Biosensors* **2013**, *3*, 44-57.

28. Khodagholy, D.; Rivnay, J.; Sessolo, M.; Gurfinkel, M.; Leleux, P.; Jimison, L.H.; Stavrinidou, E.; Herve, T.; Sanaur, S.; Owens, R.M., *et al.*, High transconductance organic electrochemical transistors. *Nature Communications* **2013**, *4*, 2133.

29. Kittler, S.; Greulich, C.; Diendorf, J.; Koller, M.; Epple, M., Toxicity of silver nanoparticles increases during storage because of slow dissolution under release of silver ions. *Chemistry of Materials* **2010**, *22*, 4548-4554.

30. Greulich, C.; Kittler, S.; Epple, M.; Muhr, G.; Koller, M., Studies on the biocompatibility and the interaction of silver nanoparticles with human mesenchymal stem cells (hmscs). *Langenbeck Arch Surg* **2009**, *394*, 495-502.

31. Tarabella, G.; Santato, C.; Yang, S.Y.; Iannotta, S.; Malliaras, G.G.; Cicoira, F., Effect of the gate electrode on the response of organic electrochemical transistors. *Appl Phys Lett* **2010**, *97*.

32. Finlay, B.B.; Falkow, S., Salmonella interactions with polarized human intestinal caco-2 epithelial cells. *Journal of Infectious Diseases* **1990**, *162*, 1096-1106.

33. Boyle, E.C.; Brown, N.F.; Finlay, B.B., Salmonella enterica serovar typhimurium effectors sopb, sope, sope2 and sipa disrupt tight junction structure and function. *Cellular microbiology* **2006**, *8*, 1946-1957.

34. Shen, L.; Turner, J.R., Actin depolymerization disrupts tight junctions via caveolae-mediated endocytosis. *Molecular biology of the cell* **2005**, *16*, 3919-3936.

35. Higashide, W.; Dai, S.; Hombs, V.P.; Zhou, D., Involvement of sipa in modulating actin dynamics during salmonella invasion into cultured epithelial cells. *Cellular microbiology* **2002**, *4*, 357-365.

36. Criss, A.K.; Casanova, J.E., Coordinate regulation of salmonella enterica serovar typhimurium invasion of epithelial cells by the arp2/3 complex and rho gtpases. *Infection and immunity* **2003**, *71*, 2885-2891.

37. Singh, J.; Batish, V.K.; Grover, S., Simultaneous detection of listeria monocytogenes and salmonella spp. In dairy products using real time pcr-melt curve analysis. *Journal of food science and technology* **2012**, *49*, 234-239.

38. Rossen, L.; Nørskov, P.; Holmstrøm, K.; Rasmussen, O.F., Inhibition of pcr by components of food samples, microbial diagnostic assays and DNA-extraction solutions. *International journal of food microbiology* **1992**, *17*, 37-45.

39. Angione, M.D.; Cotrone, S.; Magliulo, M.; Mallardi, A.; Altamura, D.; Giannini, C.; Cioffi, N.; Sabbatini, L.; Fratini, E.; Baglioni, P., *et al.*, Interfacial electronic effects in functional biolayers integrated into organic field-effect transistors. *Proceedings of the National Academy of Sciences* **2012**.

40. Lai, S.; Demelas, M.; Casula, G.; Cosseddu, P.; Barbaro, M.; Bonfiglio, A., Ultralow voltage, otft-based sensor for label-free DNA detection. *Adv Mater* **2013**, *25*, 103-107.

41. Sessolo, M.; Khodagholy, D.; Rivnay, J.; Maddalena, F.; Gleyzes, M.; Steidl, E.; Buisson, B.; Malliaras, G.G., Easy-to-fabricate conducting polymer microelectrode arrays. *Advanced Materials* **2013**, n/a-n/a.

42. Jepson, M.A.; Lang, T.F.; Reed, K.A.; Simmons, N.L., Evidence for a rapid, direct effect on epithelial monolayer integrity and transepithelial transport in response to salmonella invasion. *Pflugers Archiv : European journal of physiology* **1996**, *432*, 225-233.

43. Clarke, L.L., A guide to ussing chamber studies of mouse intestine. *Am J Physiol-Gastr L* **2009**, *296*, G1151-G1166.

44. Waswa, J.W.; Debroy, C.; Irudayaraj, J., Rapid detection of salmonella enteritidis and escherichia coli using surface plasmon resonance biosensor. *J Food Process Eng* **2006**, *29*, 373-385.

45. Hill, D.R.; Rho, H.K.; Kessler, S.P.; Amin, R.; Homer, C.R.; McDonald, C.; Cowman, M.K.; de la Motte, C.A., Human milk hyaluronan enhances innate defense of the intestinal epithelium. *Journal of Biological Chemistry* **2013**.

46. Barboza, M.; Pinzon, J.; Wickramasinghe, S.; Froehlich, J.W.; Moeller, I.; Smilowitz, J.T.; Ruhaak, L.R.; Huang, J.; Lönnerdal, B.; German, J.B., *et al.*, Glycosylation of human milk lactoferrin exhibits dynamic changes during early lactation enhancing its role in pathogenic bacteria-host interactions. *Molecular & Cellular Proteomics* **2012**, *11*.

47. Halpin, R.M.; Brady, D.B.; O'Riordan, E.D.; O'Sullivan, M., Untreated and enzyme-modified bovine whey products reduce association of salmonella typhimurium, escherichia coli o157:H7 and cronobacter malonaticus (formerly enterobacter sakazakii) to caco-2 cells. *Journal of applied microbiology* **2010**, *108*, 406-415.

48. Bernards, D.A.; Malliaras, G.G.; Toombes, G.E.S.; Gruner, S.M., Gating of an organic transistor through a bilayer lipid membrane with ion channels. *Appl Phys Lett* **2006**, *89*.

49. Weber, C.R.; Shen, L.; Wu, L.; Wang, Y.; Turner, J.R., Occludin is required for tumor necrosis factor (tnf)-mediated regulation of tight junction (tj) barrier function. *Gastroenterology* **2011**, *140*, S64-S64.

50. Behlau, I.; Miller, S.I., A phop-repressed gene promotes salmonella typhimurium invasion of epithelial cells. *Journal of bacteriology* **1993**, *175*, 4475-4484.

5 Conclusions

The work presented here contributes to the development of a system that can detect a wide range of toxins and enteric pathogens to enhance the protection and safety of people worldwide. The OECT integrated with live cells has the potential to deliver such a solution and is emerging as a viable alternative to traditional methods.

The first task realized in this project was to characterize the Caco-2 cell line with traditional techniques. Having established the parameters for intact barrier tissue, we used the same experimental conditions to perform assays with the OECT. We demonstrated that the OECT was able to detect not only faster events, but also more subtle breaches of barrier integrity caused by lower H_2O_2 concentrations. Disruption of barrier tissue by ethanol was more gradual in nature and the evolution could be followed by CellZScope and OECT alike. We postulate that the different nature of the signal shown between ethanol and H_2O_2 may be linked to the different mechanism of action of these compounds in inducing damage to the barrier tissue. The OECT was found to be able to detect EGTA-induced breaches in epithelial layers with increased temporal resolution compared to existing methods. In the last stage of this work, OECTs were integrated with a polarised epithelium and dynamically measured properties of the tissue in a multiplex fashion, under physiological conditions. A systematic dynamic study on the effect of *Salmonella typhimurium* infection of Caco-2 cells was achieved, providing a detailed view of early events, allowing further investigation of the molecular events involved by using complementary techniques. This new generation of devices underlies excellent stability in milk and the long-term operation of our devices, and further, its stable operation in milk. Our OECT also holds great promise for food and water safety. The advantage of a live-cell based technique is that the disruption of ion flow in the cell layers will be due only to live pathogens and will not be affected by dead bacteria or background flora.

Future work will include testing our prototype with viral proteins. To allow testing for toxicology, 3D culture systems with microfluidic system may be developed. The flexibility of this device shows great potential as an in line monitoring system. Ongoing work will focus on increasing device numbers compatible with high-throughput screening and an increase of device operation time. The device is also being adapted for use with additional cell lines to create new tools in different diagnostic applications. Future applications could include the use of our system to screen for compounds that restore membrane integrity following exposure to pathogenic agents. An important challenge to be addressed before these devices are ready for real-world applications relates to the packaging of the devices with cells used in clinical applications.

In summary, we have demonstrated a sensor that shows disruption of epithelial tissue sensitive to subtle breaches in barrier tissue. We think that OECTs hold great promise for food and water safety, toxicology as well as in basic research.

6 Appendix A:

Publications

Chapter 2:

L.H. Jimison, S.A. Tria, D. Khodagholy, M. Gurfinkel, E. Lanzarini, A. Hama, G.G. Malliaras, and R.M. Owens, "Measurement of barrier tissue integrity with an organic electrochemical transistor", Adv. Mater. 24, 5919 (2012)

S.A. Tria, L.H. Jimison, A. Hama, M. Bongo, and R.M. Owens, "Validation of the organic electrochemical transistor for *in vitro* toxicology", BBA - General Subjects 1830, 4381 (2013).

Chapter 3:

S. A. Tria, L.H. Jimison, A. Hama, M. Bongo, and R.M. Owens, "Sensing of EGTA Mediated Barrier Tissue Disruption with an Organic Transistor", Biosensors 3, 44 (2013).

S. A. Tria, M Ramuz, L.H. Jimison, A. Hama and R.M. Owens, Sensing of Barrier Tissue Disruption with an Organic Electrochemical Transistor, Journal of Visualized Experiments, *in press*.

Chapter 4:

S. Tria, M Ramuz, M Huerta, P Leleux, J Rivnay, L H. Jimison, A Hama, G G. Malliaras & R M. Owens, Dynamic monitoring of Salmonella typhimurium infection of polarised epithelia using organic transistors, *under review*.

École Nationale Supérieure des Mines
de Saint-Étienne

NNT: 2013 EMSE 0712

Scherrine Tria

NOVEL *IN VITRO* MODELS FOR PATHOGEN DETECTION BASED ON ORGANIC TRANSISTORS INTEGRATED WITH LIVING CELLS.

Speciality: Microelectronics

Keywords: Organic bioelectronics, Toxicology, Barrier tissue, Tight junctions, Paracellular transport.

Abstract:

In biological systems, different tissues have evolved to form a barrier. An example is the intestinal epithelium, consisting of a single layer of cells lining the wall of the stomach and colon. It restricts the passage of harmful chemicals or pathogens from the light into the tissue, while selectively absorbing the most nutrients, electrolytes and water are necessary for the host. Tight junctions are structures which limit the passage of the material through the space between the cells. The ability to measure the paracellular and transcellular transport is of vital importance because it provides a wealth of information on the state of the barrier, indicative of certain disease states , since the disruption or malfunction of the structures involved in the transport through the tissue barrier is often caused or is indicative of toxicity or disease. In addition, the degree of integrity of the barrier is a key indicator of the relevance of a particular model *in vitro* for use in toxicology and drug screening. The advent of organic electronics has created a unique opportunity to connect the worlds of electronics and biology, using devices such as organic electrochemical transistor (OECT), which provides a very sensitive way to detect ionic currents. These devices have unprecedented sensitivity in a format that can be mass produced at low cost.

The purpose of this study was to integrate a monolayer of cells representative of the gastro intestinal barrier with OECTs, to create devices that detect disruptions of the barrier in a timely and sensitive manner. This technique was demonstrated to be at least as sensitive, but a higher speed than current techniques on the market.

École Nationale Supérieure des Mines
de Saint-Étienne

NNT : 2013 EMSE 0712

Scherrine TRIA

INTEGRATION DE CELLULES AVEC DES TRANSISTORS ORGANIQUES POUR LA DETECTION RAPIDE DE PATHOGENES ET TOXINES

Spécialité: Microélectronique

Mots clefs : Bioélectronique organique, Toxicologie, Barrière Tissulaire, Jonctions serrées, Transport paracellulaire.

Résumé :

L'épithélium intestinal est un exemple de tissu qui a évolué pour former une barrière. Cette barrière limite le passage de produits toxiques d'agents pathogènes à partir de la lumière vers les tissus, tout en absorbant les nutriments, électrolytes et l'eau nécessaire à l'hôte. Les jonctions serrées sont des structures qui limitent le passage de la matière à travers l'espace intercellulaire. La capacité de mesurer le transport à travers cette barrière est d'une importance capitale car elle fournit des renseignements sur l'état de celle-ci, révélatrice de certains états pathologiques, puisque la perturbation ou dysfonctionnement des jonctions serrées est souvent due à ou est un indicatif de toxicité ou de maladie. En outre, le degré d'intégrité de la barrière est un indicateur clé de la pertinence d'un modèle *in vitro* particulier pour une utilisation en toxicologie et screening de médicaments. L'avènement de l'électronique organique a créé une occasion unique pour connecter les mondes de l'électronique et de la biologie, à l'aide des dispositifs tels que le transistor électrochimique organique (OECT), qui fournisse un moyen très sensible pour détecter des courants ioniques. Ces dispositifs ont une sensibilité sans précédent, dans un format qui peut être produit en masse à faible coût.

Le but de cette étude était d'intégrer une couche de cellules représentative de la barrière gastro intestinale avec des OECTs, pour créer des dispositifs qui permettent de détecter les perturbations de cette barrière d'une manière rapide et sensible. Cette technique a était démontrée pour être au minimum aussi sensible mais d'une rapidité supérieure que les techniques actuelles sur le marché.